NTNU

Norwegian University of
Science and Technology

Robustness of nitrifying biofilter functionality: Role of competition between heterotrophic and nitrifying bacteria on ammonium removal efficiency and microbial community structure

Maja Fjellstad Knutsen

Biotechnology (5 year)
Submission date: May 2017
Supervisor: Olav Vadstein, IBT
Co-supervisor: Ingrid Bakke, IBT

Norwegian University of Science and Technology
Department of Biotechnology and Food Science

Acknowledgements

The first person I would like to thank is my supervisor Olav Vadstein for guidance, ideas and support. I would also like to thank my Co-supervisor Ingrid Bakke for her help and the group Analysis and Control of Microbial Systems for interesting scientific discussions. Kjell Rune Johansen from VEAS has also been helpful with my experiments and practical tasks outside the University. I would also like to thank former department engineer Hege Bransegg for all practical help in the lab. My classmates have also been important for me and they have shown me invaluable support. My flat mates also deserve some attention. They have been there for me and listened to my everyday frustrations and outburst of joy over my master thesis. My parents and my two older sisters Ann-Mari and Karoline deserve a big thank you. Ann-Mari and Karoline have been my biggest supporters the last 24 years. You have been amazing!

I am eternally grateful!
Thank you!
Trondheim, May 2017

Abstract

Removal of ammonium by nitrification in biofilm systems is a common method in wastewater treatment. The ammonium removal efficiency in the nitrification process is influenced by the competition between nitrifying bacteria and heterotrophic bacteria in the biofilm, particularly for space and oxygen. The competition is affected by the ratio of organic carbon (C) to inorganic nitrogen (N) in the wastewater, since organic carbon gives advantageous conditions for the heterotrophic bacteria that can outcompete the nitrifying bacteria in the biofilm. The aim for this master thesis was to improve the knowledge about the competition between nitrifying and heterotrophic bacteria in the biofilm in order to improve ammonium removal efficiency and functionality. Experiments were done in two different nitrification biofilm systems.

The first nitrification system investigated was for biofilm carriers in moving bed biofilm reactors (MBBR) at the Department of Biotechnology. The hypothesis behind the MBBR experiments was that the biofilm with long-term exposure to organic loading (C/N ratio 1) would have reduced nitrification robustness and nitrification efficiency because of increased heterotrophic growth compared to biofilm without long-term exposure to organic loading (C/N ratio 0). Two MBBR were continuous operating for 2 separate periods of time and different short-term experiments were done to investigate the differences between the reactors.

The results from the long-term continuous operations were that nitrification activity and stability, and thus nitrification efficiency, were not decreased after long-term supply of C/N ratio 1 to the biofilm. Acute organic carbon inhibition experiments showed decreased nitrification efficiency in the biofilm with long-term exposure to organic loading. Increased loading rate of organic carbon reduced the nitrification efficiency in both the reactors and denitrification was observed. Denaturing gradient gel electrophoresis (DGGE) showed a shift in microbial community structure after increasing the organic carbon concentrations in both reactors.

The second nitrification system investigated was stationary biofilters consisting of Leca in Biological Filtration and Oxygenated Reactors (BIOFOR) at Vestfjorden Avløpselskap (VEAS) wastewater treatment plant in Asker. The hypothesis behind the study of the stationary nitrification filters consisting of Leca particles was that the automatic washing process of the

biofilters removed high amounts of heterotrophic bacteria from the outer layers of the biofilm, but not high amounts of the nitrifying bacteria in the inner layers of the biofilm.

The results from the batch oxygen experiments showed that oxygen consumption was 4 % higher and ammonium consumption rate was 19 % lower in unwashed biofilter compared to washed biofilter. The difference in ammonium consumption is a strong indication that the washing process remove heterotrophic bacteria. The DGGE analysis of microbial community structure showed that the difference between unwashed and washed biofilter was not statically significant.

Abbreviations

AOA = Ammonia oxidizing archaea
AOB = Ammonia oxidizing bacteria
AT = adenine-thymine
BC_s = Bray Curtis similarity
BIOFOR = Biological Filtration and Oxygenated Reactor
BSA = Bovine Serum Albumin
C = Organ carbon
C/N = Organic carbon / inorganic nitrogen
E_0 = Standard reduction potential
EC_{50} = Half of maximum effective concentration
EDTA = Ethylenediaminetetraacetic acid
EPS = Extracellular polymeric substance
FSA = forward scattered light
GC = guanine-cytosine
DGGE = Denaturing gradient gel electrophoresis
DMS= Dimethyl sulfoxide
DO = Dissolved oxygen
DNA = Deoxyribonucleic acid
H = Shannon diversity index
HRT = Hydraulic retention time
J = Jaccard Index
J` = Species evenness
K = Band richness or Species richness
Leca = Lightweight expanded clay aggregates
MBBR = Moving Bed Biofilm Reactor
mM = millimolar
min = Minutes
MVA = Multivariate analysis
N = Inorganic nitrogen
NOB = Nitrite oxidizing bacteria
OTU = Operational taxonomic unit
PCoA =Principal Coordinate Analysis
PCR = Polymerase chain reaction
PEHD = Polyethylene
R1 = Reactor 1 (with continuous C/N ratio 1)
R2 = Reactor 2 (with continuous C/N ratio 0)
RPM = Revolutions per minute
TAN = Total ammonia nitrogen ($NH_4^+ + NH_3$)
TOC = Total organic carbon
VEAS = Vestfjorden Avløpselskap
v = Volume
VIS = Visible
rRNA = Ribosomal RNA
RNA = Ribonucleic acid
Q = Flow rate

Table of Contents

1. Introduction

In a microbial community, multiple species compete for the resources. The results of the resource competition depend on different factors and variables (Hibbing et al., 2010). In an artificial environment, such as inside a bioreactor for ammonium removal by biofilm growth, some bacteria are more desirable than others. The bacteria that remove ammonium (nitrifying bacteria) are essential, while heterotrophic bacteria are less desirable, because of the possible negative impact on ammonium removal (Zhu and Chen, 2001). There is a resource competition for space and oxygen between the heterotrophic and nitrifying bacteria in the biofilm (Sharma and Ahlert, 1977). Organic carbon concentrations (C) can affect this competition and therefore also the ammonium removal efficiency (Zhu and Chen, 2001, Sharma and Ahlert, 1977).

1.1 The need for nitrogen removal

Nitrogen removal is an important part of modern wastewater treatment (Henze et al., 2001). Waste from agriculture, aquaculture, industrial and domestic wastewater are potential sources containing large amounts of inorganic nitrogen (N) that may be released to aquatic systems. Too high concentrations of inorganic nitrogen, often together with phosphorus, in aquatic systems may cause eutrophication, acidification and acute toxic environment for aquatic organisms (Camargo and Alonso, 2006).

Eutrophication can lead to oxygen depletion, and production of harmful toxins from algal blooms (Camargo and Alonso, 2006). Nitrogen compounds can also be harmful for humans, and especially infants are vulnerable. High concentrations of nitrite (NO_2^-) and nitrate (NO_3^-) can cause methemoglobinemia, a condition that causes decreased oxygen transport in the blood (Camargo and Alonso, 2006). An increase in human population requires higher food production. Increased food production will most likely lead to higher release of reactive nitrogen to the environment (Fields, 2004). The need for nitrogen removal from the environment will therefore increase (Galloway and Cowling, 2002).

Various processes and techniques are used for removing nitrogen from water (Crab et al., 2007). Biological treatment of wastewater is a widely used process that utilizes living organisms (usually bacteria) or products from living organisms for breaking down and transforming

unwanted substances in the water. Activated sludge or biofilter (attached growth) are two biological techniques often used for biological wastewater treatment (Henze et al., 2001). Moving bed biofilm reactor (MBBR) and Biological Filtration and Oxygenated reactor (BIOFOR) utilize biofilm growth for biofiltration of wastewater (van Kessel et al., 2010, Wien, 1995). A well-known biological method for removing nitrogen components from municipal wastewater plants and aquaculture systems is converting ammonia (NH_3) or ammonium (NH_4^+) to nitrogen gas (N_2) by nitrification and denitrification, respectively (Isaacs and Henze, 1995).

1.2 Nitrification and denitrification

Nitrification is the aerobic oxidation of ammonium (NH_4^+) to nitrate (NO_3^-) by ammonia oxidizing (AOB) and nitrite oxidizing bacteria (NOB). AOB and NOB are called nitrifying bacteria (nitrifiers) and oxidize ammonium in a two-step process. In the first step AOB oxidize ammonium to nitrite (NO_2^-) (Timmons and Ebeling, 2013). Ammonia oxidizing archaea (AOA) also oxidize ammonium to nitrite and are a central part of the nitrification process (You et al., 2009). In the second step, NOB oxidize nitrite to nitrate. The second step has lower kinetic rate than the first step, and in unbalanced systems, this may lead to nitrite accumulation. A common genus of AOB is *Nitrosomonas* and of NOB *Nitrobacter*. Equations (1.1-1.4) show the two-step oxidation of ammonium to nitrate by *Nitrosomonas* and *Nitrobacter* (Timmons and Ebeling, 2013, Ebeling et al., 2006a). Whether ammonia is protonated or not depends on the pH of the wastewater. Ammonium (NH_4^+) and ammonia (NH_3) exist in an equilibrium ($NH_3 \leftrightarrow NH_4^+$) in water and are therefore often calculated and named as one compound (ammonia, ammonium or total ammonia nitrogen (TAN)) in nitrification equations and calculations (Timmons and Ebeling, 2013). Complete ammonium oxidation (commamox) in one microorganism and not separated as for AOB and NOB, was recently confirmed to exist (Costa et al., 2006, Santoro, 2016).

Step 1: $NH_4^+ + 1.5\ O_2 \rightarrow NO_2^- + 2H^+ + H_2O$ (1.1)

Step 2: $NO_2^- + 0.5\ O_2 \rightarrow NO_3^-$ (1.2)

Sum step 1 + 2: $NH_4^+ + 2O_2 \rightarrow NO_3^- + 2H^+ + H_2O$ (1.3)

Balanced for 1 mole NH_4^+: (1.4)

$NH_4^+ + 1.83O_2 + 1.97\ HCO_3^- \rightarrow 0.0244\ C_5H_7NO_2 + 0.0976\ NO_3^- + 2.90\ H_2O + 1.86\ CO_2$

Nitrifying bacteria are chemolithoautotrophic and utilize energy from inorganic nitrogen components and use carbon dioxide (CO_2) as carbon source. This is unlike heterotrophic bacteria (heterotrophs), which utilize organic carbon as energy- and carbon source (Timmons and Ebeling, 2013). Ammonium and nitrite are weaker electron donors than organic carbon sources such as acetate (CH_3COO^-) and glucose ($C_6H_{12}O_6$). Oxidation of glucose, acetate, ammonium and nitrite and associated E_0' (standard reduction potential) values are shown in Equations (1.5-1.8). Weaker electron donors give lower free energy (ΔG), since E is proportional with ΔG (Madigian et al., 2012, Helbæk and Kjelstrup, 2009). This results in lower growth yield for the nitrifying bacteria than the heterotrophic bacteria (Zhu and Chen, 2001, Madigian et al., 2012). As a consequence, nitrifying bacteria have up to 5 times slower growth rate than for the heterotrophic bacteria (Grady and Lim, 1980). Factors that are important for the nitrification process are oxygen concentration, temperature, pH and water quality, where substrate and oxygen concentration are the two most important factors (Timmons and Ebeling, 2013). Oxygen concentrations below 2 mg/L are limiting for the nitrification process and can contribute to accumulation of nitrite (Goreau et al., 1980, Painter, 1986).

$C_6H_{12}O_6 + 6O_2 \rightarrow 6CO_2 + 6H_2O$ E_0' 0.82 - (-0,43) = 1.25 (1.5)

$CH_3COOH + 2O_2 \rightarrow 2CO_2 + 2H_2O$ E_0' 0.82 - (-0.28) = 1.10 (1.6)

$NH_4^+ + 1.5O_2 \rightarrow NO_2^- + H_2O + 2H^+$ E_0' 0.82 - (+0.43) = 0.48 (1.7)

$NO_2^- + 2H^+ + O_2 \rightarrow NO_3^- + H_2O$ E_0' 0.82 - (+0.34) = 0.39 (1.8)

For removal of high amounts of nitrate in the wastewater, the nitrification process is connected to the denitrification process in the biological treatment step. Denitrifying bacteria is a large group of facultative aerobic heterotrophic bacteria and facultative aerobic autotropic bacteria that stepwise reduce the metabolic end-product (nitrate) from nitrifying bacteria to nitrogen gas. The denitrification step is either before (pre-denitrification) or after (post-denitrification) the nitrification step in a wastewater plant. Optimal conditions for denitrifying bacteria are low oxygen and high organic carbon concentrations (Timmons and Ebeling, 2013). The heterotrophic denitrification reaction is shown in Equation (1.9) (Bruce and Perry, 2001). An anaerobic process for removing ammonium and nitrite from wastewater and converting it to nitrogen gas is carried out by Annamox (anaerobic oxidation of ammonium) bacteria. Annamox bacteria reduce nitrite and oxidize ammonium to nitrogen gas (Kuenen, 2008). The anammox reaction is shown in Equation (1.10) (Strous et al., 1998).

$$5\ CH_3COO^- + 8\ NO_3^-\ 3H^+ \rightarrow 10\ HCO_3^- + 4N_2\,(g) + 4\ H_2O \qquad (1.9)$$

$$NH_4^+ + 1.32\ NO_2^- + 0.066\ CO_2 + 0.13\ H^+ \rightarrow 1.02\ N_2 + 0.26 NO_3^- + 2.03\ H_2O + 0.066\ CH_2O_{0.5} + N_{0.5} \qquad (1.10)$$

1.3 Biofilm

Biofilm is a structure attached to a surface consisting of microorganisms and extracellular polymeric substances (EPS), that has been utilized for wastewater treatment for a long time. (Flemming et al., 2016, Donlan, 2002). Biofilm consists of several layers, and the structure is highly heterogeneous. Nutrients and oxygen are transported through water channels by diffusion to layers further down in the biofilm (Donlan, 2002). Biofilms are not unchangeable, both the structure and function will change with environmental changes (Flemming et al., 2016). For example, increased access to nutrients such as nitrogen and carbon contributes to increased biofilm thickness and a shift in the microbial community structure (Stoodley et al., 1998, Hu et al., 2009). Gradients of species, nutrients, oxygen and pH exist in the biofilm (Flemming et al., 2016).

Biofilm is advantageous for microorganisms for several reasons. Biofilm gives good utilization of extracellular enzymes and effective nutrient sorption from the surroundings. Microorganisms that are living in a biofilm are better protected from being washed out from a system compared

to planktonically living microorganism. Cooperative species exist closely in the biofilm, like AOB and NOB that have a mutualistic relationship. NOB utilize the metabolic end-product (nitrite) from AOB (Flemming et al., 2016). Nitrite is toxic for AOB and NOB remove nitrite from AOB (Cua and Stein, 2011). Some NOB provide ammonium to AOB (Flemming et al., 2016). A disadvantage of living in a biofilm is limited substrate access for the microorganisms in the deeper layers, because the organisms in the outermost layers consume substrates faster than the diffusion rate transports the substrates (Flemming et al., 2016, Madigian et al., 2012). Oxygen can penetrate to the bottom of the biofilm if the thickness is less than 300 µm (Pawlowski et al., 2007). Limited diffusion in the deepest layers reduces the growth rate for microorganisms living there and oxygen is thus often a limiting substrate in the deeper layers of the biofilm (Flemming et al., 2016, Madigian et al., 2012). Therefore are denitrifying often found in layers down in the biofilm compared to the nitrifying bacteria and other type of heterotrophic bacteria (Pawlowski et al., 2007). Substrate diffusion under 100 µm depth in the biofilm is often incomplete (Rusten et al., 2006).

1.4 Competition between nitrifying and heterotrophic bacteria

Even though heterotrophic and nitrifying bacteria utilize different energy sources, organic carbon and nitrogen components respectively, there is a resource competition for space, oxygen and essential substances in the biofilm (Sharma and Ahlert, 1977). In a resource-limited environment, like inside the biofilm, heterotrophic bacteria can outcompete or overgrow the nitrifying bacteria (Figueroa and Silverstein, 1992, Cheng and Chen, 1994, Ohashi et al., 1995).

Various factors affect the competition between heterotrophic and nitrifying bacteria. The C/N ratio, i.e. the ratio between organic carbon and ammonia, is a relevant factor, since high loading of organic carbon gives advantageous conditions for the heterotrophic bacteria (Zhu and Chen, 2001, Sharma and Ahlert, 1977). Increased C/N ratio can have acute or long-term consequences for the competition between heterotrophic and nitrifying bacteria in the biofilm. Increased competition for oxygen can be an acute event, while decrease in nitrifying bacteria populations can be a long-term consequence (Satoh et al., 2000, Zhu and Chen, 2001, Ohashi et al., 1995).

Changes in C/N ratios can lead to a shift in the microbial community structure of the biofilm, since heterotrophic bacteria populations will increase at the expense of others species. The proportion of AOB and NOB will decrease under high C/N ratios, and as a consequence of

fewer nitrifying bacteria in the biofilm, the nitrification activity will decline (Ohashi et al., 1995). Shift in microbial community structure from a large proportion of nitrifying bacteria to a large proportion of denitrifying bacteria has been shown after C/N ratio was increased (Hu et al., 2009). If the substrate conditions are changed (C/N ratio drops) and the oxygen concentration is increased, the nitrifying bacteria will most likely increase in number again (Almasi et al., 2016).

Acute increase in competition can result in oxygen deficiency. It has been shown that increased C/N ratios instantly started the competition for oxygen between the heterotrophic bacteria and the AOB in the outer layers of the biofilm. As a consequence, the AOB were inhibited and the ammonium removal rate decreased (Satoh et al., 2000). The inhibitory effect organic carbon has on AOB will decrease with increasing C/N ratio. Increasing organic carbon concentrations contribute to increasing heterotrophic growth until a maximal growth rate (saturation point) is reached. Further increase of C/N ratio after the saturation point is reached will only give a minor increase in inhibition of the nitrification process (Hu et al., 2009). NOB are also negatively affected of increased C/N ratios, since increased C/N ratios can contribute to low oxygen and nitrite concentrations inside the biofilm. Nitrite accumulation is often observed, and an explanation has been that NOB generally have lower affinity towards oxygen than AOB (Hu et al., 2009).

Even if the inlet in a reactor contains zero organic carbon, heterotrophs can still grow in the biofilm. Heterotrophic bacteria can utilize organic carbon from dead organisms (Zhu and Chen, 2001). Inhibitory substances for the heterotrophic bacteria are also often inhibitory substances for the nitrifying bacteria (Gerardi, 2016, Zhu and Chen, 2001). Increased organic loading can also contribute to nitrogen loss, since high growth of heterotropic bacteria increase the need for nitrogen for protein syntheis inside the cells (Ebeling et al., 2006b).

Measurements of oxygen concentration over time can give an indication of microbial population size or microbial growth, since metabolic activity is related to bacteria population size (Pommerville, 2004). Oxygen consumption for the heterotropic bacteria populations is often high since hetrotrophic bacteria have higher growth rate and often are higher in number in the biofilter than nitriying bacteia (Blancheton, 2000, Zhu and Chen, 2001). NOB can also have increased oxygen consumption after addition of organic carbon sources as acetate, since

some NOB are mixotrophic and can utilize acetate as carbon source (Ginestet et al., 1998, Watson et al., 1989).

1.5 Bioreactors for wastewater treatment

A bioreactor is a biological system in a container or tank where different variables can be controlled to achieve a favourable active environment and are often used for wastewater treatment. Temperature, pH, substrate concentration, retention time, oxygen concentration, pressure, stirring and volume are examples of parameters for controlling the conditions inside the reactor. Bioreactor systems can be divided into three groups: Batch, fed-batch, and continuous reactors (Doran, 2012). Hydraulic retention time (HRT) is the average time liquid spends inside a continuous reactor. HRT is defined by Equation (1.11) where v is the volume of a reactor and Q is the influent flow rate (Singh et al., 2015).

$$HRT = \frac{v}{Q} \qquad (1.11)$$

HRT can affect the competition between the microorganisms in the biofilm and the microorganisms living planktonic in the reactor. High HRT is advantageous for planktonic growth. Short HRT is advantageous for attached bacteria in the biofilm, because planktonic bacteria will be washed out when HRT is shorter than the generation time. As a consequence, the microbial communities between planktonic and biofilm are bigger at high HRT than at low HRT (Caylet et al., 2011).

1.5.1 Moving bed biofilm reactors

A well-known method used in biological wastewater treatment is moving bed biofilm bioreactor (MBBR). The MBBR system was designed in Norway and is patented by AnoxKaldnes. MBBR is based on small plastic carriers consisting of polyethylene (PEHD) designed for biofilm growth. The small plastic carriers are continuously moving inside the reactor. The movements of the biofilm carriers are created by air bubbles in aerobic systems or a mixer in anaerobic or anoxic systems (Rusten et al., 2006). An illustration of movements of biofilm carriers is shown in Figure 1.1.

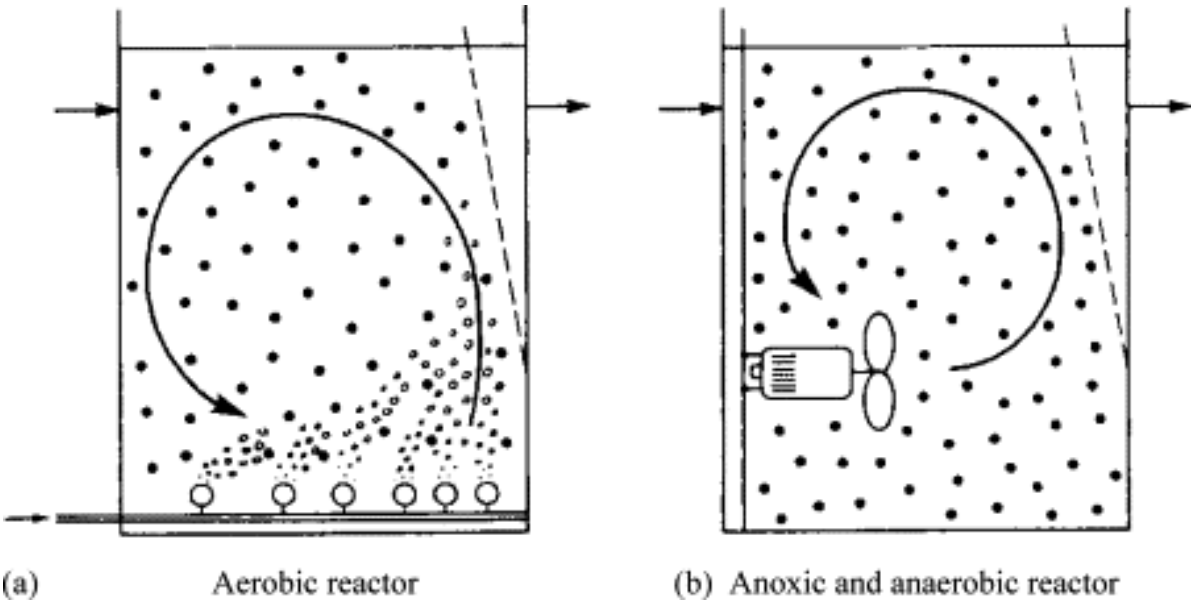

Figure 1.1 An illustration of MBBR technology by using aeration and a mixer for keeping the biofilm carriers in continuous movement in the reactor. The illustration is taken from Rusten et al. (2006)

The continuous movements of biofilm carriers from mixing and aeration create turbulence in the reactor. Turbulence contributes to transport substrates and oxygen into the biofilm, but also to limit the biofilm thickness. Too thick biofilm prevents diffusion of substrates into the biofilm and waste out from the biofilm. A thin biofilm is a key factor for optimal functioning of MBBR technology, since the penetration capabilities of substrates are usually limited in biofilms with a thickness over 100 µm. To avoid wash out of the biofilm carriers, a filter is located at the outlet of the reactor. Filling ratio (volume carrier/ volume reactor) should not exceed 70 % (Rusten et al., 2006). Neither backwashing of the biofilter or return of biomass are necessary in MBBR (Odegaard et al., 1994). The disadvantage of MBBR is the need of energy for continuously movement of the carriers (Rusten et al., 2006).

Biofilm carriers from AnoxKaldnes exist in different designs, shapes and sizes. The model K1 is often used in MBBR. K1 (Kaldnes carrier) has a cylindrical form, length of 7 mm, density of 0.95 g/cm^3 and a diameter of 10 mm. Biofilm carriers with and without biofilm growth are shown in Figure 1.2. The outside of the KI is covered by vertical ridges, while on the inside KI is divided into four identical chambers (Odegaard et al., 2000). The biofilm growth is significantly higher on the inside of the biofilm carrier, compared to the outside of the biofilm carrier, as the biofilm on the inside is more protected from external stress sources than biofilm on the outside. (Rusten et al., 2006).

.

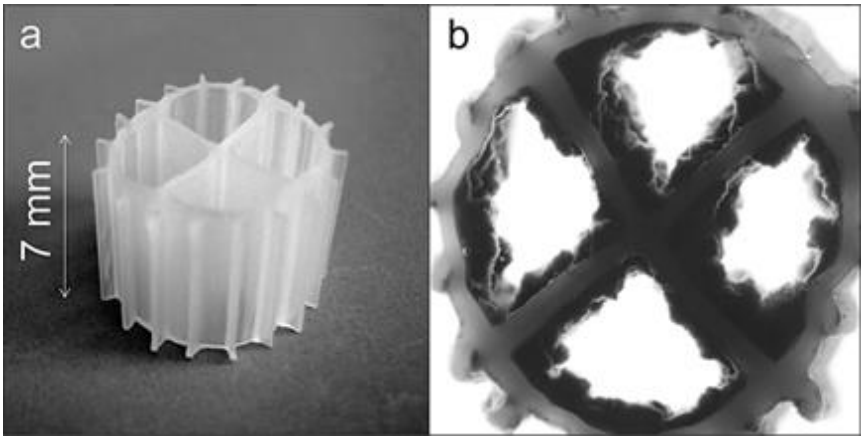

Figure 1. 2 K1 biofilm carrier with (b) and without (a) biofilm growth. The illustration is taken from Herrling et al. (2015)

1.6 Vestfjorden Avløpselskap wastewater treatment plant

Vestfjorden Avløpseskap (VEAS) wastewater treatment plant is an intermunicipal company for wastewater treatment for 600 000 citizens in Bærum, Oslo and Asker (VEAS, 2016). An illustration of the wastewater plant is shown in Figure 1.3. VEAS removes nitrogen from the wastewater by nitrification and denitrification. The wastewater reaches the nitrification step before the denitrification step. VEAS uses the BIOFOR (Biological Filtration and Oxygenated Reactor) system that consists of upstream bioreactors with stationary biofilters made from Leca (lightweight expanded clay aggregates) particles (Wien et al., 1995). The biofilm is growing on Leca particles (Mao et al., 2008). In the nitrification step, both air and wastewater arrive from the bottom of the reactors. Leca particles have, beside biofilm attachment, a mechanical filtration function for removal of suspended solids from the wastewater (Wien et al., 1995, Wien, 1995). Leca particles have a density of 1.24 g/mL and the diameter varies between 3-5 mm.

The BIOFOR process needs backwashing for proper functioning, since sludge and suspended solids will accumulate in the reactors over time (Wien, 1995). Every 14 hours, or more frequently, there is a need for an automatic backflush of the nitrification filters (Mao et al., 2008). The washing process creates wash water that is transported to the inlet of the plant for another round through the plant (Wien, 1995). Previous experiments have shown that there are high heterotrophic activity and high denitrification activity in the nitrification filters (Mao et al., 2008). There are 6 BIOFOR units with a medium volume of 800 L and with a medium depth

of 4,1 m that operate in parallel at VEAS (Wien, 1995). Ammonia concentration that reaches the biofilter varies between 0.5-2 mM. A considerable amount of organic carbon also reaches the nitrification filter and the total organic carbon (TOC) in the wastewater varies between 35-45 mg/L. Average flow (Q) is 160 L/s and average HRT is 25 min in the nitrification filters (Mao et al., 2008).

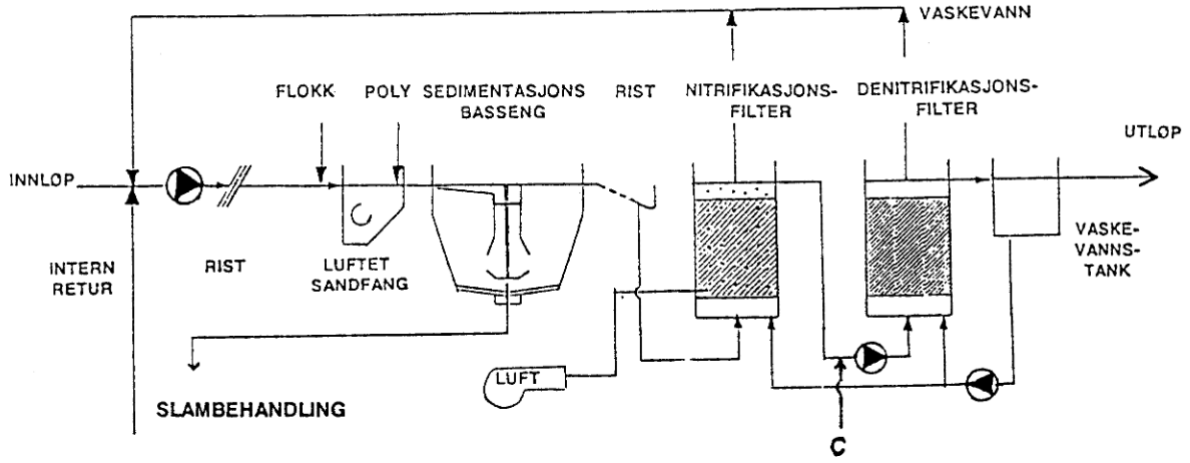

Figure 1.3 Illustration of wastewater treatment with nitrification and denitrification step at VEAS. The illustration is taken from Wien (1995).

2. Aim

The aim for this master thesis was to improve the knowledge about the competition between nitrifying and heterotrophic bacteria in order to improve ammonium removal efficiency and functionality. For this, two different biofilm systems used for nitrification were studied, MBBR and BIOFOR, but with the main focus being on the MBBR system.

The hypothesis behind the MBBR experiments at the Department of Biotechnology (NTNU) was that biofilm with long-term exposure to organic loading (C/N ratio 1) would have reduced nitrification robustness and nitrification efficiency because of increased competition with heterotrophic bacteria compared to biofilm without long-term exposure to organic loading (C/N ratio 0). Decreased nitrification robustness against changes in C/N ratio and organic loading would influence nitrification efficiency, oxygen consumption and microbial community compositions in the reactors. The following methods and experiments were used to investigate the hypothesis:

- Long-term and short-term organic carbon exposure experiments
- Organic carbon inhibition experiments
- Oxygen and organic carbon consumption experiments
- Microbial community structure characterization with DGGE

The hypothesis behind the nitrification biofilter experiment in the BIOFOR system at VEAS was that high amounts of heterotrophic bacteria exist in the outer layers of the biofilm and most of the nitrifying bacteria exist in the inner layers of the biofilm. An automatic washing process of the biofilters will therefore remove high amounts of heterotrophic bacteria from the outer layers of the biofilm and not all of the nitrifying bacteria in the inner layers of biofilm, which result in stable nitrification due to reduced competitions with heterotrophs. The following methods and experiments were done on washed and unwashed biofilter to investigate the hypothesis:

- Short-term batch experiments to investigate oxygen consumption and ammonia removal rate
- Microbial community structure characterization with DGGE

3. Materials and Methods

3.1 Principles behind core methods

Principles behind the two methods DGGE and flow cytometry are explained briefly in 3.1.1 and 3.1.2 respectively. DGGE was done for analysis of microbial community structure and flow cytometry was done for cell counting.

3.1.1 DGGE

Denaturing gradient gel electrophoresis (DGGE) is an electrophoresis technique often used for analysing variations in DNA content in microbial communities. DNA amplification by PCR is done before DGGE and the 16S rRNA gene from bacteria is used as primer (Green et al., 2010). The region V3 in the 16S rRNA gene is a highly variable region and nucleotide sequences from this region is often used in biodiversity analysis (Klammer et al., 2008, Ziembinska-Buczynska et al., 2014). The universal primers 338F-GC and 518R are primers for the region V3 in 16S rRNA in E.coli and are often used for PCR before analysis of bacterial communities by DGGE (Cocolin et al., 2001, Ceuppens et al., 2015).

In traditional agarose gel electrophoresis, DNA fragments are being separated based on the difference in fragment length as the fragments migrate through the gel to the positive anode (Lee et al., 2012). In DGGE, DNA fragments are separated based on difference in DNA sequence as fragments of similar length migrate through the gel (Green et al., 2010). The DGGE gel consists of polyacrylamide and has an increasing gradient of a denaturing agent which complete or partially denature double stranded DNA fragments to single stranded DNA fragments. Formamide and urea are commonly used as denaturing agents in DGGE. Double stranded DNA fragments with different nucleotide sequence are separated during the migration through the gel. The difference in the number of hydrogen bonds between the base pairs in the DNA fragments contributes to the separation. A DNA fragment with a high content of guanine-cytosine (GC) base pairs will migrate longer through the gel before denaturation than a DNA fragment with a high content of adenine-thymine (AT) base pairs, since GC bonds are stronger than AT bonds. DGGE is suitable for analysing multiple samples. After the electrophoresis is finish, selected DGGE bands may be cut out from the gel and further analysed by sequencing of 16S rRNA from the samples (Green et al., 2010).

The 338G-GC primer has a GC-clamp fastened at the 5`-end of the primer. GC-clamp is a DNA sequence consisting only of guanine-cytosine base pairs, typically between 30-50 base pairs long. Primers with GC-clamps transfer GC rich sequence to DNA fragments during PCR. The result is PCR fragments with greater ability to resist complete denaturation under increasing concentration of formamide and urea. A GC-clamp contributes to incomplete denaturation of double stranded DNA. The GC-clamp is therefore important for separation of bands and formation of the band pattern on the DGGE gel (Sun et al., 2015).

3.1.2 Flow cytometry

Flow cytometer (FCM) is an analytical instrument used to analysing samples containing a high number of cells. Typical microbiological applications are cell counting and DNA analyses (Picot et al., 2012). Flow cytometry uses hydrodynamic focusing to individually analyse single cells. The cells need to be in a working solution before injection into the sheat solution inside the flow cytometer (Picot et al., 2012). The DNA content in the cells are stained by a fluorescent dye before the analysis (Darzynkiewicz et al., 2010).

The principle behind hydrodynamic focusing is pressure difference between a sheat solution with high flow rate and a working solution with slow flow rate (Austin Suthanthiraraj and Graves, 2013, Kachel et al., 1990). The cells in a working solution are forced by the sheat solution to migrate towards the centre of the flow channel and further inside a narrow channel. From passing as a bunch of cells, the cells are forced to pass one by one in the centre of a narrow flow channel. Excitation wavelengths from one or more lasers hit the cells one by one. Emissions from stained the cells and scattered light are detected consecutively. The light signals are translated and analysed by a software program (Picot et al., 2012).

3.2 Medium composition

The medium used for all biofilm experiments, including experiments at VEAS, was made from macronutrients, micronutrients (stock solution) and MQ-water (Reagent water system, Millipore Corporation, France). The ammonium concentration in the medium was 100 mg/L NH_4^+-N. The amounts of macronutrients used in 1 L medium were 1.00 g $NaHCO_3$, 0.47 g $(NH_4)_2SO_4$ and 0.40 g K_2HPO_4. In the short-term organic carbon inhibition experiments (section

4.2.1), the ammonium concentration in the medium was halved from 100 mg/L NH_4^+-N to 50 mg/L NH_4^+-N, and 0.236 g/L $(NH_4)_2SO_4$ was added.

C/N ratios were calculated from mole ratios ($C_2H_3NaO_2$-C to NH_4^+-N mole ratio). For C/N ratio 1, 0.293 g/L C_2H_3NaO was added. For C/N ratio 3, 0.878 g/L $C_2H_3NaO_2$ was added. 10 mL of stock solution was added per 1 L of medium. The amounts of micronutrients in 10 mL stock solution were 2.5 g MgSO4-7H_2O, 1.5 g $CaCl_2$-2H_2O, 0.2 g $FeCl_2$-4H_2O, 0.55 g $MnCl_2$-4H_2O, 0.068 g $ZnCl_2$, 0.12 g CoCl-6H_2O, 0.12 g $NiCl_2$-6H_2O and 2.8 g EDTA.

3.3 Experimental set-ups for continuous and batch moving bed biofilm reactors

Experiments in lab scale moving bed biofilm reactors (MBBR) were done at Department of Biotechnology (NTNU). MBBR experiments were divided into long-term experiments (continuous experiments) and short-term experiments. In the long-term experiment, two MBBR with different C/N ratio were operated continuously. The reactors will from this point be referred to as reactor 1 (R1) and reactor 2 (R2). A schematic overview over the experimental design is shown in Figure 3.1. The short-term experiments were performed in two different ways; Biofilm carriers were either removed from the continuous operating reactors and transferred to batch reactors, or the conditions were changed in the long-term reactors and the consequences of the changes were measured for a limited period.

The MBBR experiments were conducted in two jacketed glass reactors (Schott Duran, Germany) with volume 0.7 L in the first period and 0.6 L in the second period. Biofilm plastic carriers (AnoxKaldnes, type K1) were added to a 50 % filling ratio (volume carriers/volume reactor). Biofilm carriers used in the experiments were given from two nitrification MBBR used in Environmental Biotechnology (TBT4130) lab course spring 2016. The biofilm carriers were in 1 month fed with a medium containing 50 mg/L NH_4^+-N (C/N ratio 0, HRT = 12 hours) in the lab course.

Poly Stat circulating water bath (Cole Parmer, USA) was used as temperature control in reactor 1, while VWR circulating water bath (VWR International, USA) was used for temperature control in reactor 2. The water baths were set to 25^{o}C and connected to the jacketed glass reactors. Silicone stoppers with 8 holes (various diameter) were used as covers. Two separate

pH controllers (Bluelab Corporation Ltd., New Zealand) for acid and base were used to regulate the pH. pH was set to 7.4 and pH probes were connected to the reactors through the silicone stopper. 0.5 M HCl and 0.5 M NaOH were used for automatically pH adjustment.

Aeration in the reactors was maintained by compressed air and an air stone. The oxygen concentration was measured by an oxygen electrode (Oxi 3351, WTW, Germany) or a Micro Fiber Optic Trace Oxygen Transmitter (PreSens, Regensburg, Germany). A magnetic stirrer and magnet were used for mixing of the medium and the biofilm carriers. Magnetic stirring was set to 300 rpm. The medium was kept in a 10 L or 20 L polypropylene autoclavable carboy with a 3 inlets polypropylene cap (Thermo Fisher Scientific, USA). A 0.2 μm membrane filter for avoiding vacuum and a silicone tubing (8 mm in diameter, VWR) for medium supply were connected to the cap. The medium (inlet) was pumped to the reactors by using Masterflex easy load L/S pump (Cole Parmer Instrument Company, USA). The glass reactors were covered by aluminium foil for avoiding light into the reactors. The outlet was transported from the reactors to a 25 L waste container by a silicon tubing (25 mm in diameter, VWR). The short-term batch experiments were carried out with the same equipment as the long-term experiments except with the medium pump off, unless otherwise is stated in the text.

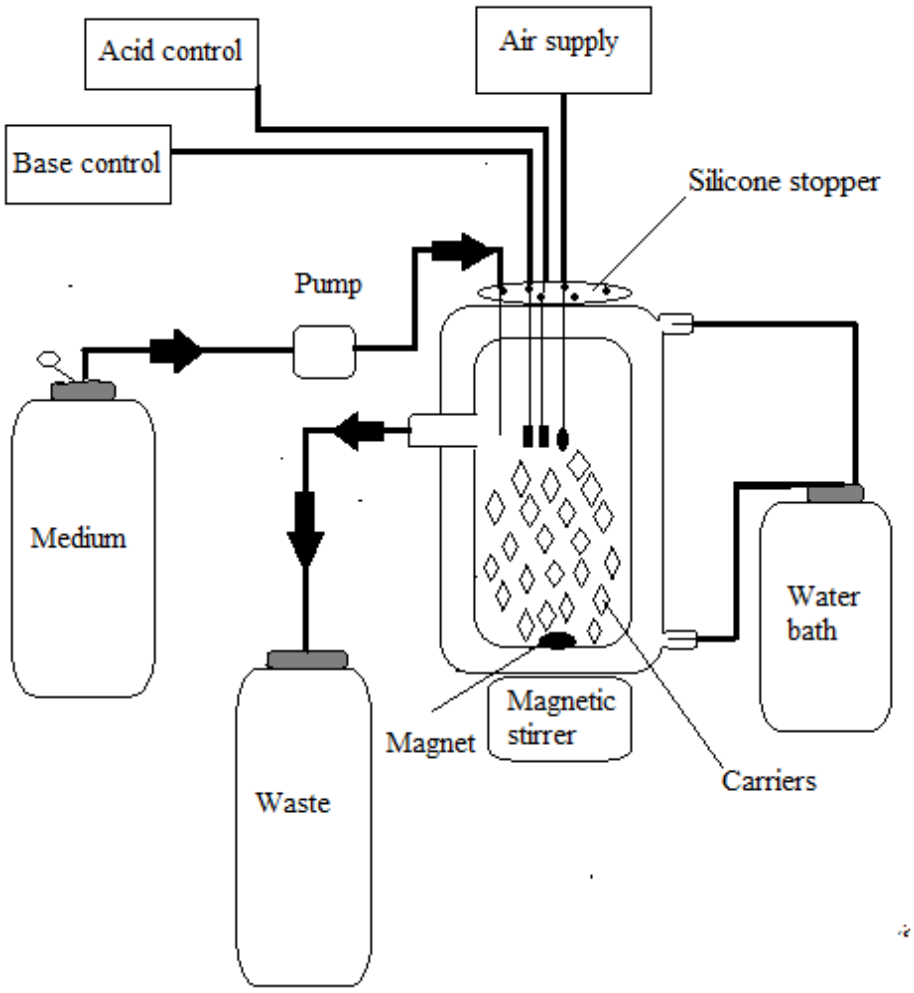

Figure 3.1 Illustration of a continuous MBBR reactor used in the long-term experiments.

3.3.1 Long-term experiments in MBBR.

The difference in nitrification activity and thus ammonium removal efficiency after long-term exposure to different C/N ratios were investigated in two nitrification MBBR. Experimental set-ups were identical between the reactors, but medium compositions were different. Biofilm carriers in reactor 1 (R1) were continuous fed with medium containing sodium acetate as carbon source (C/N ratio 1). Biofilm carries in reactor 2 (R2) were continuous fed with medium without an organic carbon source (C/N ratio 0). In the final parts of the long-term experiments medium composition were identical in both reactors.

Long-term MBBR experiments were running during two time periods. The first period (1. period) was March 2016-Mai 2016 (37 days) and the second period (2. period) was September 2016- February 2017 (152 days). During the summer, the biofilm carriers were stored in a freezer (-20ºC).

In the whole first period and in the second period until day 139, the hydraulic retention time (HRT) was 13 hours for both reactors. In reactor 1, the C/N ratio was 1 in the first period and 1 in the second period until day 130. In reactor 2, the C/N ratio was 0 in the first period and 0 in the second period until day 130. For both reactors, the C/N ratio was increased to 3 at day 131 in the second period. On day 139 in the second period, the loading rate to the biofilms was increased by lowering the HRT to 6.5 hours (i.e. flow rate increased) in both the reactors. The changes in C/N ratio and loading rate to the long-term continuous experiments were named perturbations experiments and are explained further in section 3.3.6. The level of ammonium, nitrite and nitrate were measured every 2-4 days (with few exceptions).
Acetate and oxygen concentrations were measured in selected periods. A schematic overview over experimental design is shown in Figure 3.2.

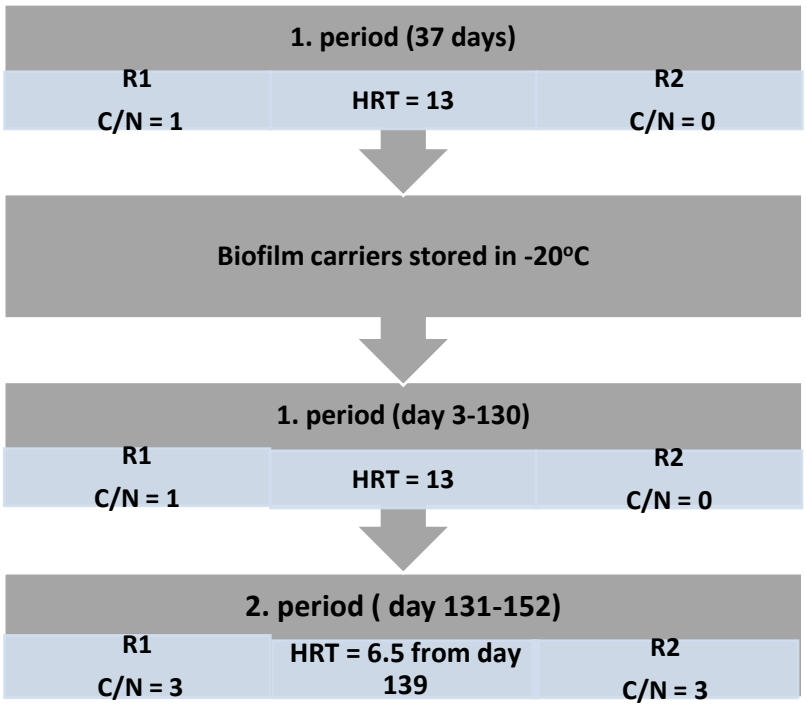

Figure 3.2: Schematic overview of experimental variables for reactor 1 (R1) and reactor 2 (R2). HRT (hours) was the same in both reactors in both periods.

Biofilm carriers from long-term continuous experiments were sampled in the first period at day 17, 30, and 37. In the second period, biofilm carries were sampled at day 1,3 43, 55, 95, 104, 118, 125, 127, 130, 137, 145, 148 and 152. Overview of carriers and water samples and short-term experiments are shown in Figure 3.3.

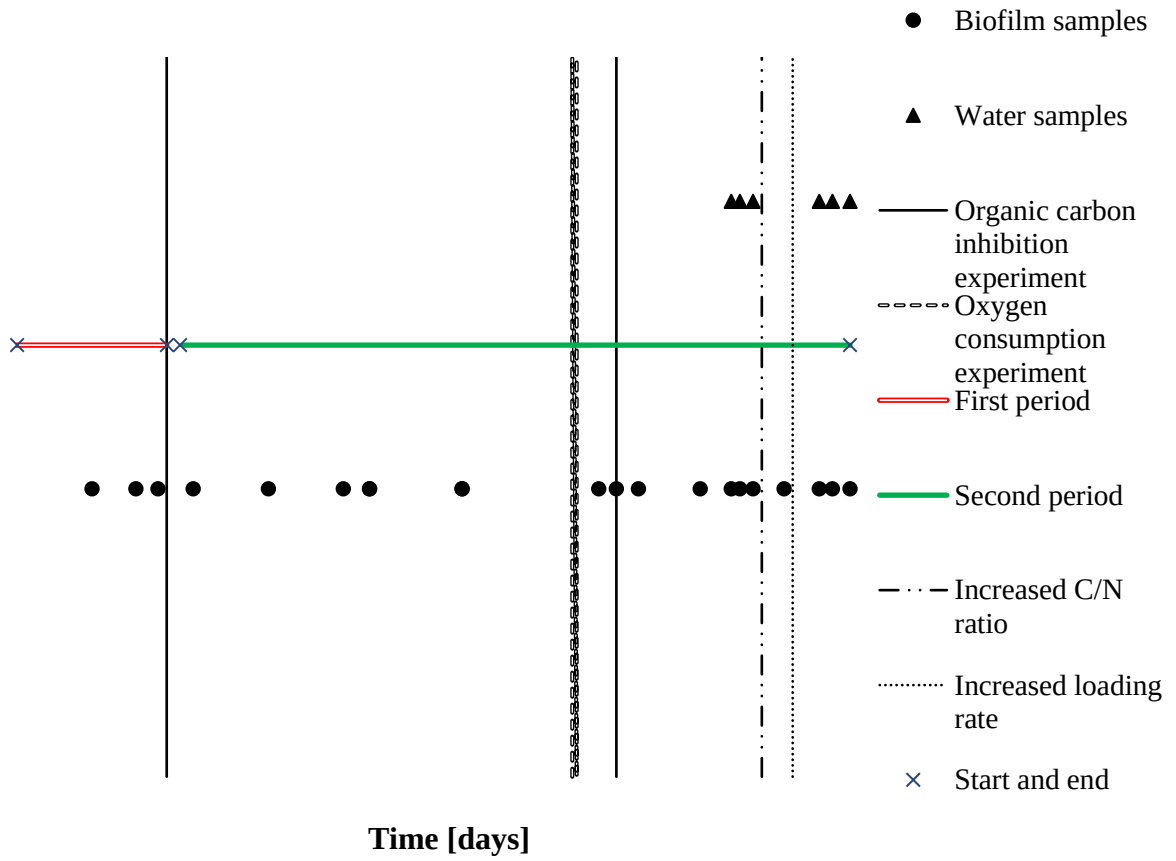

Figure 3.3 Overview of the biofilm carriers and water samples, experimental conditions and short-term experiments. Short-term organic carbon inhibition experiments were conducted at day 37 in the first period and at day 99 in the second period. Short-term oxygen consumption experiments were conducted at day 89-91 in the second period. The C/N ratio was increased at day 131 in the second period and the loading rate (increased flow) was increased at day 139 in the second period.

3.3.2 Short-term organic carbon inhibition experiments

Short-term organic carbon inhibition experiments were carried out in two MBBR in batch mode. The objective of the experiments was to investigate whether there was any difference in nitrification activity, and thus nitrification robustness, towards increasing the concentration of organic carbon between the biofilm carriers in the reactors operating in long-term continuous experiments. The biofilm carriers in reactor 1 had been continuously fed with medium containing acetate as the carbon source ($C_2H_3NaO_2$). Biofilm carriers in reactor 2 had been fed

with medium without an organic carbon source. 100 mL of carriers were removed from the long-term MBBR reactors and transferred to two batch reactors at day 37 in the first period and day 99 in the second period. Both experiments were conducted with aeration, temperature control and magnetic stirring as in the long-term experiments.

Acetate concentrations in ascending order used at day 37 in the first period were: 0 mM, 3.16 mM, 10 mM, 31.6 mM and 100 mM. At day 99 in the second period the acetate concentrations used in ascending order were: 0 mM, 10 mM, 31.6 mM, 100 mM, 316 mM and 1000 mM. The experiments started with 500 mL medium containing 0 mM. Each concentration was monitored every 30 minutes for 3 hours before replaced by a higher concentration of acetate. The programme REGTOX: macro Excel dose-response modelling (Vindimian, 2003) was used for modelling the results of increasing acetate concentrations effect on nitrification activity (dose-response).

3.3.3 Short-term oxygen consumption experiments

Short term oxygen consumption experiments were carried out in two MBBR in batch mode on days 89- 90 in the second period to determine whether there were any differences in the oxygen consumption rate between the biofilm from reactor 1 and reactor 2. Biofilm carriers in reactor 1 had continuously been fed with medium containing sodium acetate as carbon source (C/N ratio 1). Reactor 2 had been fed with a medium without an organic carbon source (C/N ratio 0). 100 mL biofilm carriers were taken out from the long-term MBBR reactors on day 89-90 in the second period and transferred to two MBBR batch reactors containing 500 mL medium. The first experiment was conducted without carbon source in the medium (C/N ratio 0). The second experiment was conducted with acetate as the carbon source in the medium (C/N ratio 1). The experiments were conducted with temperature control and magnetic stirring as in long-term experiments. The amount of dissolved oxygen in the reactors was measured by Micro Fiber Optic Trace Oxygen Transmitter (PreSens, Regensburg, Germany). Oxygen concentration was measured every 5 minutes for 6 hours. For control, the ammonium concentration was measured every 60 minutes for 6 hours for the first batch experiment (C/N ratio 0) and for 5 hours for the second experiment (C/N ratio 1).

3.3.4 Perturbations experiments: increased C/N ratio and increased organic loading to the continuous reactors

The C/N ratio was increased to 3 on day 131 in the second period in both the continuous reactors to investigate the response to increased supply of organic carbon for the continuous reactors. The experiment was carried out in the original long-term glass reactors and the new C/N ratio was kept throughout the second period (days 139-152) in both the reactors. 1 L of the new medium (C/N ratio 3) was pumped into two glass beakers in advance. When the experiment started, the liquid in the reactors was replaced by the new medium (C/N ratio 3) in the glass beakers. The idea behind this was to attain an accurate starting point for the new C/N ratio. The ammonium, nitrite, nitrate, organic carbon and oxygen concentrations were measured every 60 minutes for 9 hours. The organic carbon and oxygen concentrations were again measured 24 hours after the beginning of the experiment.

The loading rate was increased (doubled flow rate) at day 139 in the second period to investigate if there were any differences in the responses to increased loading rate between the continuous reactors. The HRT was decreased from 13 to 6.5 hours. The experiment was carried out in the original long-term glass reactors and new loading rate was kept throughout the second period (days 139-152). The ammonium, nitrite, nitrate and oxygen concentration were measured every 60 minutes for 8 hours. The concentration of organic carbon was measured every 60 minutes for 4 hours. The ammonium, nitrite, nitrate, and oxygen concentrations were again measured 24 hours after the beginning of the experiment.

3.4 Experimental set-up from VEAS wastewater treatment plant

A short-term batch experiment and sampling for microbial analysis were performed at Vestfjorden Avløpselskap wastewater treatment plant (VEAS) in Asker to investigate the competition between heterotrophic bacteria and nitrifying bacteria. The hypothesis behind the experiments and analysis was that high amounts of heterotrophic bacteria exist in the outer layers of the biofilm, while most of the nitrifiers exist in the inner layers of the biofilm. An automatic washing process of Leca biofilters will therefore remove high amounts of heterotrophic bacteria, while most of the nitrifiers will remain in the biofilm.

3.4.1 Sampling for microbial analysis

Samples to microbial analysis were taken before and after a washing process in various nitrification filters (NF) at VEAS. Samples were taken with a long stick (8 m) with a small samplings box at the end, by employees at VEAS. Samples from unwashed biofilters were taken before the washing process started and as long as possible after the last wash. Samples from washed biofilters and wash water were taken quickly after the washing process was finished. Samples were rinsed gently with water and stored in a freezer (-20^{o}C). Water samples (wash water) were taken from the top of the nitrification filters at the end of the washing process and stored in a freezer (-20^{o}C). A cooling bag with cooling elements was used to transport the samples from VEAS to NTNU, where the samples were put in a freezer and subsequently analysed.

3.4.2 Short term batch experiments with Leca

Leca from unwashed and washed filters was rinsed gently and transferred to two 1 L beakers. Leca was added to a 15 % filling ratio (volume Leca/volume beaker). The nitrogen concentration in the medium was 100 mg/L NH_4^+-N, while the C/N ratio was 1. A magnetic stirrer was used for stirring. In addition, manual stirring of Leca was performed with a spoon before each sampling. For temperature control, a 10 L bucket was filled with 5 L water (15^{o}C) and used as a water bath. Water samples for oxygen measurements were taken every 10 minutes and were put back into the batch after each measurement. The oxygen concentration was measured with a self-stirring dissolved oxygen sensor (StirrOx, WTW). Samples for ammonia, nitrite and nitrate analyses were taken every 15 minutes. The average temperature in the nitrification filters during sampling and the batch experiments was 14.8^{o}C. In the sampling period, the average total organ carbon (TOC) in the wastewater that reached the filters was 25.6 mg/L, while the average total Kjeldahl nitrogen (TKN) was 27.7 mg N/L.

3.5 Analytical methods

Water samples from the MBBR at the Department of Biotechnology (NTNU) and wash water from the nitrification filters at VEAS in Asker were taken with a 10 mL syringe (Soft-Ject, Henke sass wolf, Germany). The water samples were filtered by a 0.45 μm polyethersulfone membrane syringe filter (VWR International, USA) and transferred to 5 mL glass beaker before further chemical analysis.

3.5.1 Spectrophotometer

For chemical analysis of the water samples, a DR 3900 Benchtop VIS spectrophotometer and a DR 2800 Portable spectrophotometer were used at the Department of Biotechnology (NTNU) and at VEAS in Asker, respectively. The wavelength resolution was 1 nm in both spectrophotometers. Calibration of wavelengths and wavelengths selection was performed automatically by the instruments. Each cuvette had a label (LCK xxx) and was marked with a barcode for quick detection of correct analysis programme and measurement. Only original cuvettes from Hach Lange kit were used for analysis. When the nitrogen concentration in the water sample exceeded the concentration range in the Hach Lange kits, the samples were diluted with MQ-water.

3.5.2 Analysis of inorganic nitrogen compounds

The concentration of ammonium, nitrite and nitrate in the water samples were analysed with Hach Lange kits of high and low concentration range as the concentration varied in the medium and in the reactors (Table 3.1). For ammonium and nitrite analyses, the filtered sample was added to the cuvette and the DosiCap (cuvette cap with powder) was turned upside-down and tightened before the cuvette was shaken repeatedly. For nitrate analysis, the filtered sample and an extra solution (A LCK 339 or A LCK 340) were added to the cuvette before the cuvette was inverted several times. After incubation in a specific period of time, the cuvettes were analysed in the spectrophotometer (Table 3.1).

Ammonium (NH_4^+) and ammonia (NH_3) exist in an equilibrium ($NH_3 \leftrightarrow NH_4^+$), and are therefore often calculated and named as one compound: total ammonia nitrogen (TAN). In pH 7.4, the largest part of TAN is ammonium, which is why the term ammonium is used further in this thesis.

Table 3.1 Detailed information about Hach Lange kit cuvettes

Label	Test for	Range (mg/L)	Sample added (mL)	Extra solution (mL)	Mixing method	Incubation time (min)
LCK 304	NH_4^+-N	0.015-2.0	5	No	Shake	15
LCK 303	NH_4^+-N	2-47	0.2	No	Shake	15
LCK 341	NO_2^-- N	0.05-0.6	2	No	Shake	10
LCK 342	NO_2^-- N	0.6-6.0	0.2	No	Shake	10
LCK 339	NO_3^-- N	0.23-13.5	0.2	A LCK 339	Invert	15
LCK 340	NO_3^-- N	5-35	0.2	A LCK 340	Invert	15

3.5.3 Organic carbon analysis

The concentration of organic acids was measured by an organic acids kit (LCK 365) containing cuvettes and 4 extra solutions (A, B, C & D). The concentration range of the organic acids kit was 50-2500 mg/L for CH_3COOH and 75-3600 mg/L for C_3H_7COOH. 0.4 mL of solution A and 0.4 mL of the water sample were added to the cuvette. The cuvette was inverted repeatedly and heated in a dry block heater (Grant QBD2, Grant Instruments, Cambridge, UK) at 100°C for 10 minutes. The cuvette was cooled down to room temperature (18-22°C) before 0.4 mL of solution B, 0.4 mL of solution C and 2 mL of solution D were added to the cuvette. The cuvette was inverted repeatedly between every addition of liquid. After incubation (3 minutes), the cuvette was analysed by the spectrophotometer. Acetic acid (CH_3COOH) exist in an equilibrium with acetate (CH_3COO^-). The term acetate is used further in this thesis.

3.5.4 Flow cytometry

The number of cells in the water samples from the MBBR were investigated in a flow cytometer. Water samples from reactor 1 and reactor 2 were taken on days 125, 127, 130, 137, 145, 148 and 152 in the second period. The water samples from day 137, 144, 147 and 150 were taken after the C/N ratio had been increased in both reactors, and for the water samples from day 144, 147 and 150 the loading rate (decreased HRT) had been increased in both reactors as well. The samples were fixated shortly (max 30 minutes) after sampling. 990 µL sample and 10 µL Glutaraldehyde (50% in H_2O) were added to 2 mL polypropylene Cryo.S cryogenic tubes (Greiner Bio-One, Frickenhausen, Germany) and gently mixed with a minishaker. Samples were defrosted, mixed with a minishaker and diluted (1:10 or 1:100) with 0.1x TE-buffer (Appendix E) to a final volume of 1 mL in flow cytometer plastic tubes. 10000x concentrate of SYBR green I nucleic acid stain (Life technologies, USA) in DMSO was diluted 1:50 with 0.1x TE-buffer. 10 µL of the diluted stain solution was added to each sample. The samples were mixed with a minishaker and incubated for 15 minutes in the dark.

Cell counts were conducted on a BD Accuri C6 flow cytometer (BD Biosciences, San Jose). The flow rate was controlled by measuring the weight of 2 mL MQ-water in a cytometer tube before and after a 5 minutes run with a medium flow rate (35 µL/min). The deviation in the measured flow rate was less than 3 % from the stated flow rate (35 µL/min). Every sample was run with medium flow rate (35 µL/min) in 3 minutes. An analysis program with automatically run of samples, shaking of test tubes and washing of the test needle between every sample was

chosen. Excitation wavelengths of 488 nm were sent out by a Solid State Blue laser. Green fluorescence emission within 533 nm from stained bacteria was detected by a optical filter (FL1). SYBR green I nucleic acid stain has excitation maximum at 497 nm and an emission peak around 520 nm (ThermoFisher). The threshold for detecting events/cells was set to 2000 µg/sec. Samples with > 1000 countings/µL were reanalysed with a new dilution.

BD Accuri C6 software (Accuri Cytometer, Version 1.0.264.21) was used for analysing the results. Signals detected from FL1 (optical filter) were plotted against forward scattered lights (FSA) by the software. FSA are correlated to cell size (Shapiro, 2003). Global gating was used to investigate the specific areas of interests in every plot. Detected emission under 10^{-4} was removed from the results. The results were transferred and further processed in Microsoft Excel.

3.6 Microbiological community analysis

Biofilm carriers from MBBR and Leca particles from VEAS were taken for microbial analyses. All microbial community analyses were conducted at Department of Biotechnology (NTNU).

3.6.1 DNA extraction

The biofilm carriers were cut into 4 pieces by a scalpel, while the Leca particles were crushed to smaller pieces by a ceramic mortar. The water samples were transferred to 50 mL syringes (Soft-Ject, Henke sass wolf, Germany) and filtered with a 0.2 µm syringe tip filter (DynaGard, Spectrum Laboratories, Inc., Rancho Dominguez) before DNA extraction. DNA was isolated by Power Soil DNA kit (Mo Bio Laboratories, Inc., Carlsbar). The DNA kit used chemical and mechanical separation techniques for extraction of DNA, and PowerBEAD tubes for cell lysis and homogenization of the samples. In several washing steps, organic and inorganic substances were separated from the DNA. The DNA got attached to a silica filter under high salt concentration in a spin column, while impurities in several steps flowed through. In the last step, water was added and DNA was released from the silica filter. Isolated DNA samples were frozen (-20^{o}C) in collection tubes. The protocol for DNA isolation kit is presented in Appendix B.

3.6.2 PCR

Extracted DNA from microbial samples were amplified with polymerase chain reactions (PCR) (T100 Thermal Cycler, BIO-RAD, USA). PCR master mix used for DNA amplification was prepared from 2.5 µL key buffer (10x, VWR), 0.5 µL dNTP mix (10 mM), 0.5 µL MgCl (25 mM, VWR), 0.75 µL Bovine Serum Albumin (BSA) (20 mg/L, BioLabs), 0.125 µL Taq DNA Polymerase (VWR), 18.125 µL filtered MQ-water, 0.75 µL 338F-gc primer (100 µm, Sigma) and 0.75 µL 518R primer (100 µL, Sigma). The primer sequences are shown in Table 3.3.

Taq DNA Polymerase was added as the last component in the master mix to avoid degradation of the enzyme, and the master mix was mixed with a minishaker. The PCR tubes were placed on a PCR cooling block (Eppendorf, Sigma-Aldrich) and 24 µL of the master mix was added to each of the PCR tubes. Extracted DNA from microbial samples (DNA templates) were defrosted in room temperature and mixed with a minishaker. 1µL of each microbial sample (DNA template) was added to each PCR tube. The PCR tubes (total concentration of 25 µL) were again mixed with a minishaker. A negative control (without DNA template) was used for discovering potential contaminations in the components used in the master mix. The programme (cycle sequence) for PCR is shown in Table 3.2. The denaturation, annealing and elongation step (marked in Table 3.2) were repeated in 35 cycles in the PCR programme. The PCR products were stored at 4^{o}C before further analysis.

The result of the DNA amplification (the PCR products) were investigated by agarose gel electrophoresis. 5 µL PCR products were mixed with 1 µL DNA Loading dye (6x,Thermo scientific) before the PCR products were loaded into the wells on the agarose gel. 3 µL 1 kb Plus DNA ladder (0.5 µg/µL, Thermo Scientific) was used to approximately determine the size of the different DNA fragments on the gel. The DNA fragments were run on the agarose gel in 140 volts for 45 minutes in 1xTAE (Tris-acetate-EDTA) buffer. Pictures were taken of the agarose gels in UV light (G:box, Syngene, Cambridge) by GeneSnap (SynGene, Cambridge).

1xTAE buffer was made from 40 mL 50xTAE buffer (Appendix C) and 1960 mL MQ-water. Agarose gel solution was made from 4 g agarose and 400 mL 1xTAE buffer heated to boiling point in a microwave. Solution was cooled to 65^{o}C before 20 µL Gel Red (10000x in water, Biotium, Hayward) gel staining for nucleic acid was added. The agarose gel solution was stored in a heating cabinet at 65^{o}C.

Table 3. 2 Programme for PCR run on Thermal cycler

Step	Temperature [°C]	Time[min]	Cycles [numbers]
Pre-warming	95	∞	
Denaturation	95	3	
Denaturation	95	0.5	
Annealing	50	0.5	35
Elongation	72	1	
Elongation	72	30	
Cooling	10	∞	

Table 3.3 Primer sequences used in PCR

Primer	Sequences
338F-GC	5'-cgcccgccgcgcgcggcgggcggggcgggggcacgggggg actcctacgggaggcagcag-3'
518R	5'-attaccgcggctgctgg-3'

3.6.3 DGGE

Denaturing gradient gel electrophoresis (DGGE) for analysing microbial communities from PCR products was performed with the PhorU2 DGGE system (Ingeny, Netherlands). All the equipment used for DGGE was from the PhorU2 system, unless stated otherwise in the text.
0 % and 80 % denaturing acrylamide solutions (Appendix C) were used to create a denaturation gradient. The denaturing gradient gel was made from distribution of the three solutions: low denaturing solution (35 % denaturing), high denaturing solution (55% or 60 %) and stacking gel solutions (0 % denaturing) between two glass plates. The contents of the three solutions are shown in Table 3.4. 80 % denaturing solution was filtered with a 0.45 μL polyethersulfone membrane syringe filter (VWR International, USA). TEMED (Sigma-Aldrich) was added as the last component of the three solutions to avoid premature polymerization, since a mix of ammonium persulfate (APS, Appendix C) and Tetramethylenediamine (TEMED) in acrylamide solutions immediately starts polymerization of the solutions.

The denaturing gradient gel was made between two cleaned glass plates fastened with a spacer inside a gel box. A comb (48 wells) was placed between the glass plates for the wells formation. A syringe connected to a plastic hose was also placed between the glass plates for distribution of the gel solutions. High denaturing gel solution (55 % or 60 %) was pumped first between the glass plates for highest denaturing percent at the end of the gel. Low and high denaturing solutions were mixed and pumped inside the glass plates. Stacking gel was pumped as the last

solution inside the glass plates for formation of 0 % denaturing in the wells (at the beginning of the gel). The gel stood 2 hours in the fume hood for polymerization. The comb was removed and the spacer was pushed completely down after the gel was polymerized.

The gel box was immersed in a water bath (60ºC) with 17 L 0.5x TAE-buffer (Appendix C). The voltage was set to 100 V. A recirculation function was turned on for 5 minutes, while the PCR samples were mixed with a shaker. The wells were stained with loading dye to investigate the quality of the wells. A mixture of 5 µL loading dye and 4 or 5 µL PCR sample were added to each well. 5 µL DGGE ladder was used as standard and for separating sets of samples. The six outermost wells on both sides of the gel were not used because of a high risk for a smiling effect at the outer edges of the gel. The high voltage function was turned on. The recirculation function was turned on after 10 minutes. The ampere was checked. Large deviations from 27-32 mA indicated problems with equipment, buffer solution or current flow through the gel. The gel was running vertically for 22 hours.

Table 3.4 Solutions used for making denaturing gradient gel.

Solution	**0 % denaturing acrylamide solution [mL]**	**80 % denaturing acrylamide solution [mL]**	**APS [µL]**	**TEMED [µL]**
35 %	13.5	9.5	87	16
55 %	9.5	13.5	87	16
60 %	6	18	87	16
Stacking gel	8	-	40	10

After 22 hours, the gel box was removed from the water bath. The gel was released from the glass plates and transferred to a plastic sheet. A gel staining solution containing 3 µL SYBR Gold (Invitrogen), 600 µL 50x TAE-buffer and 30 mL MQ-water was distributed over the gel. An opaque plastic box was placed over the gel for 1 hour, and every 15 minutes the gel was gently shaken for achieving a more even distribution of the staining solution. Excess staining solution was removed with MQ-water after 1 hour. The gel was transferred to a UV plate. Pictures were taken of the DGGE gels in UV light (G:BOX,Syngene, Cambridge) using the programme GeneSnap (SynGene, Cambridge).

3.7 Analysis of DGGE data

The DGGE images were cropped, reduced from 16-bit to 8-bit and converted to tiff-files in the ImageJ 1.51j8 software (Rasband, 1997-2012). The band patterns on the DGGE images were analysed in the Gel2K software (Norland, 2004). Gel2K transformed fluorescence strength in one lane into densitometric curves, where peaks correspond to the DGGE bands in each sample. Fluorescence signals from the bands matched the area of each peak. Bands with similar migration lengths were sorted by the program and were manually put into different band groups. This resulted in a sample/peak area matrix, which was exported and further processed in Microsoft Excel. The peak areas were normalized by calculating the fractional peak area for each peak in a sample. This normalization was done by dividing individual (n_i) peak areas by the sum area of all the peaks ($\sum n_i$) in the same lane/sample (Equation 3.1). Diversity analysis and calculations on the values obtained from band patterns in Gel2K were done using the PAST 3.14 software (Hammer et al., 2001).

$$p_i = \frac{n_i}{\sum n_i} \quad (3.1)$$

Analyses of diversity of bacterial community data from the DGGE data were performed to explore similarities and differences in microbial communities in the biofilms and the water samples from MBBR and BIOFOR. Biological diversity can be divided between alpha- and beta-diversity. Alpha-diversity describes the diversity in one sample while beta-diversity describe the diversity between different samples (Whittaker, 1960, Rosenzweig, 1995). Species richness (K), species evenness (J`), Shannon diversity index (H`) describe alpha-diversities. Bray-Curtis and Jaccard similarities/dissimilarities can be used to describe beta-diversities (Pepper et al., 2015).

Species richness (S`) or band richness (K`) is the number of species in a sample or the number of bands in each lane on the DGGE gel. Species evenness (J`) describe the distribution of the number of species in a sample (Pepper et al., 2015, Shannon and Weaver, 1949). Species evenness ($E^{H/S}$) is calculated by dividing the Shannon diversity index on the number of species (bands) (Peet, 1975). Shannon diversity index (H`) describes the diversity in a community by considering both species richness and species evenness. High Shannon index indicates a community with high species richness and high species evenness (Shannon and Weaver, 1949).

The Shannon index in each sample was calculated by Equation 3.3 where p_i is the fractional peak area from each band on the DGGE gel (Pepper et al., 2015, Shannon and Weaver, 1949).

$$J` = e^{H`}/K` \quad (3.2)$$

$$H` = -\Sigma\, piln(pi) \quad (3.3)$$

Bray Curtis similarity describes the difference between two samples (Bray and Curtis, 1957). Bray Curtis similarities between the samples were visualized by Principle coordinate analysis (PCoA) in an ordination scatter plot based on a distance/similarity matrix. Multidimensional scaling (MDS) is another name for PCoA. PCoA gives eigenvalues (coordinates) and their associated percentage of variance explained of the distance/similarity matrix. (Anderson, 2005, Davis, 1986, Podani and Miklos, 2002).

One-way PERMANOVA or Non-Parametric MANOVA tests were performed to test whether the differences between groups in Bray Curtis similarities were significant (Anderson, 2001). p-values under 0.005 were considered to be significant (Hammer et al., 2001). One-way PERMANOVA test based on Jaccard similarity were also performed in PAST. Jaccard index describes the similarity between two samples or communities by the absence and presence of species. The index is calculated by dividing the number of shared species between two samples by the sum of species in both communities (Equation 3.4). The Jaccard index is between 0 (no common species) and 1 (only shared species) (Pepper et al., 2015, Jaccard, 1908).

$$J(A,B) = \frac{|A \cap B|}{|A \cup B|} \quad (3.4)$$

The difference between Bray Curtis similarity and Jaccard similarity is that Jaccard similarity is based on absence/presence of species, while Bray Curtis similarity also includes the abundance of species. For example, two microbial communities can have the same species present (high Jaccard), but with different dominance of species (different Bray Curtis) (Bray and Curtis, 1957, Jaccard, 1908).

Species richness (K), Busaz and Gibson`s species evenness (J`), and Shannon diversity index (H`) were calculated for each sample in PAST. One-way PERMANOVA tests based on Bray

Curtis or Jaccard similarities were performed in PAST to test if there were statistically significant differences in community structure and composition between groups of samples.

4. Results

4.1 Long-term MBBR experiments

The objective of the long-term experiments in the first and the second period was to investigate the differences in nitrification activity and thus ammonium removal efficiency between biofilm carriers operating with different C/N ratios. Adaption and response to changes as increased C/N ratio and increased organic loading were also investigated (perturbations experiments). Reactor 1 was continuous fed with C/N ratio 1 and reactor 2 was continuous fed with C/N ratio 0. The perturbation experiments were performed by increasing the C/N ratio and the loading rate (increased flow rate). From day 131 in the second period, both of the reactors were fed with C/N ratio 3, and from day 139 in the second period, the loading of C/N ratio was doubled (increased loading rate) as well. Nitrification activities were calculated as NH_4^+-N consumption for AOB and NO_3^--N production for NOB in order to estimate the difference in the nitrification activities between AOB and NOB.

The nitrate, nitrite and ammonia concentration in the reactors were measured over 36 days in the first period (Figure 4.1, Table 4.1). On day 37, the organic inhibition experiment was performed (section 4.21). The reactors started with biofilm carriers from two nitrification MBBR that had been operated for some weeks before start-up (Inlet = 50 mg/L NH_4^+-N, HRT = 12 hours, C/N ratio 0). From day 11 to day 27 in the first period, the nitrite concentration elevated in reactor 1 (Figure 4.1 A). The nitrite concentration in reactor 1 increased from average 0.32 ± 0.14 mg/L NO_2^--N before day 11 to average 2.53 ± 0.93 mg/L NO_2^--N between day 11 and day 27.

Unstable pumps and worn pump tubings caused unstable flow rate in both reactors (marked in Figure 4.1). On day 36, reactor 1 had problems with the pump, and therefore reactor 1 was set on batch conditions for 12 hours. The average ammonium, nitrite and nitrate concentrations are shown in Table 4.1. The differences in nitrification activities given as NH_4^+-N consumption and NO_3^--production in reactor 1 and reactor 2 were small in the first period. Both reactors showed stable nitrification activity over time. The average nitrification activities in the first period were 7.26 ± 1.02 mg NH_4^+-N/ L h and 7.12 ± 0.97 mg NO_3^--N/ L h for reactor 1 and 7.17 ± 0.85 mg NH_4^+-N/ L h and 7.43 ± 0.95 mg NO_3^--N/ L h for reactor 2 (Table 4.2).

The nitrate, nitrite and ammonium concentrations in the reactors were measured over 152 days in the second period (Figure 4.1, Table 4.1). The reactors started with frozen biofilm carriers from the first period, and were in batch modus for 24 hours before the pumps were turned on. Unstable nitrification activities were shown in both reactors during the first half of the experiment. Also in the second period, different minor problems occurred. On day 24, the ammonium and nitrite concentrations were high in both reactors because of unstable flow rate (marked in Figure 4.1), and the reactors were set on batch conditions for 12 hours after this incidence. On day 24, the aeration source in reactor 2 was turned off by accident, and the incident resulted in high nitrite and ammonium concentration in reactor 2. On day 69, reactor 1 was finally stable, and at day 77, reactor 2 was finally stable.

The difference in nitrification activity given as NH_4^+-N/ L h consumption and NO_3^-- N/ L h production, between reactor 1 and reactor 2 was small in the second period (days 3-130). The average nitrification activities until day 131 with the long-term operating conditions were 7.67 ± 0.67 mg NH_4^+-N/ L h and 7.95 ± 1.13 mg NO_3^-N/ L h for reactor 1, while for reactor 2 the average nitrification activities with the long-term operating conditions until day 131 were 7.95 ± 1.13 mg NH_4^+-N/ L h and 7.94 ± 0. 79 mg NO_3^--N (Table 4.2).

After the increase in C/N ratio (day 131) and loading rate (day 139) (perturbation experiments), bigger differences were observed in the nitrogen concentrations in the reactors and in the nitrification activities. Both reactors showed some unstable nitrification activities after increased C/N ratio to 3. Reactor 2 had one short nitrite peak after increased C/N ratio, but managed to stabilize (Figure 4.1 F). Reactor 1 showed a tendency of nitrite accumulating, but the nitrite concentrations were lowered again in both reactor after increased loading (Figure 4.1 E-F). Few samplings point and varying nitrogen concentrations gave high standard deviations in the average nitrogen concentrations, especially for nitrite concentration, after increased C/N ratio (days 131-138) (Table 4.1).

After increased loading rate, the average nitrification activities for reactor 1 was 12.52 ± 1.75 mg NH_4^+-N/ L h and 8.75 ± 1.83 mg NO_3^--N/L h. Average nitrification activity after increased loading for reactor 2 was 13.85 ± 1.13 mg NH_4^+-H/ L h and 11.24 ± 3.13 mg NO_3^--N/L (Table 4.2). Varying nitrogen concentrations measured in the reactors gave high standard deviation in the average nitrogen concentrations after increased loading (days 139-152). The ammonium

concentrations increased and the nitrate concentrations decreased in both the reactors when the loading rate increased (Figure 4.2 E-F) (Table 4.1).

It is possible to observe a gap between nitrification activity given as NH_4^+-N consumption (mg/L h) and NO_3^--N-production (mg/L h) after increased loading rate (days 145-152) for both the reactors (Figure 4.2 C-D). In the days 145-152, average loss of nitrogen was 20.68 ± 12.70 mg N/L in reactor 1 and average loss of nitrogen was 19.50 ± 15.79 mg N/L for reactor 2. Nitrification activities given as NH_4^+-N/ L h consumption were higher than the average nitrification activities given as NO_3^-- N production for both the reactors when the loading was increased, but reactor 2 had a moderate standard deviation at nitrification activity given as NO_3^--N production (Table 4.2 C).

Loss of nitrogen was observed from both the reactors after increased loading rate (Figure 4.E-F). Average sum of nitrogen compounds (NO_3^-- N + NH_4^+-N + NO_2^-- N) was 80.88 ± 3.59 mg N /L in reactor 1 and 80.47 ± 13.26 mg N /L in reactor 2 after increased loading rate (days 139-152). In the periods before increased organic concentrations to the reactors, loss of nitrogen had not been observed. Before the perturbation experiments, the average sum of nitrogen compounds (NO_3^-- N + NH_4^+-N + NO_2^-- N) in the reactors had been stable around 100 mg N /L and been in mass balance with the inlet concentrations of nitrogen. Loss of nitrogen was observed in reactor 1 shortly after increased C/N ratio (section 4.2.3).

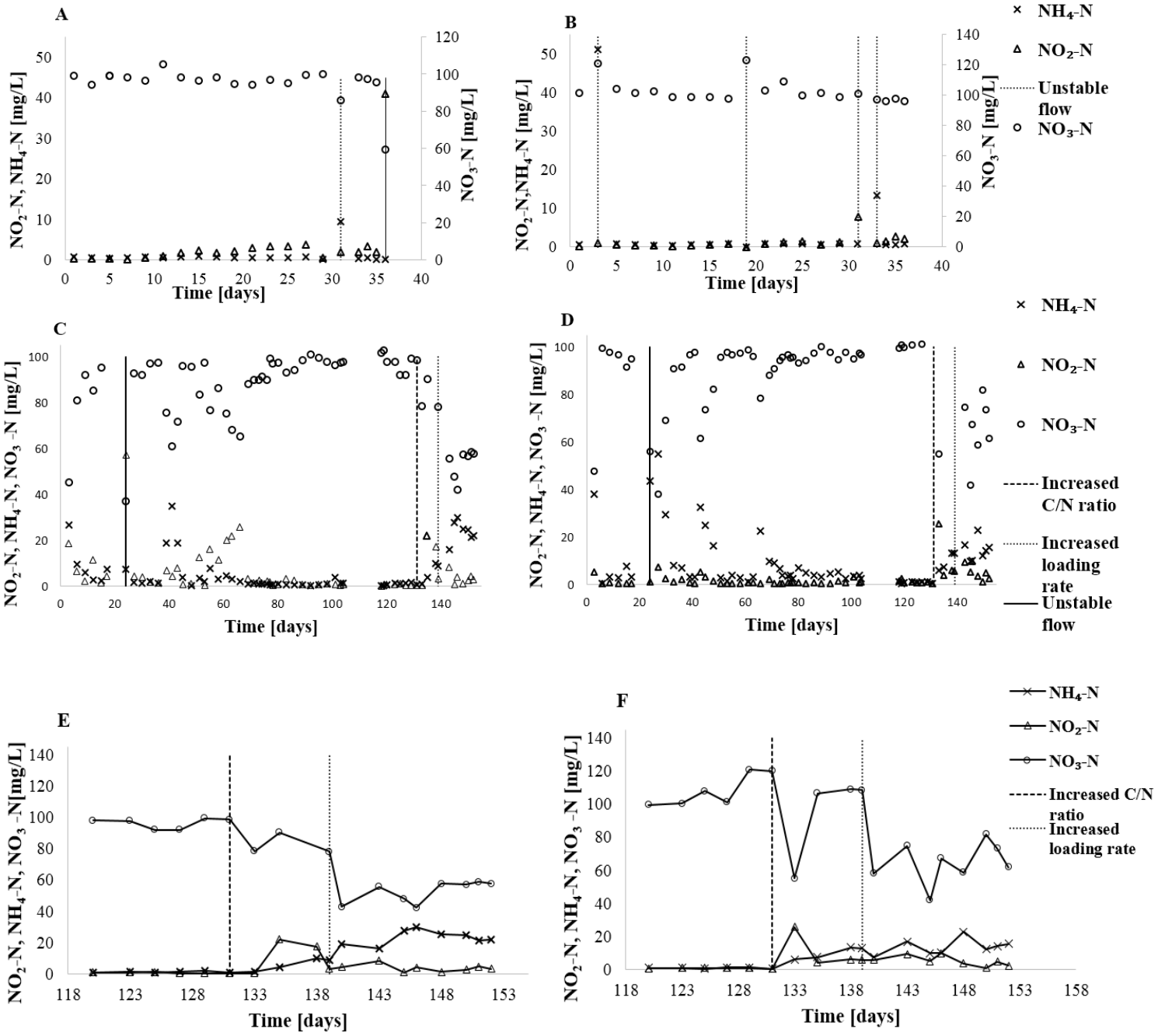

Figure 4.1 Ammonium (NH_4^+-N), nitrite (NO_2^--N) and nitrate (NO_3^--N) concentrations in reactor 1 and reactor 2 in the first period (36 days) and in the second period (152 days). A) reactor 1 in the first period. B) reactor 2 in the first period. C) reactor 1 in the second period. D) reactor 2 in in the second period. E) reactor 1 in the second period (days:120-152). F) reactor 2 in the period (days: 120-152). E and F is to increase the resolution during the two perturbation experiments (days 120-152).

Table 4.1 The average ammonium, nitrite and nitrate concentrations (mg N /L) in reactor 1 and reactor 2 in the first and the second period. Deviation values were excluded from the average calculations (Appendix A). The second period were divided into the 3 groups: A is before the two perturbation experiments (days ≥131). B is after increased C/N ratio and before increased loading (days 132 -138), and C is after increased loading rate (days ≥139).

1. Period	**Reactor 1**			**Reactor 2**		
	NH_4^+-N	NO_2^--N	NO_3^--N	NH_4^+-N	NO_2^--N	NO_3^--N
	mg/L	mg/L	mg/L	mg/L	mg/L	mg/L
Average	0.540 ± 0.22	1.837 ± 1.32	97.95 ± 2.64	0.643 ± 0.11	0.856 ± 0.66	100.8 ± 3.21
2. Period (A)	**Reactor 1**			**Reactor 2**		
	NH_4^+-N	NO_2^--N	NO_3^--N	NH_4^+-N	NO_2^--N	NO_3^--N
	mg/L	mg/L	mg/L	mg/L	mg/L	mg/L
Average	3.17 ± 6.13	3.37 ± 4.65	92.19 ± 8.66	3.76 ± 3.79	0.57 ± 0.60	97.16 ± 6.92
2. Period (B)	**Reactor 1**			**Reactor 2**		
	NH_4^+-N	NO_2^--N	NO_3^--N	NH_4^+-N	NO_2^--N	NO_3^--N
	mg/L	mg/L	mg/L	mg/L	mg/L	mg/L
Average	5.02 ± 4.54	13.21 ± 11.41	84.23 ± 8.30	8.72 ± 3.80	11.73 ± 11.96	90.13 ± 30.45
2. Period (C)	**Reactor 1**			**Reactor 2**		
	NH_4^+-N	NO_2^--N	NO_3^--N	NH_4^+-N	NO_2^--N	NO_3^--N
	mg/L	mg/L	mg/L	mg/L	mg/L	mg/L
Average	21.57 ± 6.40	3.53 ± 2.22	54.60 ± 11.61	13.34 ± 4.56	5.06 ± 2.92	64.59 ± 12.44

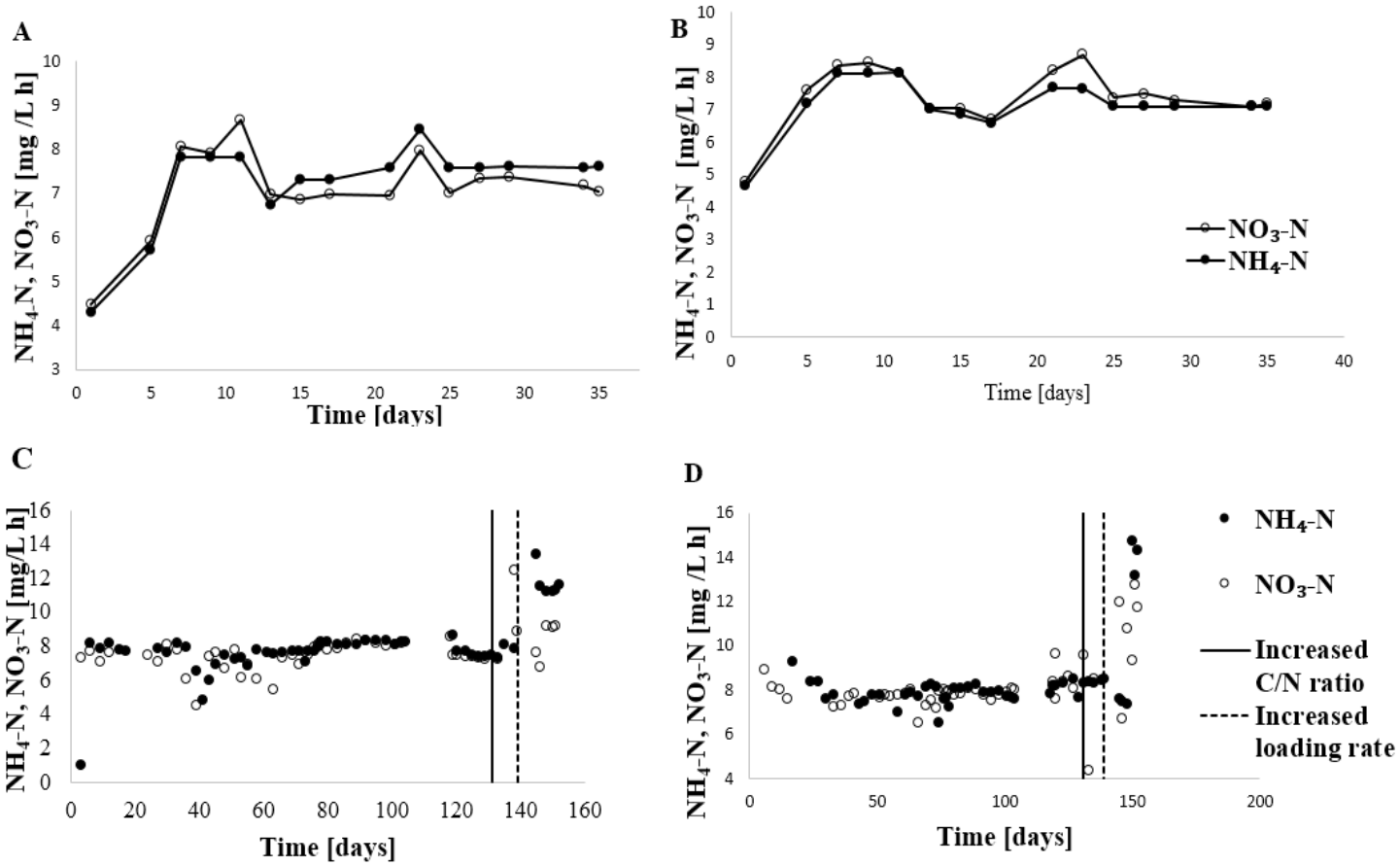

Figure 4.2 The nitrification activity given as NH_4^+-N consumption (($[NH_4^+\text{-}N]_{in}$ - $[NH_4^+\text{-}N]_{out}$)/ HRT) and NO_3-N production ($[NO_3^-\text{-}N]_{in}$/ HRT) for reactor 1 and 2. A) reactor 1 in the first period. B) reactor 2 in the first period). C) Reactor 2 in the second period. D) Reactor 2 in second period. Deviation values were removed from the nitrification activities calculations (Appendix A).

Table 4.2 The average nitrification activity given as NH_4^+-N consumption (mg/L h) and NO_3^--N production (mg/L h) in reactor 1 and reactor 2 in the first and the second period. Deviation values were excluded from the average calculations (Appendix A). The second period was divided into the 3 groups: A is before the two perturbation experiments (days $\geq$131), B is after increased C/N ratio and before increased loading rate (days 131-138), and C is after increased loading rate (days $\geq$139).

1. period	**Reactor 1**		**Reactor 2**	
	NH_4^+-N	NO_3^--N	NH_4^+-N	NO_3^--N
	mg/L h	mg/L h	mg/L h	mg/L h
Average	7.26 ± 1.02	7.12 ± 0.97	7.17 ± 0.85	7.43 ± 0.95
2. period (A)	**Reactor 1**		**Reactor 2**	
	NH_4^+-N	NO_3^--N	NH_4^+-N	NO_3^--N
	mg/L h	mg/L h	mg/L h	mg/L h
Average	7.67 ± 0.67	7.45 ± 0.77	7.95 ± 1.13	7.94 ± 0.79
2. period (B)	**Reactor 1**		**Reactor 2**	
	NH_4^+-N	NO_3^--N	NH_4^+-N	NO_3^--N
	mg/L h	mg/L h	mg/L h	mg/L h
Average	7.72 ± 0.41	8.03 ± 3.02	7.49 ± 0.13	7.21 ± 2.44
2. period (C)	**Reactor 1**		**Reactor 2**	
	NH_4^+-N	NO_3^--N	NH_4^+-N	NO_3^--N
	mg/L h	mg/L h	mg/L h	mg/L h
Average	12.52 ± 1.75	8.75 ± 1.83	13.85 ± 1.13	11.24 ± 3.13

4.2 Short-term experiments

4.2.1 Short-term organic carbon inhibition experiments

The objective of the experiments was to investigate whether there was any difference in acute organic carbon inhibition of nitrification activity between the biofilm from reactor 1 (with continuous organic carbon supply) and the biofilm from reactor 2 (without continuous organic carbon supply). The organic carbon inhibition experiments were performed in two batch reactors on day 37 in the first period and on day 99 in the second period. The rate of nitrate accumulation (slope of NO_3^--N versus time) at 0 mM sodium acetate added was defined as 100 % nitrification activity. Dose response curve and EC_{50} (effective concentration for 50 inhibition) were calculated using REGTOX based on the nitrate accumulation rates calculated from data in Figure 4.3.

The difference in nitrate accumulation rate (mg NO_3^--N/L h) was small on day 37 in the first period between the biofilm carriers from reactor 1 and reactor 2. Start concentrations of nitrate

(time 0) at 0 mM sodium acetate were high for both the reactors. This was due to nitrate carried over in the biofilm carriers from the continuous operations to the batch reactors used in the short-term organic carbon inhibition experiment (Figure 4.3 A-B). The nitrate accumulation rate was slightly higher for the biofilm from reactor 2 than for the biofilm from reactor 1 for all the sodium acetate concentrations.

At 3.16 mM sodium acetate, the nitrification activity (%) for biofilm from reactor 1 was 82 %, while the nitrification activity for the biofilm from reactor 2 was 96 %. EC_{50} value of sodium acetate for the nitrification in the biofilm from reactor 2 was 205 mM (Figure 4.4). Dose-response curve and EC_{50} could not be calculated from the results in reactor 1. The biofilm from reactor 1 was inhibited by all concentrations of sodium acetate, however, the degree of inhibition did not increase with increasing sodium acetate concentration. For control, nitrite and ammonium concentration were measured after 3 hours for each sodium acetate concentration (0 mM – 100 mM) in both reactors. The nitrite concentration was higher than the nitrate concentration in both reactors for all the sodium acetate concentrations (0 mM – 100 mM).

The difference in nitrate accumulation was high on day 99 in the second period between the biofilms in the reactors (Figure 4.3 C- D). The biofilm from reactor 2 showed higher nitrification robustness towards increased sodium acetate concentration than reactor 1. The EC_{50} value of sodium acetate was 27.3 mM for the nitrification in the biofilm from reactor 1 (Figure 4.4 C), while for the biofilm from reactor 2, the EC_{50} value of sodium acetate was 308.2 mM (Figure 4.4 D).

For control, nitrite and ammonium were measured after 3 hours for each sodium acetate concentration. At 0 mM sodium acetate, the nitrite concentration was equal to the nitrate concentrations in both the reactors. For sodium acetate concentrations above 10 mM, the nitrite concentration was higher than the nitrate concentration in both the reactors. This result indicates accumulation of nitrite and decreased NO_3^--N-production (mg/L h) compared to NH_4^+-N consumption (mg/L h).

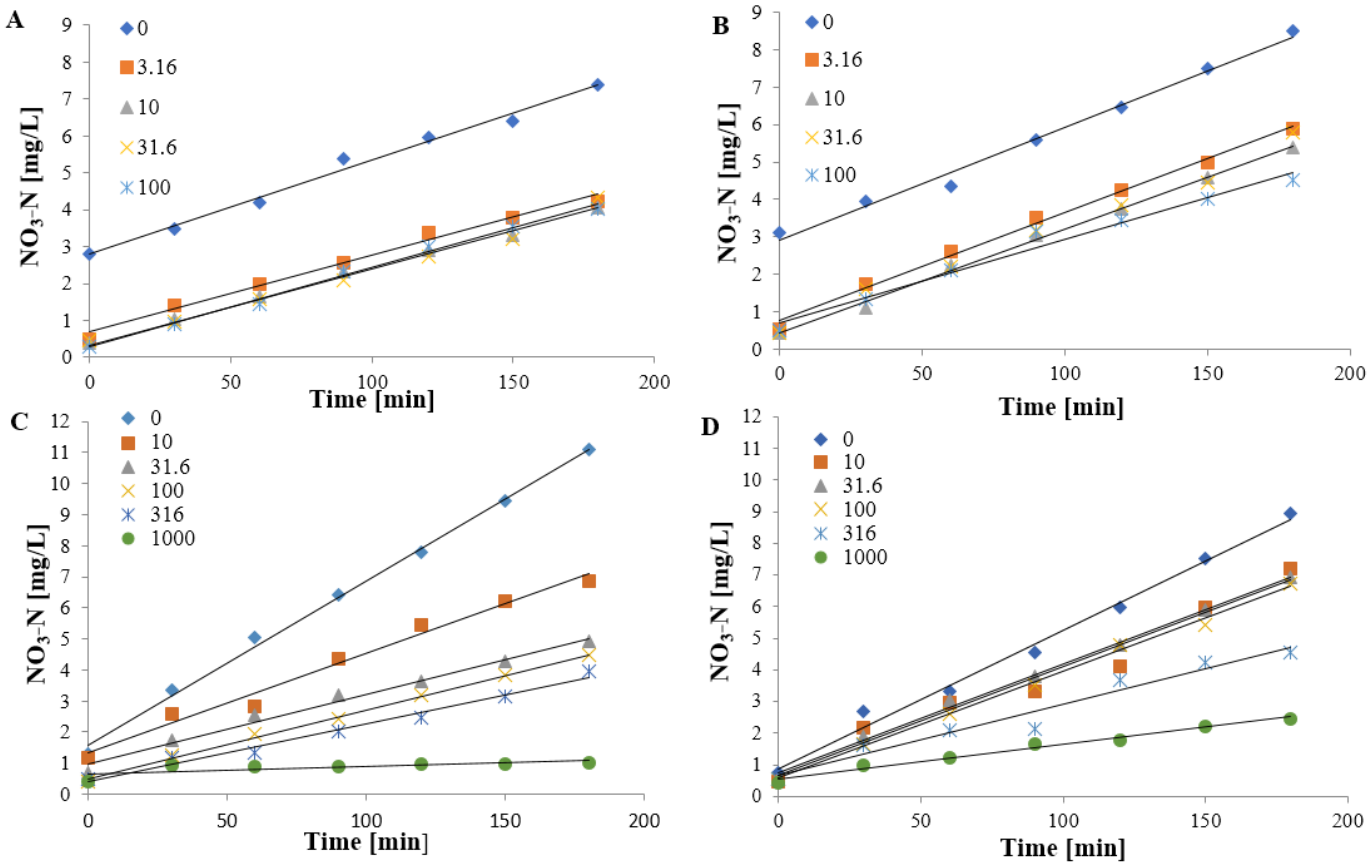

Figure 4.3 Organic carbon inhibition experiment on biofilm carriers from reactor 1 and reactor 2 on day 37 in the first period (A and B) and on day 99 in the second period (C and D). The effect on nitrate accumulation due to increasing sodium acetate concentration was investigated. A) Biofilm carriers from reactor 1 in the first period. B) Biofilm carriers from reactor 2 in the first period. C) Biofilm carriers from reactor 1 in the second period. D) Biofilm carriers from reactor 2 in second period.

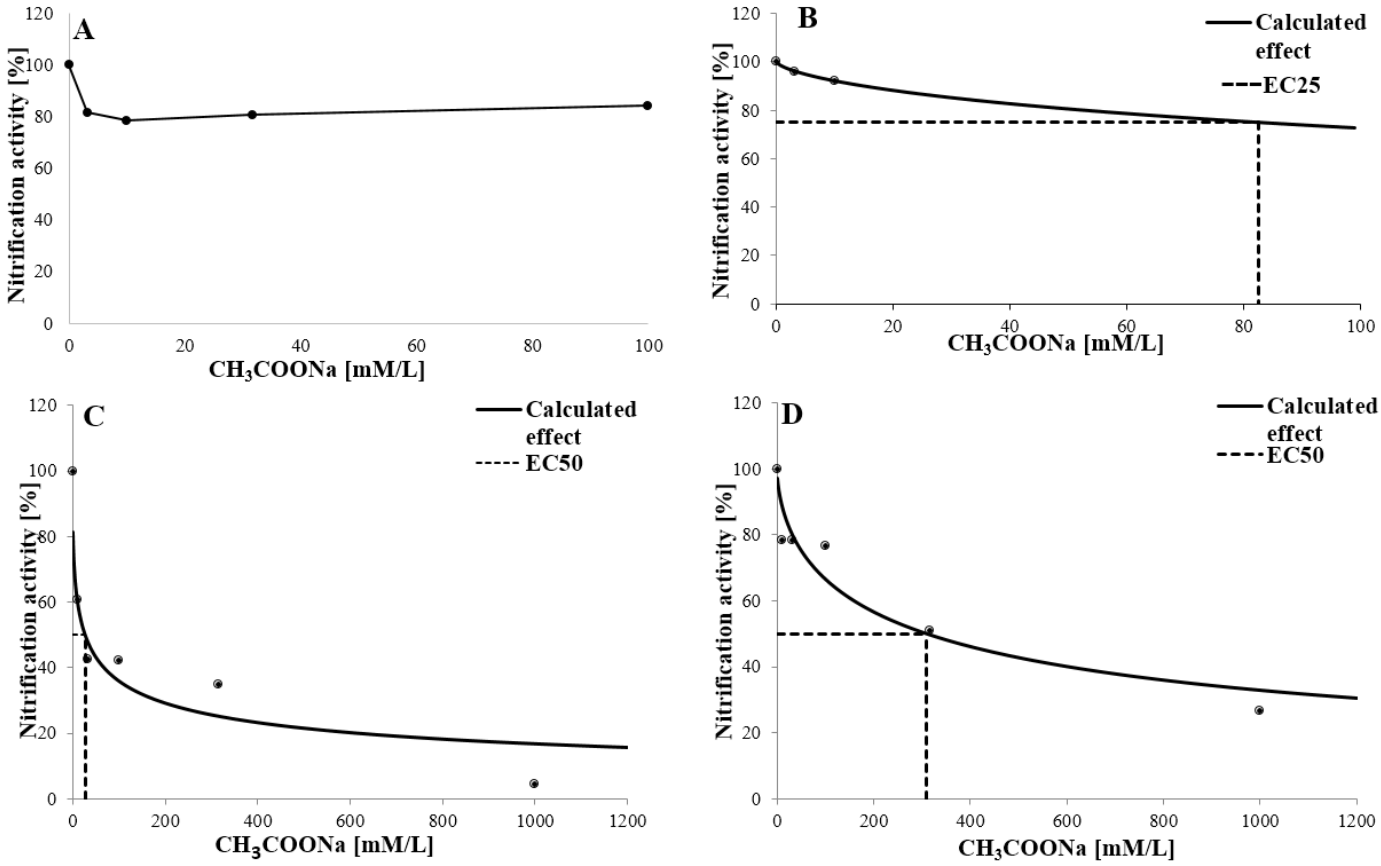

Figure 4.4 Calculated dose-response curves for sodium acetate inhibitory effect on nitrification activity using REGTOX. 0 mM was set as 100 % nitrification activity. A) Biofilm carriers from reactor 1 in the first period. Nitrification activity (%) is based on nitrate accumulation rate and not calculated effect in REGTOX (EC_{50} not calculated). B) Biofilm carriers from reactor 2 in the first period (EC_{50} 205 mM). EC_{25} marked in the figure. C) Biofilm carriers from reactor 1 in second period (EC_{50} 27.3 mM). D) Biofilm carriers from reactor 2 in the second period (EC_{50} 308.2 mM).

4.2.2 Short-term oxygen consumption experiments in batch mode

The objective of the experiments was to investigate whether there was any difference in oxygen consumption between the biofilm from reactor 1 (continuous C/N ratio 1) and the biofilm from reactor 2 (continuous C/N ratio 0). The batch experiments were conducted on day 89 with C/N ratio of 0 and on day 90 with C/N ratio of 1 (Figure 4.5). For control, the changes in the ammonium concentration were measured (Figure 4.6).

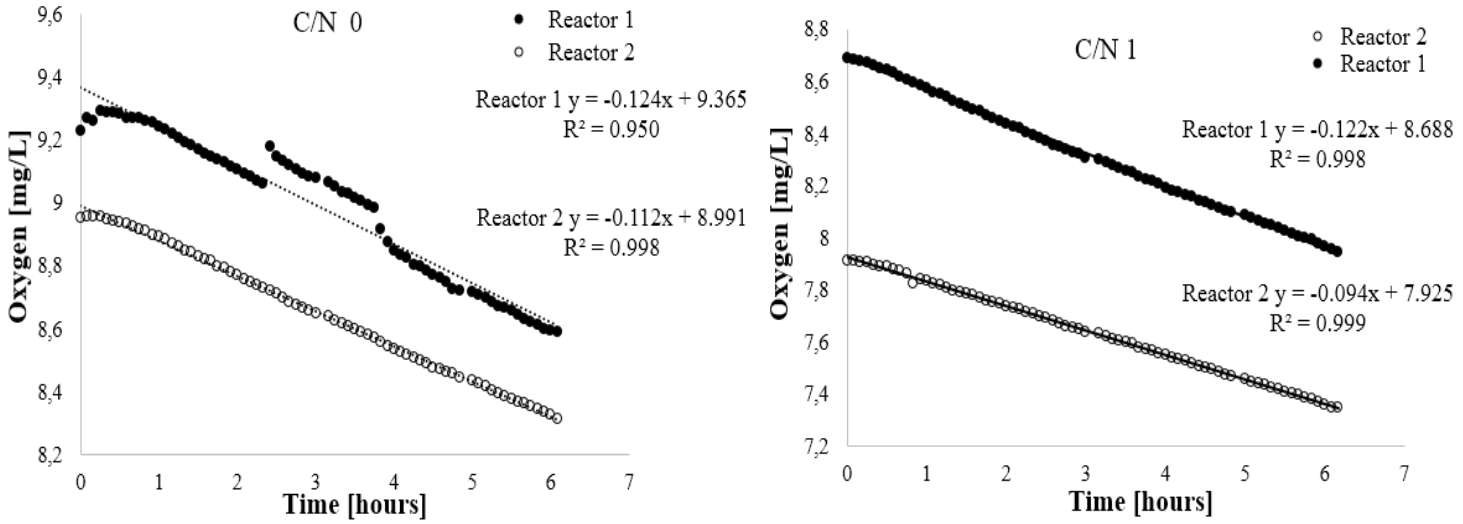

Figure 4.5 Oxygen consumption experiments with biofilm carriers from reactor 1 and reactor 2 with C/N ratio of 0 (left) on day 89 and C/N ratio of 1 (right) on day 90 in the second period. The sudden increase in oxygen concentration for biofilm carriers from reactor 1 in C/N ratio 0 (left) was due to the extra oxygen caused by the sensor loosening from the attached position in the batch reactor. The experiments were conducted in batch mode.

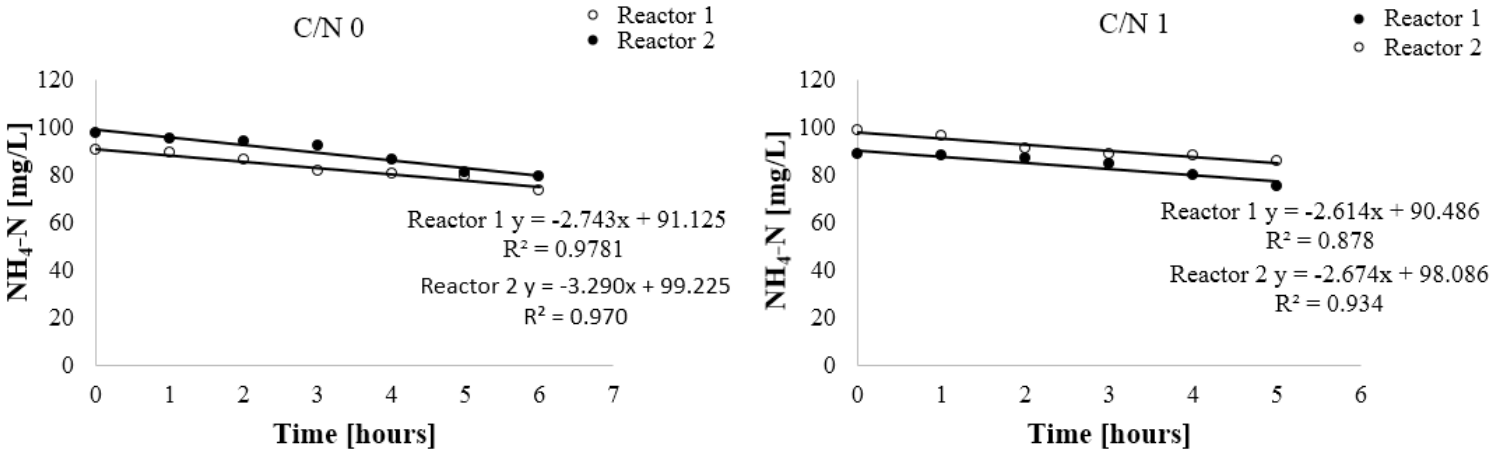

Figure 4.6 The change in ammonium concentration (NH_4^+-N) with time in reactor 1 and reactor 2 from the oxygen consuming batch experiment (Figure 4.5) with C/N ratio of 0 (left) on day 89 and C/N ratio of 1 on day 90 (right) in the second period.

The results showed higher oxygen consumption rate for the biofilm from reactor 1 than for the biofilm from reactor 2 during both experiments. The consumption rate was calculated by linear regression. In the batch experiment with C/N ratio of 0 in the medium, the oxygen consumption rate was 10 % higher for the biofilm carriers from reactor 1 than reactor 2. The ammonium consumption rate was 16 % higher for the biofilm carriers from reactor 2 than biofilm carriers from reactor 1 in the batch experiment with C/N ratio 0. In the batch experiment with C/N ratio 1, the oxygen consumption rate was 23 % higher for the biofilm carriers from reactor 1 than reactor 2. The ammonium consumption rate was 2 % higher for the biofilm carriers from reactor 2 than for the biofilm carriers from reactor 1 in the batch experiment with C/N ratio of 1 (Figure 4.6).

4.2.3 Organic matter and oxygen consumption experiment with increased C/N ratio

The objective of the experiment was to investigate whether there were any differences in organic matter (acetate) and oxygen consumption between the reactors after increased C/N ratio. On day 131 in the second period, the C/N ratio was increased to 3 in the medium for both the reactors. The organic carbon (Figure 4.7), oxygen (Figure 4.9) and nitrogen (NH_4^+-N, NO_2^--N, NO_3^--N) (Figure 4.8) concentrations were measured for 9 hours after the C/N ratio was increased to 3 in the reactors. The organic carbon consumption rate was considerably higher in reactor 1 than reactor 2 the 9 first hours after increased C/N ratio (Figure 4.7). The oxygen consumption rate was slightly higher in reactor 1 (0.052 mg/L h) compared to reactor 2 (0.042 mg/L h) during these 9 hours after C/N ratio was increased (Figure 4.9). A weak decline in oxygen concentration was observed in both reactors from day 131 to 152 in the second period (Figure 4.11).

The experiments showed 13 % higher ammonium consumption rate in reactor 2 compared to reactor 1 the first 9 hours after increased C/N ratio. Nitrite and nitrate accumulation were higher in reactor 2 compared to reactor 1. Figure 4.8 showed that considerable amount of nitrogen was lost from reactor 1 after increased C/N ratio. Therefore, the loss of nitrogen (NH_4^+-N, NO_2^--N, NO_3^--N) from the nitrogen budget was calculated (Figure 4.10). The loss of nitrogen increased as a function of time for reactor 1, while the nitrogen budget in reactor 2 was stable. After 9 hours, the nitrogen loss in reactor 1 was 34.4 %.

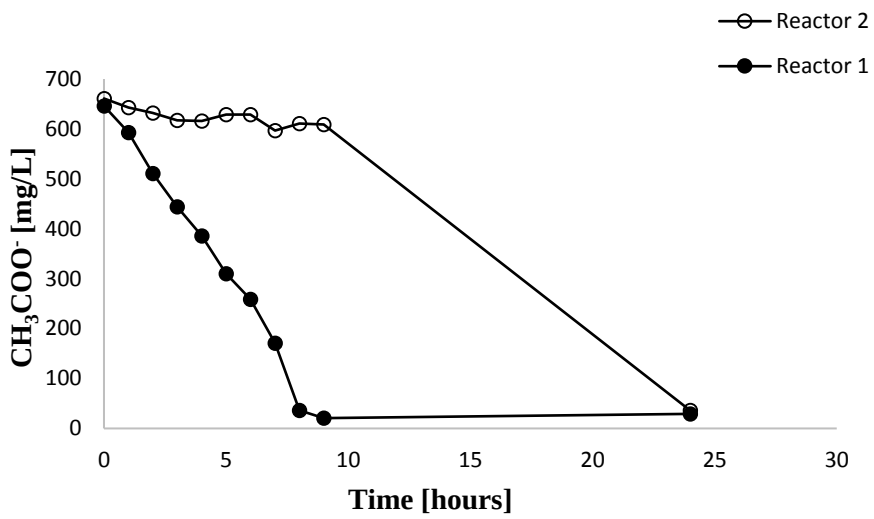

Figure 4.7 The changes in acetate (CH_3COO^-) with time after the C/N ratio was increased to 3 on day 131 in the second period for reactor 1 (previous C/N ratio 1) and reactor 2 (previous C/N ratio 0).

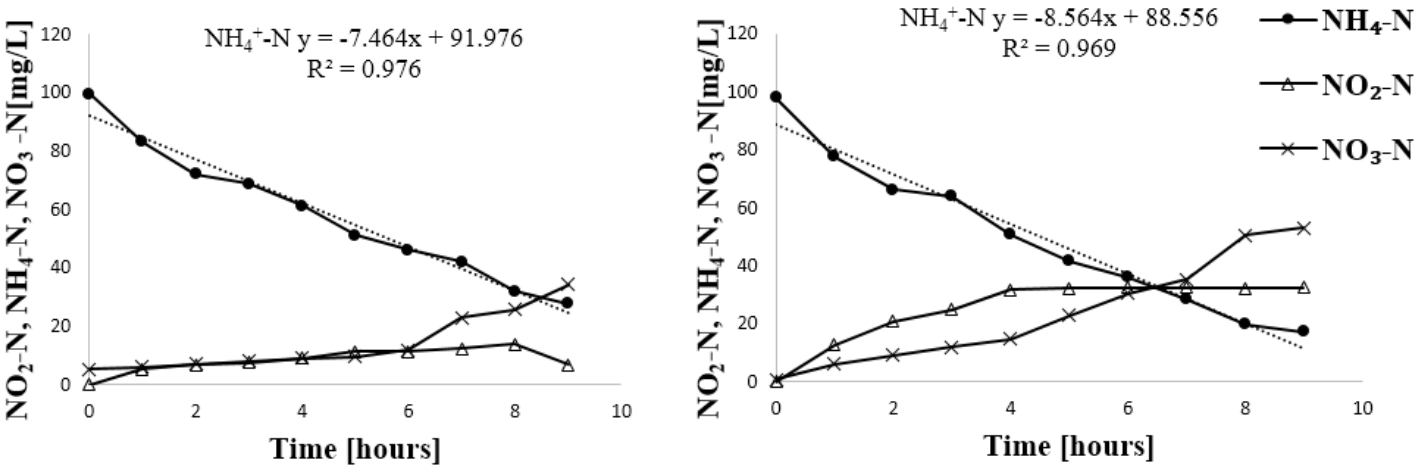

Figure 4.8 The changes in ammonium (NH_4^+-N), nitrite (NO_2^--N) and nitrate (NO_3^--N) concentration in reactor 1 (left) and reactor 2 (right) after the C/N ratio was increased to 3 on day 131 in the second period.

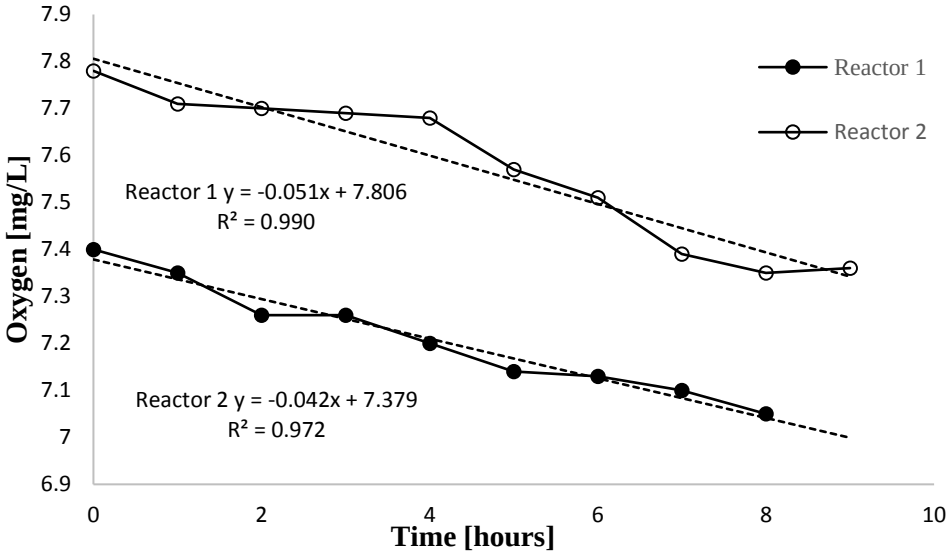

Figure 4.9 The decline in oxygen after the C/N ratio was increased to 3 on day 132 in the second period for reactor 1 and reactor 2.

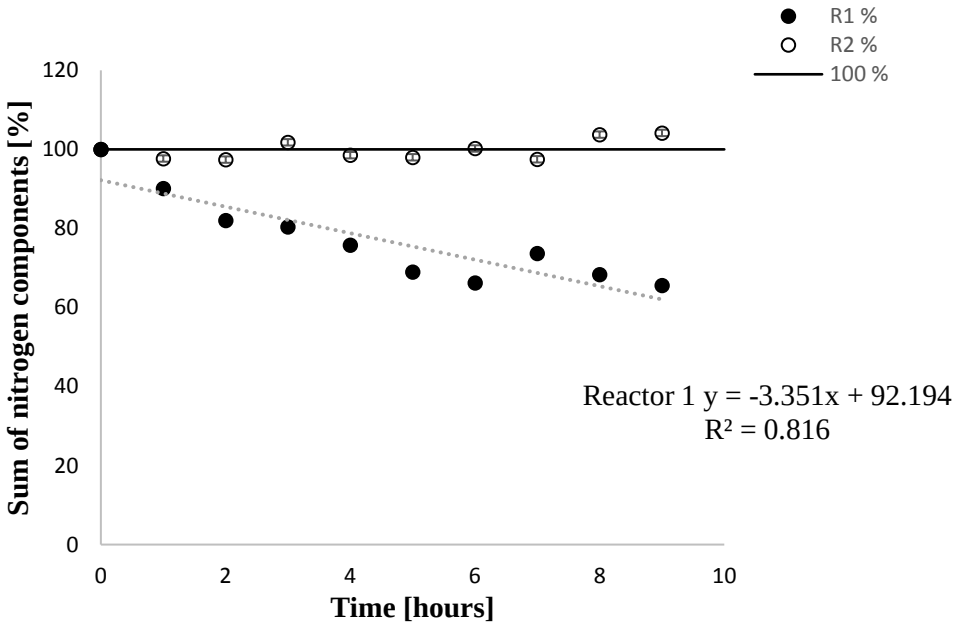

Figure 4.10 The sum of nitrogen components (%) calculated from the nitrogen concentrations in Figure 4.8 after the C/N ratio was increased to 3 at day 131 in the second period for reactor 1 (R1) and reactor 2 (R2). The sum of nitrogen components (%) was calculated from the sum nitrogen (NH_4^+-N, NO_2^--N, NO_3^--N) at a specific time divided by the sum nitrogen (NH_4^+-N, NO_2^--N, NO_3^--N) at time 0.

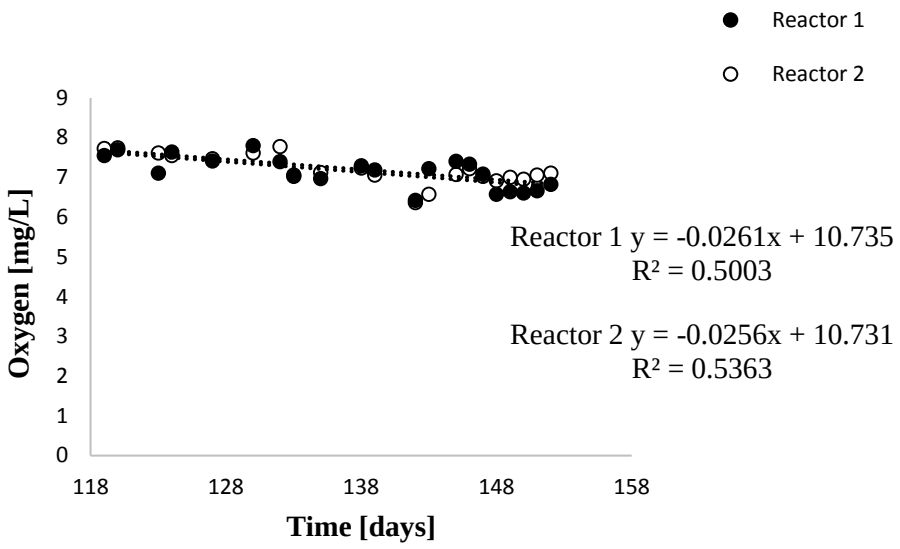

Figure 4.11 The oxygen concentration in reactor 1 and reactor 2 from day 118 to day 152 in the second period. On day 131, the C/N ratio was increased to 3, while on day 139 the loading rate of C/N ratio of 3 was doubled.

4.2.4 Ammonium consumption and oxygen concentrations after increased loading

The objective of the experiment was to investigate whether there were any differences in consumption of ammonium, organic carbon and oxygen between reactor 1 and reactor 2 after the loading rate (HRT decreased) was doubled at day 139 in the second period. The HRT was decreased from 13 to 6.5 hours. The nitrate concentration was high in both reactors due to a combination of water samples taken for DGGE analysis and a low flow rate at day 138. This resulted in an unbalance in the nitrogen budget and a high nitrate concentration for the reactors before the experiment started.

The main difference between reactor 1 and reactor 2 after increased loading rate was the development in ammonium accumulation (Figure 4.12). After 8 hours, the ammonium concentration was higher in reactor 2 than reactor 1. The ammonium concentration in reactor 2 started to decrease after 6 hours, while the ammonium concentration in reactor 1 was increasing still after 8 hours. 24 hours after the loading rate was increased, the ammonium concentration in reactor 1 was 19.00 NH_4^+-N mg/L, while the ammonium concentration in reactor 2 was 7.29 NH_4^+-N mg/L.

The nitrite and nitrate concentration showed a similar development after loading rate was increased (Figure 4.12). The oxygen concentration decreased in both reactors during the first

24 hours (Figure 4.13). Organic carbon concentrations were measured in both reactors in the 4 first hours after increased loading and both the reactors managed to keep the organic concentrations at the same level as before increased loading rate (< 40 mg CH_3COO^-/L).

Organic carbon concentrations were measured again 8 hours after the loading rate was increased and the acetate concentration was higher in reactor 2 (65.1 mg/L) than reactor 1 (22.8 mg/L). However, after a few days and rest of the period, the acetate concentration in reactor 2 was similar with the acetate concentration in reactor 1 (Figure 4.14). The organic carbon concentration (acetate) was low in both reactors (< 50 mg/L) the rest of the period when the reactors were running (Figure 4.14). The ammonium concentrations throughout the second period are shown in Figure 4.15.

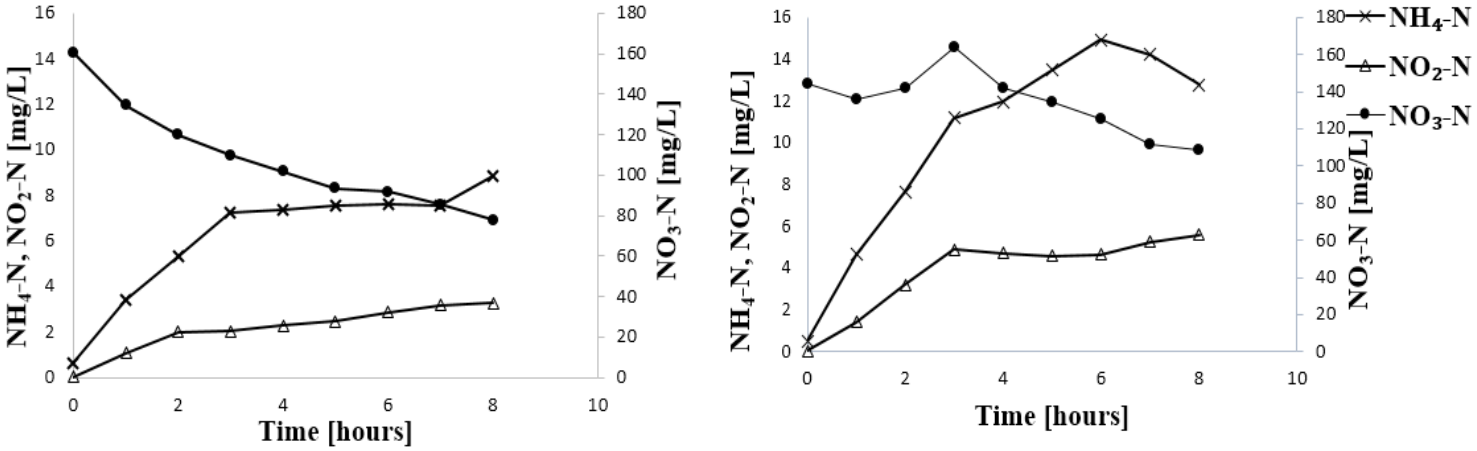

Figure 4.12 The changes in ammonium (NH_4^+-N), nitrite (NO_2^--N) and nitrate (NO_3^--N) concentration in reactor 1 (left) and reactor 2 (right) after organic loading rate was increased at day 139 in the second period.

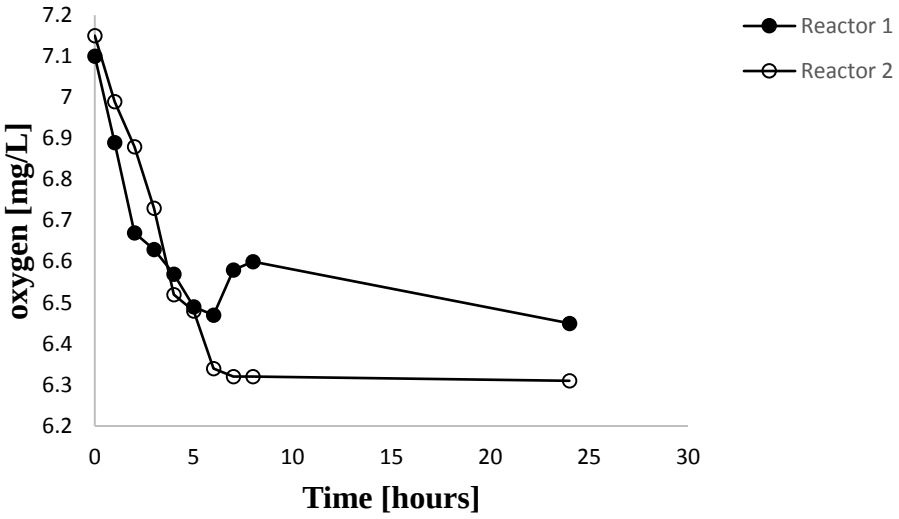

Figure 4.13 The change in oxygen concentration (mg O_2/L) in reactor 1 and reactor 2 after the loading rate was increased on day 139 in the second period.

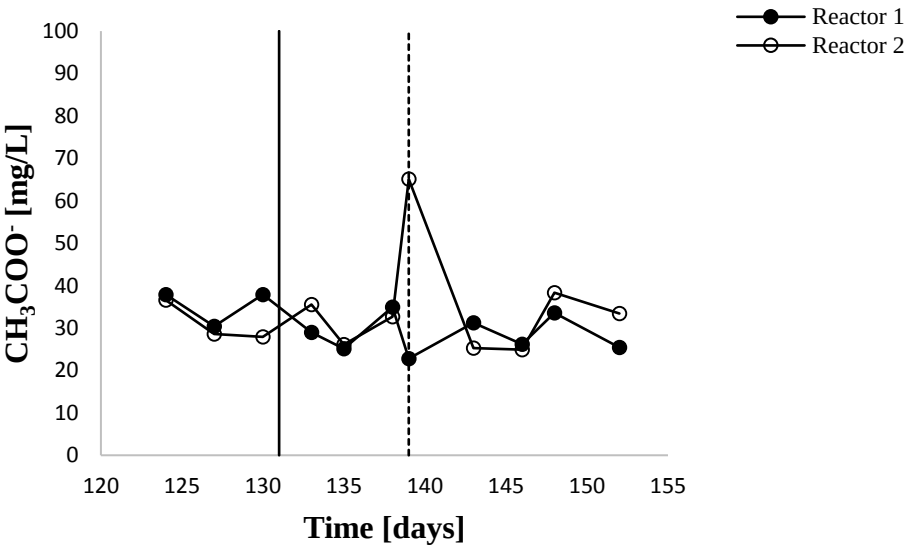

Figure 4.14 The acetate concentration (CH_3COO^-) in reactor 1 and reactor 2 in the second period before and after the C/N ratio (solid line) and the loading rate (dotted line) were increased in the reactors.

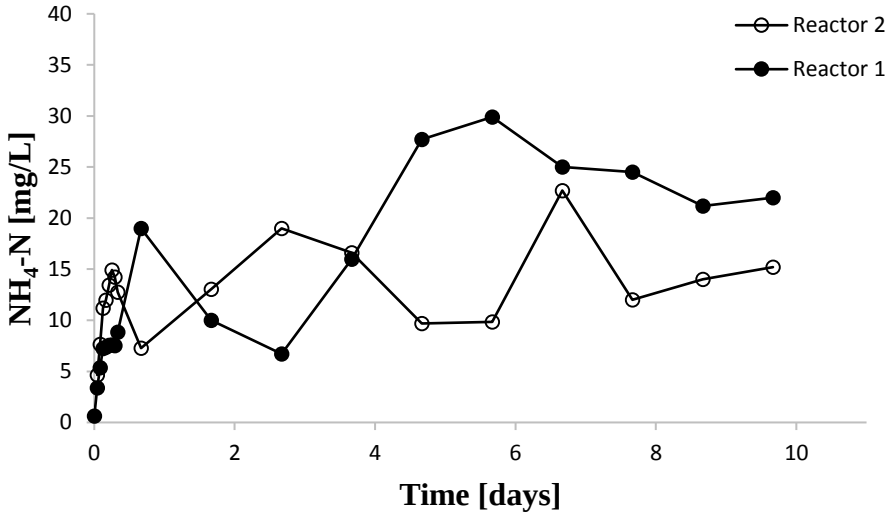

Figure 4.15 The change in ammonium (NH_4^+-N) concentration in the days after the organic loading rate was increased and until the end of the second period in reactor 1 and reactor 2. The day the organic loading rate was increased (day 139 in the second period) is set as day 0.

4.2.5 Cell and aggregate counting by flow cytometer

The aim of the cell counting was to investigate the difference in the number of free-living cells and cell aggregates in water between reactor 1 and reactor 2, and the change in the number of cells after increasing the C/N ratio and the loading rate.

The flow cytometry plots were divided into two global gates: planktonic cells (P) and cell aggregates (CA). Cell aggregates were defined as larger cell clusters of living planktonic cells or cell clusters torn from the biofilm carriers. Gating was based on the identification of populations based on plotting DNA fluorescence (FL1) versus side scatter (FSC), and an example of the global gating from day 137 is shown in Figure 4.16. The number of planktonic cells (Figure 4.17) and cell aggregates (Figure 4.18) before and after the C/N ratio and the loading rate were increased for reactor 1 and reactor 2 were compared.

Before the C/N ratio and the loading rate was increased, the number of planktonic cells was 22 times higher in reactor 1 than in reactor 2, while the number of cell aggregates was 428 times higher in reactor 1 than in reactor 2. After the C/N ratio and the loading rate were increased, the gap between the number of planktonic cells and cell aggregates in reactor 2 was smaller. Exceptions from the decline in the gap were seen at day 148 for planktonic cells (Figure 4.17) and on day 152 for cell aggregates/µL (Figure 4.18).

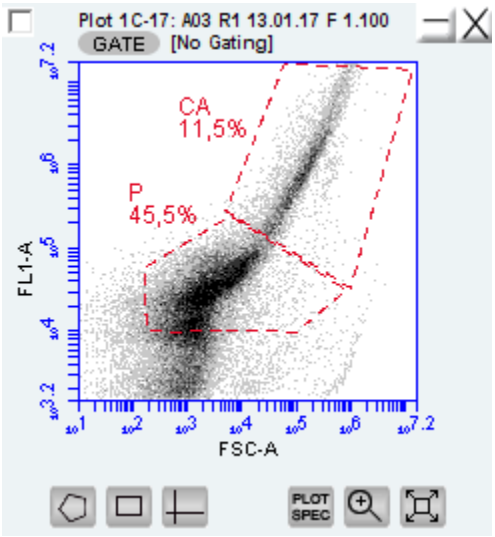

Figure 4.16 Global gating used for all samples, indicating gating for planktonic cells (P) and cell aggregates (CA), based on forward scatter (FSC) and DNA fluorescence (FL1).

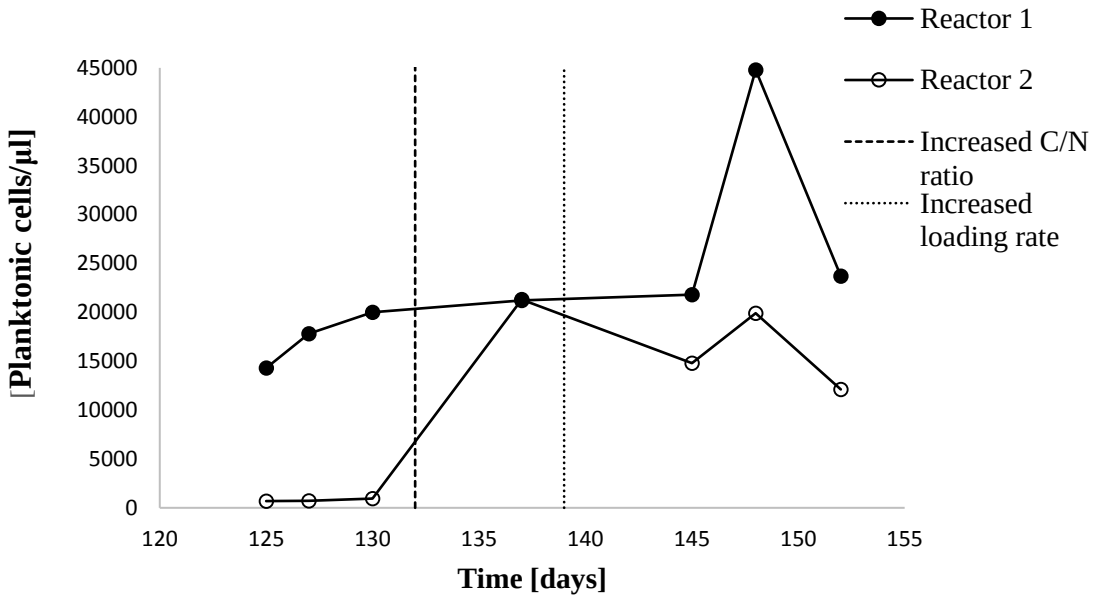

Figure 4.17 The changes in cell number (cells/µL) with time (days) for planktonic cells in reactor 1 and 2. The time the C/N ratio (day 131) and the loading rate (day 139) were increased are indicated by vertical lines.

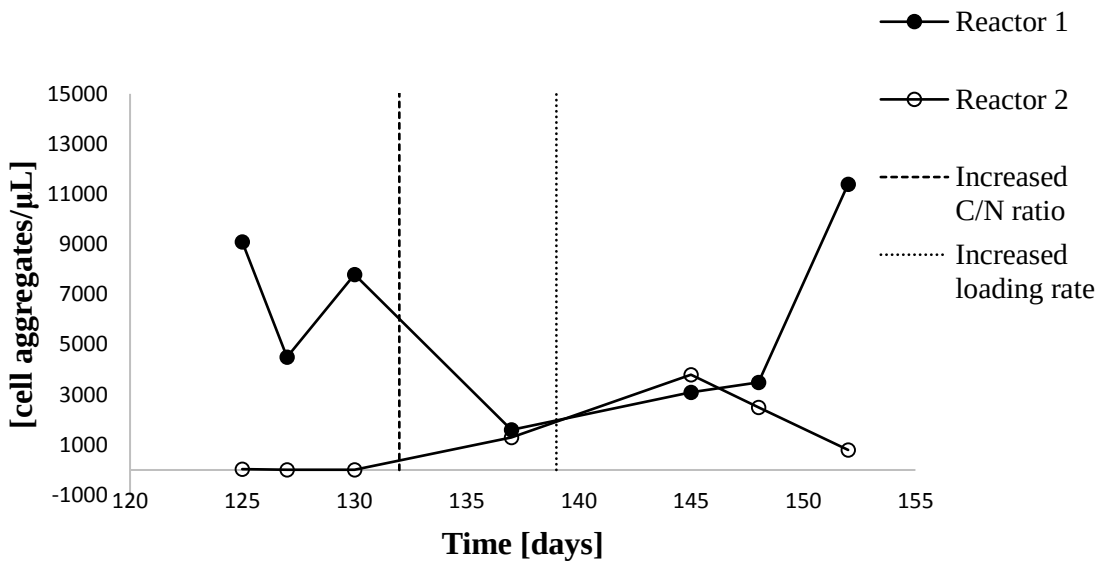

Figure 4.18 The changes in the number of cell aggregates (aggregates/µL) with time (days) in reactor 1 and 2. The time the C/N ratio (day 131) and the loading rate (day 139) was increased are indicated by vertical lines.

4.3. Diversity and structure of microbial communities in MBBR

Two DGGE gels were analysed based on samples taken from reactor 1 and reactor 2 during first and second period. The objectives of the two DGGE gels analysed were to investigate changes in diversity and structure of microbial communities on biofilm carriers during different stable nitrification phases, but also investigate changes after long and short-term exposure to different C/N ratios and increased loading.

4.3.1 Changes in microbial communities after changes in C/N ratio and loading rate

PCR products from biofilm carriers (C) and water samples (W) from reactor 1 (R1) and reactor 2 (R2) taken before (B) and after (A) the C/N ratio (day 131, second period) and the loading rate (day 139, second period) was increased, were analysed on DGGE gel 1 (Figure 4.19). 65 bands were identified on the analysed gel. The samples were divided into 8 groups based on three conditions: type of reactor (R1 or R2), type of sample (biofilm carrier or water) and time (before or after the C/N ratio and the loading rate was increased). Abbreviations for the 8 groups are therefore: R1WB, R1WA, R2WB, R2WA, R1CB, R1CA, R2CB, R2CA.

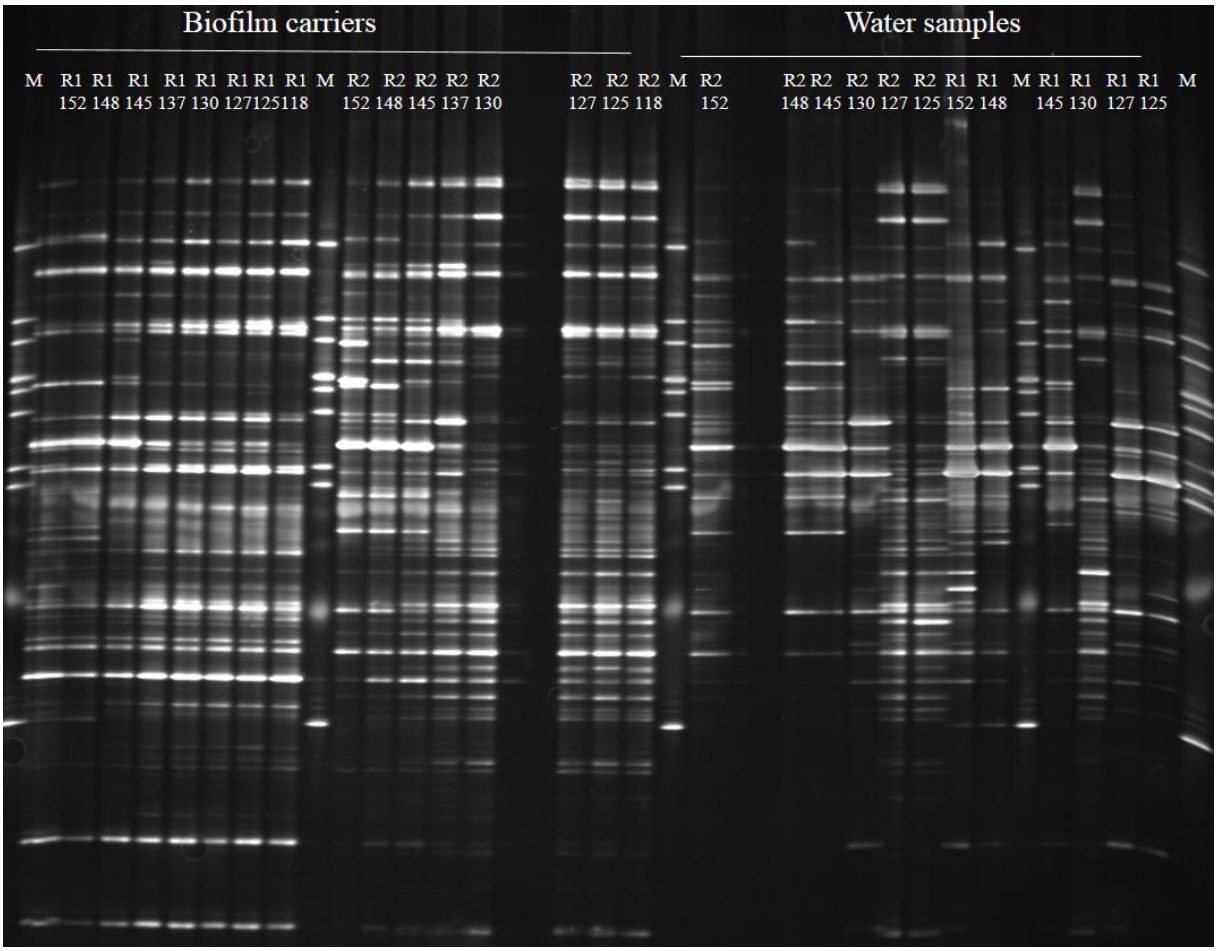

Figure 4.19 DGGE gel 1 of samples from biofilm carriers and water from reactor 1 and reactor 2 before and after increased C/N ratio and loading rate. Abbreviations: R1 (reactor 1), R2 (reactor 2), M (marker). Numbers (118-152) represent the day biofilm carriers and water samples were taken. On day 131, the C/N ratio was increased in the medium and on day 139 the loading rate was increased.

Alpha-diversities were calculated based on the 8 groups (Table 4.3). The band richness ranged from 26-49, the Shannon Diversity ranged from 2.48-3.46, while the evenness ranged from 0.53-0.73 between the samples (Table 4.3). The variance in band richness within the groups of water samples was high, especially for water samples taken before increased C/N ratio and loading rate. The variance in evenness within the 8 groups was though low. The average Shannon Diversity and the band richness decreased for all the 8 groups after increased C/N ratio and loading rate. The average band richness and the average Shannon Diversity were higher for biofilm carriers from reactor 2 than from reactor 1, both before and after increased C/N ratio and loading rate.

Table 4.3 The band richness (k`), the Shannon diversity index (H`) and the evenness (J`) were calculated based on analysis of DGGE gel 1 (Figure 4.19). Comparisons of alpha-diversities in biofilm carriers (C) and water samples (W) from reactor 1 (R1) and reactor 2 (R2) before and after increased C/N ratio and loading rate. The numbers 1-4 represent samples taken before (B) increased C/N ratio and loading rate, while the numbers 5-8 represent samples taken after (A) increased C/N ratio and loading rate. The numbers (118-152) in the name-column represent the day the biofilm carriers and the water samples were taken. The average and the standard deviation of alpha-diversities were calculated for the different groups.

Group	Number	Name	Band richness (k`)	Shannon Diversity (H`)	Evenness $e^{H`}/k`$ (J`)
	2	R1W125	24	2.73	0.64
	3	R1W127	30	2.88	0.59
R1WB	4	R1W130	41	3.28	0.65
		Average	32 ± 8.6	2.96 ± 0.28	0.63 ± 0.03
	6	R1W145	26	2.71	0.58
	7	R1W148	26	2.67	0.55
R1WA	8	R1W152	36	3.15	0.65
		Average	29 ± 5.8	2.48 ± 0.27	0.59 ± 0.05
	2	R2W125	44	3.32	0.63
	3	R2W127	47	3.54	0.73
R2WB	4	R2W130	31	2.79	0.53
		Average	41 ± 8.5	3.22 ± 0.38	0.63 ± 0.10
	6	R2W145	26	2.66	0.55
	7	R2W148	24	2.74	0.65
R2WA	8	R2W152	31	2.86	0.56
		Average	27 ± 3.6	2.75 ± 0.10	0.59 ± 0.05
	1	R1C118	42	3.23	0.60
	2	R1C125	41	3.24	0.62
R1CB	3	R1C127	40	3.13	0.57
	4	R1C130	37	3.12	0.61
		Average	40 ± 2.2	3.18 ± 0.06	0.60 ± 0.02
	5	R1C137	37	3.16	0.64
	6	R1C145	34	3.02	0.60
R1CA	7	R1C148	33	2.96	0.58
	8	R1C152	35	3.04	0.60
		Average	35 ± 1.7	3.04 ± 0.09	0.60 ± 0.02
	1	R2C118	48	3.50	0.69
	2	R2C125	48	3.42	0.64
R2CB	3	R2C127	49	3.40	0.61
	4	R2C130	49	3.46	0.65
		Average	49 ± 0.6	3.44 ± 0.04	0.65 ± 0.03
	5	R2C137	49	3.38	0.60
	6	R2C145	44	3.20	0.56
R2CA	7	R2C148	39	3.13	0.59
	8	R2C152	33	2.98	0.60
		Average	41 ± 6.8	3.17 ± 0.16	0.59 ± 0.02

The change in community structure (beta-diversity) was also investigated. Principle coordinate analysis (PCoA) based on ordination by Bray-Curtis similarity indicated changes in community structure after the C/N ratio and the loading rate was increased (Figure 4.20). How scattered the samples are on the PCoA, give information about the variance in the community structure between the samples. In other words, how similar or how different the samples are in terms of community structure. A low variance between the samples is visualized as points clustered together, while high variance between the samples is visualized as scattered points on the plot.

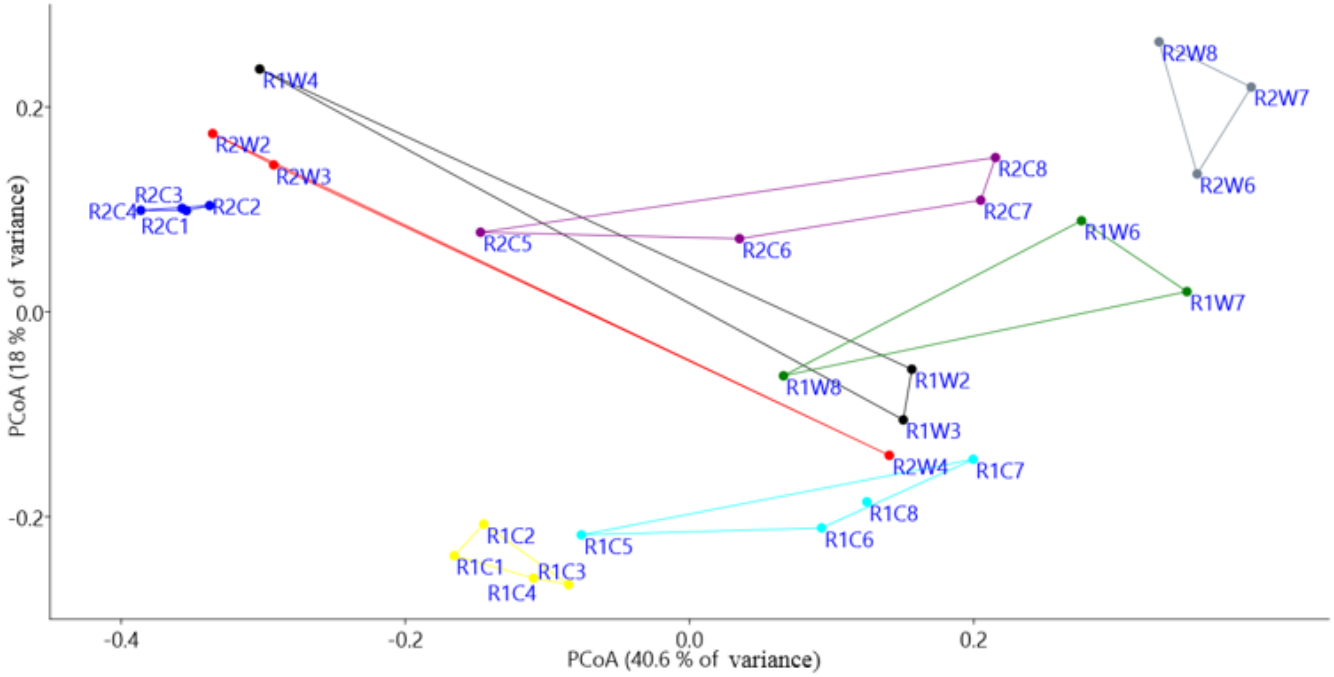

Figure 4.20 Principle coordinate analysis (PCoA) based on Bray-Curtis similarity of the microbial communities in biofilm carriers (C) and water samples (W) from reactor 1 (R1) and reactor 2 (R2) analysed from DGGE gel 1 (Figure 4.19). The numbers 1-4 represent samples taken before the C/N ratio and the loading rate of the medium was increased (before perturbations). The numbers 5-8 represent samples taken after the C/N ratio and the loading rate was increased (after perturbations) (Table 4.4). Different colors are used to separate the different groups. Yellow group: Biofilm carriers from reactor 1 before perturbations. Light blue group: Biofilm carriers from reactor 1 after perturbations. Dark blue group: Biofilm carriers from reactor 2 before perturbations. Purple group: Biofilm carriers from reactor 2 after perturbations. Brown group: Water samples from reactor 1 before perturbations. Green group: Water samples from reactor 1 after perturbations. Red group: Water samples from reactor 2 before perturbations. Grey group: Water samples from reactor 2 after perturbations.

PCoA indicated that biofilm carriers from reactor 1 and 2 went through a succession in the community structure after increased carbon to the biofilm. In the PCoA plot (Figure. 20), the point representing the biofilm communities moved along the x-axis (explains 40.6 of the variance) after increased organic carbon concentrations were introduced to the reactors. In addition, PCoA indicated that biofilm carriers from reactor 1 and 2 were closer in community structure after increased C/N ratio and loading rate. PCoA also indicated that the variance between the water samples within the water groups was high, compared to the biofilm samples.

The changes in community structure (beta-diversity) were confirmed by statistical analyses. The P values (Sequential Bonferroni correlation) from one-way PERMANOVA test based on Bray Curtis similarity showed a significant difference in community structure between water samples and biofilm carriers (Figure 4.4). The difference in community structure in biofilm carriers in reactor 1 and reactor 2 before and after increased C/N ratio was also significant, however the groups of water samples were not. The P values (Sequential Bonferroni correlation) from one-way PERMANOVA based on Jaccard similarity indicated a shift in species inventory after the C/N ratio and the loading rate was increased for the biofilm carriers in reactor 1 and reactor 2 (Table 4.5). This is based on that the difference between the biofilm groups before and after the perturbation experiments in Jaccard similarity was significant difference.

Table 4.4 The results from one-way PERMANOVA based on Bray Curtis similarity with the groups identified in Figure 4.20. The biofilm carriers (C) and the water samples (W) from reactor 1 (R1) and reactor 2 (R2) before (B) and after (A) increased C/N ratio and loading rate. Multiple comparisons of the various groups based on Sequential Bonferroni correlation (P-value column) and significant difference if $P < 0.05$.

Comparisons	**P value**	**F**	**P(same)**	**Total sum of square**
R1WB & R1WA	0.3000	5.321	0.0001	3.921
R2WB & R1WA	0.1010			
R1CB & R1CA	0.0262			
R2CB & R2CA	0.0272			
R1WB & R1CB	0.0287			
R2WB & R2CB	0.0281			
R1CB & R2CB	0.0282			
R1CA & R2CA	0.0288			
R1WA & R1CA	0.0278			
R2WA & R2CA	0.0313			
R2WB & R1WB	0.8990			

Table 4.5 The results from one-way PERMANOVA test based on Jaccard similarity with the groups identified in Figure 4.20. The biofilm carriers (C) and the water samples (W) from reactor 1 (R1) and reactor 2 (R2) before (B) and after (A) increased C/N ratio. Significant difference if $P < 0.05$. Multiple comparisons of the various groups based on Sequential Bonferroni correlation (P-value column).

Comparisons	P value	F	P (same)	Total sum of square
R1WB & R1WA	0.1055	7.599	0.0001	3.096
R2WB & R1WA	0.0961			
R1CB & R1CA	0.0262			
R2CB & R2CA	0.0272			
R1WB & R1CB	0.0287			
R2WB & R2CB	0.0281			
R1CB & R2CB	0.0282			
R1CA & R2CA	0.0288			
R1WA & R1CA	0.0278			
R2WA & R2CA	0.0313			
R2WB & R1WB	0.1994			

4.3.2 DGGE analysis from the stable nitrification phases and for replicated samples.

PCR products from biofilm carriers taken in stable phases form both the first and second period and biofilm carriers taken the same day (replicates) from reactor 1 (R1) and reactor 2 (R2) were analysed on DGGE gel 2 (Figure 4.21). 80 bands were identified on the analysed gel. The samples were divided in 8 groups based on type of reactor (R1 or R2) and different phases (A, B, C and X) (Table 4.6). Phase A is from day 17, 30 and 37 in the first period. Phase B is from day 99 and 104 in the second period. Phase C is day 125, 127 and 130 in the second period. Replicates from day 152 in the second period are marked with X. Abbreviations for the 8 groups are therefore: R1A, R2A, R1B, R1B, R1C, R2C, R1X and R2X.

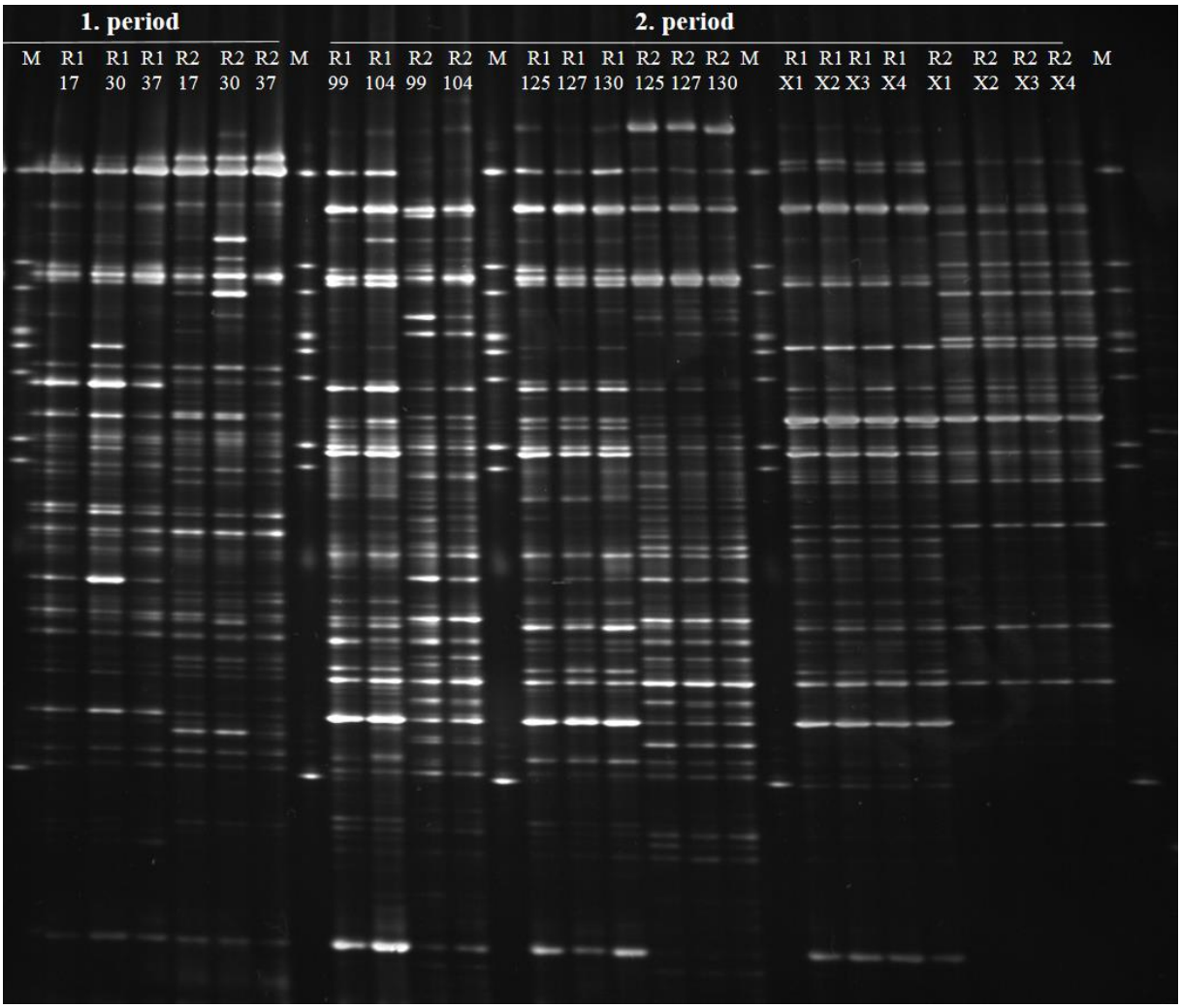

Figure 4.21 DGGE gel 2 of biofilm carriers from reactor 1 and 2 in the first and the second period. Abbreviations: R1 (reactor 1), R2 (reactor 2), M (marker). The numbers (1-152) represent the day biofilm carriers were sampled. Replicates sampled on day 152 are marked with X.

The alpha-diversities were calculated based on the 8 groups (Table 4.6). The band richness ranged from 25-48, the Shannon Diversity ranged from 2.17-2.38, while the evenness ranged from 0.21-0.33 (Table 4.6). The standard deviations of the average alpha-diversities in the groups R1X and R2X (replicates) were small, especially for Shannon diversity and evenness which had standard deviations varying between 0.004-0.03. The Shannon diversity and the evenness were similar between the phases A, B and C.

Table 4.6 Band richness (k`), Shannon diversity index (H`) and evenness (J`) calculated from the microbial community data from DGGE gel 2 (Figure 4.21). The diversity date was used to compare the biofilm carriers obtained from reactor 1 (R1) and 2 (R2) during three stable periods and for replicates sampled the same day. The average and the standard deviation of alpha-diversities were calculated for the different groups. The numbers (17-152) in the sample name-column represent the day the biofilm carriers were sampled. Replicates sampled on day 152 in the second period are marked with X. Samples from group with A are from the first period. Samples from group with B, C and X are from the second period.

Group name	**Sample name**	**Band richness (k`)**	**Shannon Diversity (H`)**	**Evenness $e^{H`}/k`$ (J`)**
	R2X4	25	2.09	0.32
R2X	R2X3	26	2.15	0.33
	R2X2	26	2.15	0.33
	R2X1	27	2.16	0.32
	Average	26 ± 0.8	2.14 ± 0.03	0.33±0.004
	R1X4	34	2.2	0.27
	R1X3	34	2.2	0.27
R1X	R1X2	39	2.23	0.24
	R1X1	39	2.21	0.23
	Average	37 ± 2.9	2.21 ± 0.01	0.25 ± 0.02
	R2 130	42	2.22	0.22
	R2 127	44	2.22	0.21
R2C	R2 125	47	2.35	0.22
	Average	44 ± 2.5	2.26 ± 0.08	0.22 ± 0.01
	R1 130	43	2.28	0.23
	R1 127	38	2.19	0.23
R1C	R1 125	44	2.28	0.22
	Average	42 ± 3.2	2.25 ± 0.05	0.23 ± 0.01
	R2 104	46	2.27	0.21
R2B	R2 99	43	2.36	0.25
	Average	45 ± 2.1	2.32 ± 0.06	0.23 ± 0.02
	R1 104	48	2.38	0.22
R1B	R1 99	45	2.28	0.22
	Average	47 ± 2.1	2.33 ± 0.07	0.22±0.004
	R2 37	42	2.26	0.23
	R2 30	42	2.27	0.23
R2A	R2 17	41	2.31	0.25
	Average	42 ± 0.6	2.28 ± 0.03	0.23 ± 0.01
	R1 37	37	2.21	0.25
R1A	R1 30	36	2.21	0.25
	R1 17	33	2.17	0.26
	Average	35 ± 2.1	2.20 ± 0.02	0.25 ± 0.01

Changes in community structure (beta-diversity) were also investigated. Ordination by Bray-Curtis similarity principle coordinate analysis (PCoA) indicated changes in community structure (Figure 4.22). PCoA indicated larger variance between the samples from the first period (phase A) than the samples from the second period (phase B and C). In addition, PCoA indicated small variance between the samples taken the same day (replicates), however, the variance in community structure between the samples from reactor 1 in the second period (R1C) was smaller.

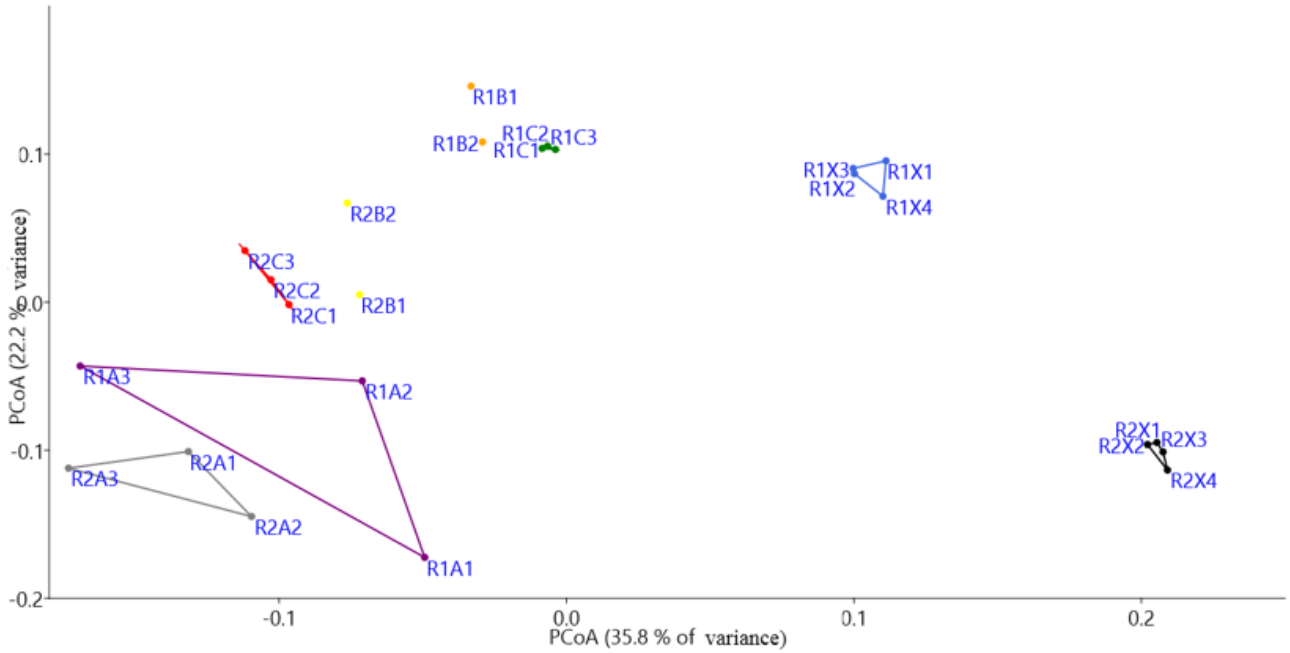

Figure 4.22 Principle coordinate analysis (PCoA) based on Bray-Curtis similarity of the microbial communities on the biofilm carriers from reactor 1 (R1) and 2 (R2) based on data from the DGGE gel (Figure 4.21). The biofilm carriers were sampled in three different stable phases (A, B and C). Phase A corresponds to day 17, 30 and 37 in the first period, phase B corresponds to day 99 and 104 in the second period, while phase C corresponds to day 125, 127 and 130 in the second period. Replicates sampled on day 152 in the second period are marked with X.

Changes in community structure (beta-diversity) were further investigated by statistical analysis. P values (Sequential Bonferroni correlation) from one-way PERMANOVA test based on Bray Curtis similarity showed significant difference in community structure between the replicate samples from reactor 1 (R1X) and reactor 2 (R2X). The difference in community structure between biofilm carriers taken in the different stable phases were not statically significant (Table 4.7). One-way PERMANOVA test from based on Jaccard similarity showed

that the species inventory in the samples in the three stable phases was not significant different and thus indicate similar species present in the three stable phases (Table 4.8).

Table 4.7 Results from one-way PERMANOVA test based on Bray Curtis similarity for the groups identified in Figure 4.22. Biofilm carriers from reactor 1 (R1) and 2 (R2) were sampled in three different stable phases (A, B & C). Phase A corresponds to day 17, 30 and 37 in the first period, phase B corresponds to day 99 and 104 in the second period, while phase C corresponds to day 125, 127 and 130 in the second period. Replicates from day 152 in the second period are marked with X. Multiple comparisons of the various groups based on Sequential Bonferroni correlation (P-value column). Significant difference if $P < 0.05$.

Comparisons	**P value**	**F**	**P(same)**	**Total sum of squares**
R2X & R1X	0.0291	10.36	0.0001	0.974
A1 & A2	0.1011			
A1 & B1	0.1009			
A 1& C1	0.0961			
A2 & B2	0.100			
A2 & C2	0.1002			
B2 & B1	0.3443			
B2 & C2	0.104			
C1 & C2	0.1047			
C1 & B1	0.0957			

Table 4.8 Results from one-way PERMANOVA test based on Jaccard similarity with the groups identified in Figure 4.22. Biofilm carriers from reactor 1 (R1) and 2 (R2) were sampled from three different stable phases (A, B & C). Phase A corresponds to day 17, 30 and 37 in the first period, phase B corresponds to day 99 and 104 in the second period, while phase C corresponds to day 125, 127 and 130 in the second period. Replicates from day 152 in the second period are marked with X. Multiple comparisons of the various groups based on Sequential Bonferroni n (P-value column). Significant difference if $P < 0.05$.

Comparisons	**P value**	**F**	**P(same)**	**Total sum of square**
R2X & R1X	0.0291	14.51	0.0001	3.515
A1 & A2	0.3034			
A1 & B1	0.3006			
A 1& C1	0.0961			
A2 & B2	0.1000			
A2 & C2	0.1002			
B2 & B1	0.3443			
B2 & C2	0.104			
C1 & C2	0.1047			
C1 & B1	0.0957			

4.4 VEAS wastewater treatment plant: Competition between nitrifying and heterotrophic bacteria

The hypothesis behind the experiments at VEAS was that the automatic washing process of Leca biofilters removed high amounts of heterotrophic bacteria from the outer layers of the biofilm, and not high amounts of the nitrifying bacteria in the inner layers of the biofilm.
If this was the case, the washing process should promote the stabilisation of the nitrification process. Oxygen consumption experiments and DGGE analysis were performed to investigate the hypothesis.

4.4.1 Oxygen consumption experiment at VEAS

The oxygen consumption experiments between washed and unwashed biofilter showed a 4 % difference in oxygen consumption between the unwashed and washed biofilter (Figure 4.23). The lines of regression were calculated from the linear regions (5 first samplings points: time 0-4) (Figure 4.23). In the unwashed biofilter, the oxygen consumption rate was 0.252 mg O_2/L min, while in the washed biofilter, the oxygen consumption rate was 0.241 mg O_2/L min.

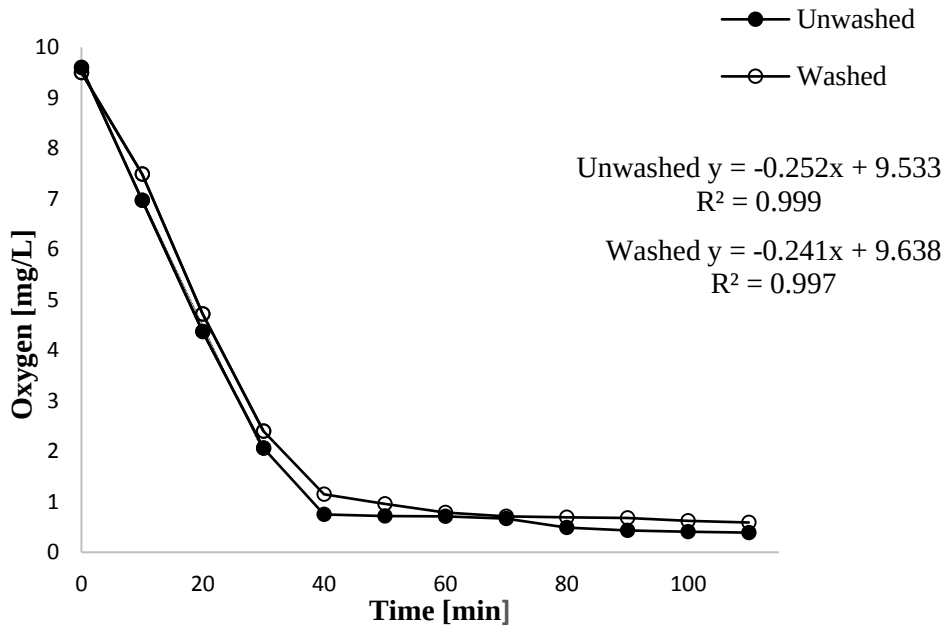

Figure 4.23 The oxygen consumption in the washed and the unwashed biofilter (nitrification filter 83). The lines of regression were calculated from the linear regions (time: 0-40 min).

The unwashed and washed biofilters showed similar changes in ammonium, nitrite and nitrate concentration (Figure 4.24), and thus nitrification activity. The nitrite and the nitrate concentration increased in the beginning of the experiment, but decreased in the final part of the experiment for both unwashed and washed biofilters. Linear regression was performed on the ammonium concentration in unwashed and washed biofilters, which showed a 19 % difference in ammonium consumption rate (Figure 4.24). The ammonium consumption rate was higher in the washed biofilm (0.077 mg NH_4^+-N/L min) than in the unwashed biofilm (0.062 mg NH_4^+-N /L min). When the oxygen concentration was under 1 mg O_2 /L, the ammonium consumption stopped in the washed and the unwashed biofilters. The loss of nitrogen from the nitrogen budgets (sum of NO_3^--N + NO_2^--N + NH_4^+-N) from the washed and the unwashed biofilters increased with time in the oxygen consumption experiment (Figure 4.25). The loss of nitrogen was higher in washed biofilters than in unwashed biofilters.

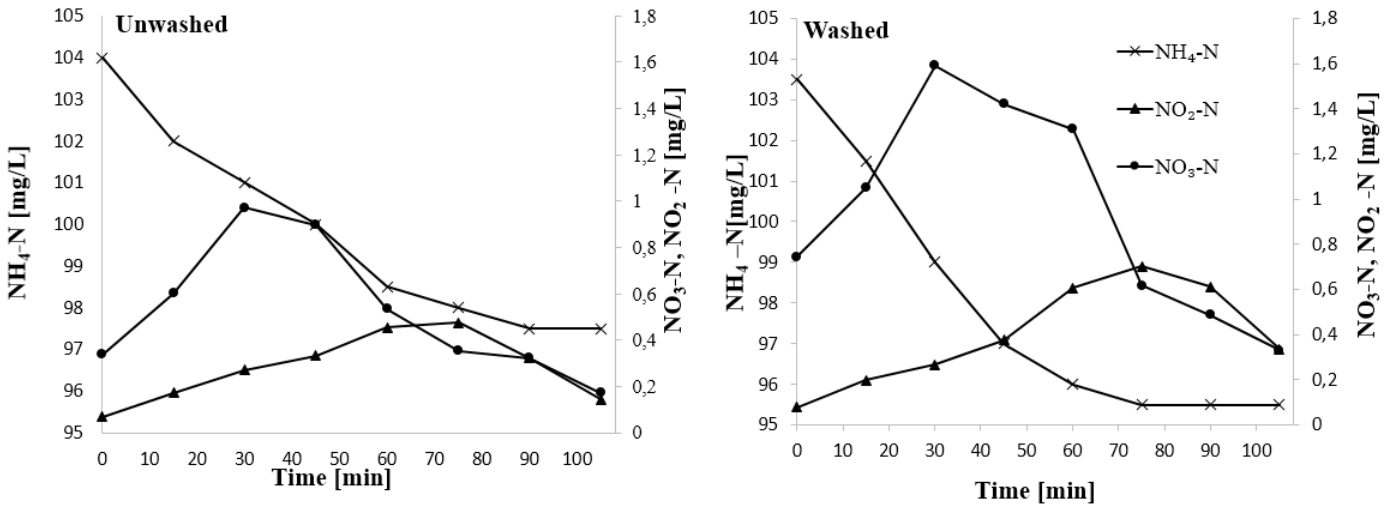

Figure 4.24 The change in ammonium (NH_4^+-N), nitrite (NO_2^--N) and nitrate (NO_3^--N) concentration with time (minutes) in the washed (left) and the unwashed biofilter (right) from nitrification filter 83.

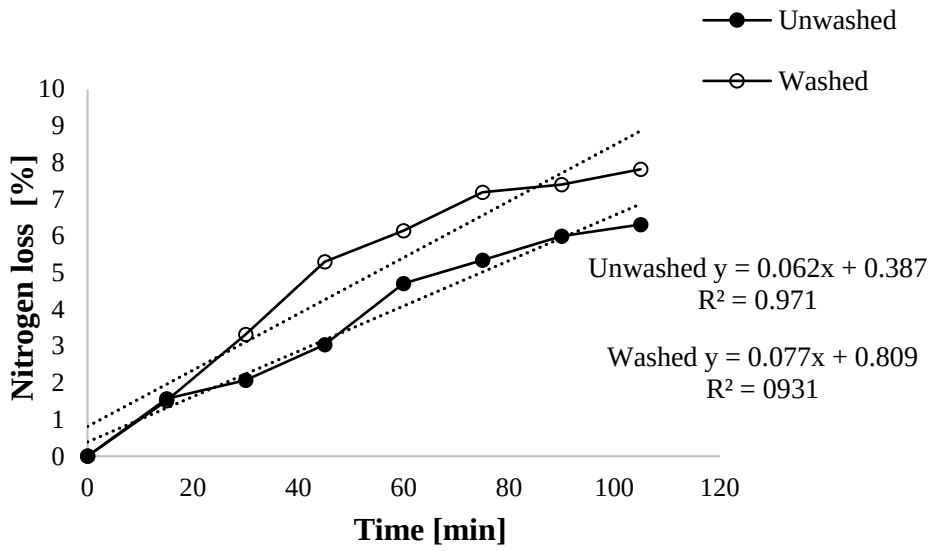

Figure 2.25 The nitrogen loss (%) as a function of time (min) from washed and unwashed biofilter from nitrification filter 83 (Table 4.9 C). The nitrogen loss was calculated from the sum of nitrogen (NO_3^--N + NO_2^--N + NH_4^+-N) compounds at a specific time divided on the sum of nitrogen compounds (NO_3^--N + NO_2^--N + NH_4^+-N) at time 0.

4.4.2 DGGE analysis of nitrification biofilter at VEAS

The objective of DGGE analysis was to investigate if the microbial community structure was different for washed and unwashed biofilters, as part of testing the hypothesis in section 4.4. Wash water from the washing process was also analysed. Nitrification filters identification and sampling times are shown in Table 4.9 and 4.10.

Table 4.9 Sampling details for the first period at VEAS. Nit refers to nitrification filter. Letters (C-G) represent samples taken from a nitrification filter at the same day.

Date	**28.09.2016**	**28.09.2016**	**29.09.2016**	**29.09.2016**	**30.09.2016**
Letter	G	F	E	D	C
Unwashed	Nit-81	Nit-84	Nit-83	Nit-82	Nit-83
Time	07:00-07:15	09:55-10:00	13:00-13:10	13:30-13:35	07:10-07:15
Washed	Nit-81	Nit-84	Nit-83	Nit-82	Nit-83
Time	07:55-08:07	10:52-11:00	13:40:13:52	14:28-14:37	07:40-07:50
Wash water	Nit-81	Nit-84	Nit-83	Nit-82	Nit 83
Time	07:50	10:15	13:15	13:58	07:37

Table 4.10 Sampling details for the second period at VEAS. Nit refers to nitrification filter. Letters (A-B) represent samples taken from a nitrification filter at the same day.

Dato	**27.10.2016**	**27.10.2016**
Letter	B	A
Unwashed	Nit-84	Nit-82
Time	14:20	14:57
Washed	Nit-84	Nit-82
Time	15:03	15:45
Wash water	Nit-84	Nit-82
Time	14:42	15:26

PCR products from unwashed biofilters (U), washed biofilters (W) and wash water (Ww) were analysed on DGGE gel 3 (Figure 4.26). 47 bands were identified on the analysed gel. The last part of the gel picture was removed because of an irregularity in the lower band lines that made analysis in Gel2K difficult (Appendix D). The gel picture showed (by observation) clear difference in band pattern between biofilters and wash water, and almost identical band pattern between washed and unwashed biofilters.

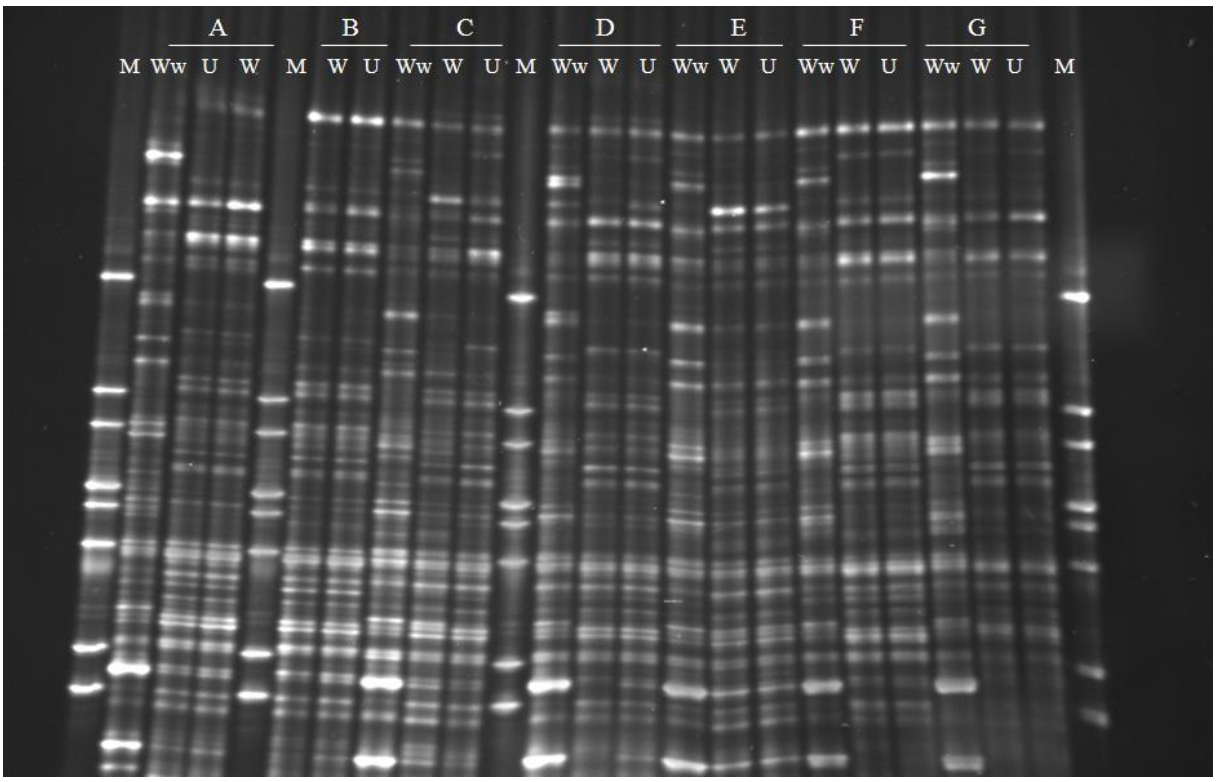

Figure 4.26 DGGE gel from unwashed biofilters (U), washed biofilters (W) and wash water (Ww). The letters A-G represent samples taken from the same biofilter at the same day (Table 4.9 and 4.10). The letter M represent marker (ladder). The removed part of the gel (lower part with high denaturation) is presented in Appendix D.

Alpha-diversities were calculated based on these groups: unwashed biofilters, washed biofilters and wash water (Table 4.11). The band richness varied between 26-37, the Shannon diversity varied between 2.84-3.20, while the evenness varied between 0.50-0.75. The average band richness, the average Shannon diversity and the average evenness were similar for the three groups (Table 4.11).

Table 4.11 Band richness (k`), Shannon diversity index(H`), evenness (J`) calculated for unwashed biofilters (U), washed biofilters (W) and wash water (Ww). The letters A-G represent samples taken from the same biofilter at the same day (explained in table 4.9 and 4.10). The averages and the standard deviations of alpha-diversities were calculated for the three group.

Group name	Biofilter	Samples	Band richness (k`)	Shannon Diversity (H`)	Evenness $e^{H`}/k`$ (J`)
	G	U81	26	2.89	0.69
	F	U84	29	3.02	0.71
	E	U83	30	3.11	0.75
U	D	U82	33	3.19	0.74
	C	U83-2	35	3.18	0.68
	B	U84-2	33	3.12	0.69
	A	U82-2	32	3.00	0.63
		Average	31 ± 3.0	3.07± 0.11	0.70 ± 0.04
	G	W81	27	2.95	0.71
	F	W84	28	2.96	0.69
	E	W83	29	2.96	0.66
	D	W82	33	3.16	0.71
W	C	W83-2	33	3.11	0.68
	B	W84-3	33	3.08	0.66
	A	W82-2	30	2.96	0.64
		Average	30 ± 2.6	3.02 ± 0.09	0.68 ± 0.03
	G	Ww81	27	2.93	0.69
	F	Ww84	29	2.99	0.69
Ww	E	Ww83	31	3.03	0.66
	D	Ww82	37	3.20	0.66
	C	Ww83-2	34	2.84	0.50
	A	Ww82-2	37	2.96	0.52
		Average	33 ± 3.8	2.99± 0.12	0.62 ± 0.09

Changes in community structure (beta-diversity) were also investigated. Ordination by principle coordinate analysis (PCoA) based on Bray Curtis similarities of microbial community structure from DGGE gel 3 (Figure 4.26) indicated high variance between the wash water and the biofilters (both unwashed and washed).

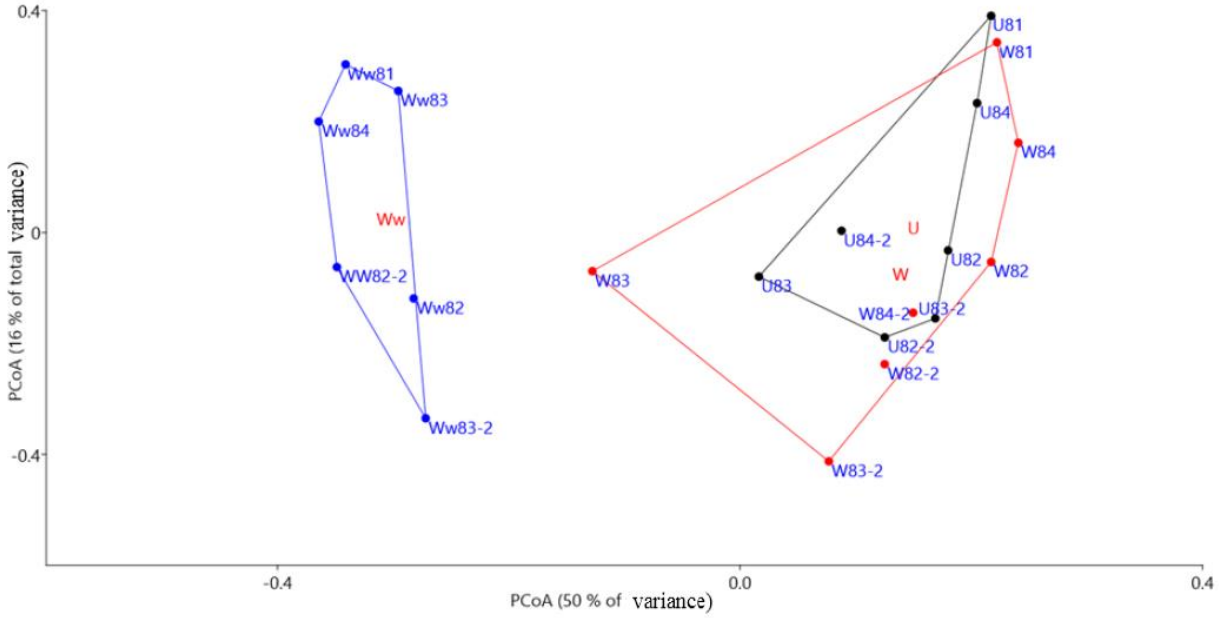

Figure 4.27 Principle coordinate analysis (PCoA) based on Bray Curtis similarity calculated from banding pattern in DGGE gel 3 (Figure 4.26). U represents the samples from unwashed biofilters (black dots), W represents samples from washed biofilter (red dots) and Ww represent samples from wash water (blue dots). The numbers 81-84 represent the different nitrification filters explained in Table 4.9 and 4.10.

PCoA indicated also that the community structure was similar in the unwashed and the washed biofilters (Figure 4.27). One-way PERMANOVA based on Bray Curtis similarities between the three groups confirmed this (Table 4.12). P values from multiple comparisons (Sequential Bonferroni correlation) showed that the difference in community structure between unwashed and wash biofilter was not significant, whereas the difference in community structure between the wash water and the biofilters (unwashed and washed) was significant. One-way PERMANOVA test based on Jaccard similarity showed that the difference in species inventory between washed and unwashed biofilters was not significant, whereas the species composition in biofilters and in wash water was significant different (Table 4.13).

Table 4.12 Results from one-way PERMANOVA based on Bray Curtis similarity for the groups identified in 4.21. Unwashed biofilters (U), washed biofilters (W) and wash water (Ww) were compared. Multiple comparisons of the various groups based on Sequential Bonferroni correlation (P-value column). Significant difference if $P < 0.05$.

Comparisons	**P value**	**F**	**P (same)**	**Total sum of square**
U and W	0.8895			
U and Ww	0.0008	6.778	0.001	4198
W and Ww	0.002			

Table 4.13 Results from one-way PERMANOVA test based on Jaccard similarity with the groups identified in Figure 4.27. Unwashed biofilters (U), washed biofilters (W) and wash water (Ww) were compared. Multiple comparisons of the various groups based on Sequential Bonferroni correlation (P-value column). Significant difference if $P < 0.05$.

Comparisons	**P value**	**F**	**P (same)**	**Total sum of square**
U and W	0.9806			
U and Ww	0.0005	6.78	0.002	1.119
W and Ww	0.0005			

5. Discussion

The competition between nitrifying and heterotrophic bacteria was investigated in two different nitrification biofilm systems in order to improve the ammonium removal efficiency and functionality. The nitrification activity and the microbial community structure in two lab-scale MBBR at Department of Biotechnology (NTNU) were investigated. In addition, the effect of organic carbon concentration on the nitrification process was studied. Furthermore, the oxygen consumption, the ammonium consumption and the microbial community structure in nitrification biofilters consisting of Leca particles in the BIOFOR system at VEAS were investigated.

5.1 Evaluation of selected methods, experimental set-up and instruments

Oxygen measurements were only performed in the end of the long-term MBBR experiments due to lack of an oxygen electrode earlier. Continuous oxygen measurements could have been interesting for investigation of the development of heterotrophic bacteria over time. In addition, continuous oxygen measurements with an oxygen electrode would have given a higher resolution of the difference in the oxygen consumption rate between the washed and unwashed biofilter in the experiments at VEAS (Figure 4.23). Multiple parallels of the oxygen consumption batch experiments at VEAS could also have given a better answer on the difference in ammonium removal efficiency and oxygen consumption between the washed and the unwashed biofilters.

For long-term MBBR experiments in the future, newer pumps would be an advantageous for improved accuracy and time saving. The Masterflex easy load L/S pumps used in the long-terms experiments maintained correct flow rates over longer time periods. However, the main disadvantages of the Masterflex pumps were abrasion on the plastic tubings and adjustment of the flow rate. Considerable time was spent on obtaining correct flow rate as the flow rate was manually adjusted and measured with a stopwatch and a measuring cylinder. The plastic tubings were replaced every time a new medium was made. Strong abrasion on the pump tubings was discovered because of inaccuracies in the flow rates. Deviation values caused by the various problems in the long-term continuous experiments were removed from the calculation of the averages (Appendix A). Most likely, these problems had minor impact on the results obtained

in the present work as the reactors stabilized after the different incident. In addition, the deviation values were removed from the calculation of the averages in further analyses, discussion and conclusion.

DGGE was used for analysing the microbial community structure in the biofilm samples from MBBR and BIOFOR. It has been claimed that species under 1 % of the total community are rarely shown on the DGGE gel (Eiler et al., 2003). Changes in the number of nitrifying bacteria or other species in biofilms during increasing C/N ratios can be difficult to detect because of the high numbers of heterotrophic bacteria. The weakest band detected in the two DGGE gels from the MBBR experiments (Figure 4.21 and 4.26) was 0.01 % of the total sample. The weakest gel band detected in the DGGE gel from VEAS (gel 3, Figure 4.26) was 0.04 % of the total sample. Most likely some of the bands were not properly separated on the gel, however, this had probably little impact on the result of the microbial community analyses.

5.2 MBBR: Competition between nitrifying and heterotrophic bacteria

5.2.1 Long-term MBBR experiments

Two MBBR with different C/N ratios were continuous operated during two separate periods (first period: 36 days, second period: 152 days) to investigate the impact of organic carbon on the nitrification activity and the ammonium removal efficiency in the biofilms. Adaption to changes such as increased C/N ratio and increased organic loading were also investigated (perturbation experiments). The difference in nitrification activity between reactor 1 (continuous C/N ratio 1) and reactor 2 (continuous C/N ratio 0) was small in both periods (Figure 4.2). In the first period (day 3-36), nitrite was accumulating from day 11-27 in reactor 1, whereas in reactor 2, no nitrite accumulation over time was observed. This was the only clear difference between the reactors in the first period. The accumulation of nitrite in reactor 1 indicated weak inhibition of NOB, most likely because of increased competition with heterotrophic bacteria. Piculell et al. (2016) observed that thicker biofilms in MBBR most likely was advantageous for the NOB. Their results indicated that the ratio of NOB to AOB decreased when the biofilm was thinner than 300 μm. This might explain why not an increase in the nitrite concentration was seen in the continuous operating reactors in the second period (days 3-130), as the reactors had been operated for a longer period and the biofilm therefore most likely was thicker than 300 μm.

In the long-term experiments (second period: day 3-130), no clear difference was observed between reactor 1 and reactor 2 with respect to nitrification activity (Figure 4.2, Table 4.2). A reduction in nitrification activity was not observed in reactor 1, which had been continuous fed with a C/N ratio of 1 (Figure 4.2). The results indicate that the nitrifying bacteria were not hindered by the heterotrophic bacteria in the biofilm in reactor 1, even though the reactor had been continuously operated for over 100 days. The combination of high HRT (13 hours), high oxygen concentration in the reactors (Figure 4.11), and high ammonium concentration in the inlet (100 NH_4^+-N mg/L) gave most likely the nitrifying bacteria satisfying conditions in both reactors. Hu et al. (2009) showed that nitrifying and heterotrophic bacteria can grow together at the same time in a biofilm if the substrate and oxygen concentrations are not limiting. In most wastewater plants, varying amounts of organic carbon are reaching the nitrification filters, still the nitrification process works at a satisfactory level most of the time. Hu et al. (2009) and Zhu and Chen (2001) have investigated the impact of C/N ratios on nitrification, and the studies have clearly shown that organic carbon has a negative impact on the nitrification process. Therefore, the results obtained here, demonstrating that reactors with a C/N ratio of 0 and 1 have a similar long-term nitrification activity, are surprising.

The microbial community structure of the biofilms from three different stable nitrification phases in the first and the second period of the long-term continuous experiments were investigated in DGGE gel 2 (Figure 4.21). One-way PERMANOVA test based on Bray Curtis similarity showed that the microbial community structure of biofilms from the different stable nitrification phases were not significant different (Table 4.7). Furthermore, the alpha-diversity was similar for the all the stable nitrification phases (Table 4.6). These results indicate that the microbial community structure in the reactor 1 (C/N ratio 1) and reactor 2 (C/N ratio 0) were similar and stable, even though the reactors had been operating for two long periods and with different C/N ratios. The results confirm the findings related to the nitrification activity, which was similar for reactor 1 and 2 in long-term operations in first and the second period (day 3-130) (Table 4.2).

A high HRT and a C/N ratio of 1 might have given advantageous conditions for the heterotopic planktonic bacteria, hence the heterotrophic bacteria in the biofilm may have been fed less organic carbon than expected. This is another possible explanation for the small difference in nitrification activity between the reactors. Cell counting by flow cytometer (Figure 4.17)

showed a high number of planktonic cells and cell aggregates in reactor 1, which supports the explanation for the small difference in nitrification activity between the reactors stated above. The high number of planktonic cells and cell aggregates may also explain the small difference between the reactors in the first organic carbon inhibition experiment at day 37 in the first period (Figure 4.3). It is possible that a reduction in the nitrification activity in reactor 1 might have been discovered if the reactor had been operated for a longer period of time (200-300 days).

Since the long-term continuous experiments (second period: days 3-130) showed small differences in nitrification activity between the reactors, the biofilms in the reactors were challenged with higher organic carbon concentrations in two perturbation experiments. The first perturbation experiment, where the C/N ratio was increased to 3 (day 131-138), showed 13 % higher ammonium consumption rate in reactor 2 than in reactor 1 for 9 hours after C/N ratio was increased (Figure 4.8). This result indicates a higher ammonium removal efficiency in reactor 2 shortly after increased C/N ratio.

Two days after the C/N ratio was increased, the nitrite concentration increased in reactor 2, however, the reactor managed to stabilize quickly (Figure 4.1 E). Reactor 1 showed a tendency of nitrite accumulating, but after the loading rate was increased, the nitrite concentration was lowered in reactor 1 as well. This results may indicate that reactor 2 managed to stabilize quicker than reactor 1 and thus had higher nitrification robustness. This result indicate that NOB were inhibited after increased C/N ratio, but that the strong inhibition was short-term. The difference in average nitrification activity was similar for the reactors after the C/N ratio was increased, however, there were few sampling points and high standard deviations for the average nitrogen concentrations (day 131-138).

The acetate consumption rate was considerably higher for the biofilm in reactor 1 than reactor 2 in the 9 hours after the C/N ratio was increased (Figure 4.7). This result is a strong indication that continuously supply of C/N ratio of 1 for over 130 days had contributed to increased growth of heterotrophic bacteria in the biofilm from reactor 1 compared to reactor 2. This assumption is supported by the short-term oxygen consumption in the batch experiment. The oxygen consumption rate was 23 % higher for the biofilm carrier from reactor 1 than for biofilm carriers from reactor 2 (second period: days 89-90) (Figure 4.5).

High heterotrophic activity after increased C/N ratio to the biofilm can contribute to increased oxygen competition in the biofilm. This can create anaerobic zones in the deeper layer of the biofilm, which can be a good environment for denitrifying bacteria. Loss of nitrogen was observed in reactor 1 the first hours after the C/N ratio was increased to 3, while no nitrogen loss was seen in reactor 2 in the same period of time (Figure 4.10). Loss of nitrogen indicates a high number of denitrifying bacteria present in reactor 1 and anaerobic conditions in the biofilm. These results are corroborating by Hu, Li et al. (2009), who detected increased nitrogen loss, increased denitrification, lowered ammonia removal rate and a shift in the microbial community after the C/N ratio to the biofilm was increased.

The development of the organic carbon consumption rate in reactor 2 indicated that even though no organic carbon was introduced (unlike in most wastewater plants) to reactor 2 before day 131, the response time was short (< 24 hours) before reactor 2 consumed organic carbon equally to reactor 1 (Figure 4.7). The short response time indicate that heterotrophic bacteria already were present on the biofilm carriers from reactor 2, and that they most likely have been living on organic carbon from dead organisms. The oxygen consumption rate was higher in reactor 2 than reactor 1 after the C/N ratio was increased to 3 (Figure 4.9). This supports the dramatically planktonic cell growth in reactor 2 after the C/N ratio and the organic loading rate were increased (Figure 4.17). The results showed that previous continuous supply of organic carbon (as in reactor 2) is not necessary for the biofilm to be able to handle higher amounts of organic carbon in the wastewater. Gonzalez-Silva et al. (2016) showed by pyrosequencing that the biofilm communities in three nitrifying MBBR without organic carbon in the medium were dominated by heterotrophic bacteria. For the three reactors, 71, 57, and 67 % of the sequence reads representing the biofilm communities were classified as heterotrophic bacteria, and 90 % of OTUs identified (in the data set) did not represent nitrifying bacteria.

After increased loading rate (second period, days 139-152), the main difference in response between the reactors was the development of ammonium concentration. Both the reactors showed varying ammonium concentration in the first days after the loading rate was increased, but after some days, the average ammonium concentration was increased in both the reactors compared to average ammonium concentration before the perturbations experiments (Figure 4.1). This is an indication of decreased ammonium removal efficiency in both the reactors. The nitrifying bacteria did not manage to adjust to the increased loading of nitrogen and removed nitrogen with the same efficient as before. This is unlike the heterotrophic bacteria, which

managed to adapt to the increased loading rate of organic carbon. The organic carbon concentration remained low in both the reactors throughout the period (Figure 4.14). Increased ammonium concentration indicate that the growth rate of the nitrifying bacteria was inhibited by the higher growth rate of heterotrophic bacteria.

At day 145-152, a gap was observed between the nitrification activity calculated from the nitrate production (NO_3^--N/L h) and the nitrification activity calculated from the ammonium consumption (NH_4^+-N /L h) in both the reactors (Figure 4.2 E-F). The result can be in agreement with the organic carbon experiments (day 99, 2. Period) (Section 4.2.1), where the final concentration of nitrite was higher than the final concentration of nitrate after the sodium acetate concentration was increased. The results indicate that NOB were inhibited more than AOB after the organic carbon concentration was increased, and that the competition for oxygen presumably increased in the biofilm. Hu, Li et al. (2009) observed lower nitrate production with higher C/N ratios, and concluded that NOB utilize oxygen slower than AOB.

Nitrogen loss was observed in both the reactors after loading rate was increased (Figure 4.2 E-F). This is a strong indication of denitrification activity in the reactors. The degree of inhibition of NOB can therefore be overestimated based on the nitrification activity calculations. Denitrifying bacteria consume nitrate in the reactors, and therefore, high amounts of denitrifying bacteria will contribute to lower nitrate concentration in the reactors, which will give lower nitrate production values (NO_3^--N/L h), as were observed in Figure 4.2 E-F. Based on the nitrification activity calculations after increased loading rate, it cannot be concluded that NOB were more inhibited than AOB. A conclusion might be that AOB were inhibited by the higher average ammonium concentration in the reactors after the second perturbation experiment. This conclusion corresponds with Satoh et al. (2000), who detected that increased C/N ratio almost immediately started to inhibit AOB in the biofilm due to increased oxygen competition in the biofilm. The tenedency seen in the two pertubation experiments was inhibition of NOB shortly after increased C/N ratio and AOB after increased loading.

The difference in nitrification activity was similar between the reactors, also after increased loading rate, but reactor 2 showed higher variation in nitrification activity given a nitrate production (NO_3^--N/L h) (Table 4.2). The ammonium concentrations were lower in reactor 2 than reactor 1 the last days before shut-down of the reactors (Figure 4.15). It is difficult to conclude that there was a difference between the reactors with respect to nitrification efficiency,

stability and response due to variations in the nitrogen concentrations and short operation time after the loading rate was increased (Figure 4.1). Based on the average calculations and observations, it seems that reactor 1 was further weakened in nitrogen efficiency compared to reactor 2, but reactor 2 had higher variation in nitrification activitiy (NO_3^--N/L h) and higher ustability in the nitrification process (Figure 4.1, Table 4.2) The main conclusion is that increased organic loading was negative affecting both the reactors. Furter statistical tests are needed for significant to determine if reactor 2 handled the pertubations better, and maybe a longer operation time had been neseccary for cleary see if both reactors manged to stabilize the nitrfication process and see the difference in nitrification efficiency.

The microbial community structure was investigated before and after the C/N ratio and the loading rate were increased (perturbation experiments). One-way PERMANOVA test based on Bray Curtis Similarity showed that biofilm carriers taken before increased C/N ratio were significantly different in community structure compared to the biofilm carriers taken after the C/N ratio and the loading rate were increased (Table 4.4). The changes in species inventory were confirmed by One-Way PERMAMOVA test based on Jaccard similarity (Table 4.5). This is most likely a result of increased heterotrophic growth, and the result illustrate how fast a stable microbial community structure can change after the organic carbon concentration is increased. The average band richness and the Shannon diversity were lowered in the biofilm in both the reactors after the C/N ratio and the loading rate was increased (Table 4.3). This result corresponds with Michaud et al. (2006) who found a reduction of taxa richness and diversity after the C/N ratio was increased in a moving bed biofilm system.

5.2.2 Short-term organic carbon inhibition experiments

The organic carbon inhibition experiment was repeated twice to investigate if there was a difference in acute organic carbon inhibition of the nitrification activity between the biofilm from reactor 1 (with continuous organic carbon supply) and the biofilm from reactor 2 (without continuous organic carbon supply). The difference in nitrate accumulation rate between reactor 1 and reactor 2 was small the first time the experiment was performed (day 37, 1. period) (Figure 4.2). The nitrate accumulation rate was slightly higher in the biofilm from reactor 2 than for the biofilm from reactor 1 for every concentration of sodium acetate. High degree of inhibition of nitrate accumulation was not shown for neither of the reactors. The result indicates that the ammonium removal efficiency in the biofilm from reactor 2 was higher, however, the difference

between the nitrate accumulation rates was too small to conclude if there was a difference in the nitrification robustness. In the second experiment, the organic carbon inhibition of the nitrification process was greater, which may be explained by thicker biofilms, increased heterotrophic growth due to longer operations time, and higher organic carbon concentrations (Figure 4.3).

The maximum organic carbon concentration was increased from 100 mM to 1000 mM the second time the organic carbon inhibition experiment was performed (day 99, 2. period) (Figure 4.3) EC_{50} value of sodium acetate for the nitrification activity was 11 times higher for the biofilm from reactor 2 than the biofilm from reactor 1. This result support the hypothesis that long-term supply of organic carbon has a negative impact on ammonia removal efficiency. The nitrification activity was almost completely inhibited in reactor 1 at 1000 mM. Nitrification robustness against acute toxic concentrations of organic carbon was thus considerably higher for reactor 2 than for reactor 1. This is based on the fact that the biofilm from reactor 2 managed to obtain nitrification activity even at an organic carbon concentration as high as 1000 mM. Similar results have been shown in nitrification MBBR by Henry et al. (2016), where EC_{50} for sodium acetate dropped from 274 mM to 15 mM after the biofilm was chronically exposed to organic carbon. In the study by Henry et al. (2016), heterotrophic growth caused lower robustness of the nitrification process against acute toxic organic carbon concentrations compared to the control reactors without continuous organic carbon loading over time.

A relevant comparison between the long-term continuous experiment (Figure 4.1) and the organic carbon inhibition experiment (Figure 4.3) is the intensity of the organic loading. A C/N ratio of 1 and 3 is equivalent to 3.57 mM and 10.7 mM sodium acetate, respectively. The organic loading is coming dropwise in the continuous MBBR and high numbers of heterotrophic planktonic bacteria are present in the reactors. In the organic carbon inhibition experiments, the organic loading was added all at once to the biofilm carriers and at the start the medium did not contain heterotrophic planktonic bacteria that could immediately start consumption of organic carbon. Therefore, the oxygen competition was probably higher between heterotrophic and nitrifying bacteria in the biofilm in the organic carbon inhibition experiment. This can be an explanation for the immediate inhibition of nitrification activity after addition of organic carbon in the organic carbon inhibition experiments.

The summary of the long-term and short-term experiments is that a long-term supply of a C/N ratio of 1 reduced the nitrification robustness towards acute toxic organic carbon loadings. This was shown clearly in the short-term organic carbon inhibition experiment. This give a clear indication of the negative impact increased competition with heterotrophic bacteria has on the efficiency in the nitrification process. The long-term nitrification stability did not decrease after long-term supply of a C/N ratio of 1. After the perturbations experiments, the average nitrification activity did not decrease in the reactors. However, the nitrification efficient did decrease because the average ammonium concentration was increased in both the reactors after the loading rate was doubled.

5.3 VEAS wastewater treatment plant: Competition between nitrifying and heterotrophic bacteria

The objective of the oxygen consumption/nitrification experiment at VEAS and the DGGE analysis of the microbial communities was to investigate whether the automatic washing process of nitrification biofilters consisting of Leca removed high amounts of heterotrophic bacteria from the outer layers of the biofilm, and not high amounts of the nitrifying bacteria in the inner layers of the biofilm.

The oxygen consumption rate was 4 % higher in the unwashed biofilter than the washed biofilter, while the ammonium consumption rate was 19 % lower in the unwashed biofilter than in the washed biofilter. The results indicate that the washing process removed some of the heterotrophic bacteria as the oxygen consumption decreased and ammonia removal efficiently increased in the washed biofilter. In addition, these differences indicate that high amounts of heterotrophic bacteria existed in the biofilm even after the washing process was finished. However, the 4 % difference in oxygen consumption seemed to increase the oxygen penetration into the biofilm. The results may also indicate that the nitrification process at VEAS is oxygen limited, and thus may have room for improvements. The organic carbon concentration in the wastewater that reached the nitrification filters gave good growth conditions for the heterotrophic bacteria in the biofilm. High heterotrophic growth might contribute to the decrease the nitrification efficiency due to increased competition for oxygen in the biofilm, and the washing process contributed to better oxygen penetration by removing biofilm layers. The oxygen consumption experiment was performed without parallels, and the differences observed

between the washed and the unwashed biofilter may have been considered to be statistically insignificant if the experiment had been repeated.

The nitrogen budget for the washed and unwashed biofilter showed loss of nitrogen, which suggest that denitrification takes place in the nitrification reactors (Figure 4.25). Mao et. al (2008) detected high denitrification activity and heterotrophic activity in the nitrification biofilters at VEAS. High denitrification and anaerobic activity in the biofilter is a good explanation for the loss of nitrogen as the nitrite and the nitrate concentration decreased when the oxygen concentration went under 1 mg O_2/L (Figure 4.24). The 19 % inhibition of the ammonium removal rate in the unwashed biofilter indicates that the nitrification process is oxygen restriction in the biofilm. Mao et al. (2008) showed that nitrification in the biofilm on the Leca particles declined strongly when oxygen concentration was low in the batch.

The one-way PERMANOVA test based on Bray Curtis similarity of the microbial community composition (Table 4.12) showed no significant difference between the washed and the unwashed biofilter. The P-value from one-way PERMANOVA test based on Jaccard similarity comparing washed and unwashed biofilter was close to 1, which is a strong indication that certain species was not removed from the biofilm after the washing process (Table 4.13). Measurements of alpha-diversities also indicated that the microbial community structure in washed and unwashed biofilter was similar. Mao et al. (2008) showed that the microbial community composition (DGGE profil) in three different nitrification filters at VEAS was similar at all depths of the nitrification filters and between the filters. This support the results in the present work showing low variance in alpha- and beta diversities between different filters and between washed and unwashed biofilter.

The results from DGGE, showing that unwashed and washed biofilters were similar, are not supported by the results from the oxygen consumption experiments.
DGGE and oxygen consumption measurements are not methods with a high degree of accuracy. The washing process most probably removed only a small fraction of the total biomass in the stationary biofilter. The amount of biomass (microorganisms) was probably high in the washed biofilter, and therefore, the oxygen consumption rate will be equally high in the washed biofilter. DGGE are used for analysing variations in microbial community structure, and if changes in the microbial community only occur in a small fraction of the total sample, these changes can be suppressed in the DGGE analysis.

The results from the oxygen consumption experiments indicated that the washing process removed heterotrophic bacteria from the outer layers of the biofilm. Since the microbial community composition analysis showed no significant difference between unwashed and washed biofilters, the hypothesis can only be partially confirmed.

To improve ammonium removal efficiency and functionality, the nitrification process should be favoured. The results obtained from the two systems in the present work indicated that the ammonium removal efficiency decreased due to the negative impact of the heterotrophic bacteria. Especially, the competition for oxygen increased when organic carbon reached the biofilm. Therefore, it is recommended that research in the future focus on removing higher amounts of organic matter before the nitrification filter, even though the nitrification process might work at a satisfactory level with current C/N ratios in the wastewater.

5.4 Future works

There is still much more to learn and investigate when it comes to the competition between nitrifiers and heterotrophs. Partial sequencing of the 16S-rRNA gene would give more detailed taxonomic information about the microbial communities, and would be a natural next step to continue the reached conducted in this thesis. Sequencing of 16S rRNA from biofilm samples was not performed in the present work due to time constrains. Illumina sequencing is an appropriate method for complete microbial community analysis as it gives genus information for the organisms present. It will thus be possible to divide the community into heterotrophs, AOB and NOB, and in that way, get more detailed information on the dynamics of the communities, especially for the samples from the MBBR under different C/N ratios. Sequencing of 16S rRNA from the nitrification biofilters at VEAS and measurements of bacteria concentrations before and after the washing process would probably have given better results regarding the amounts of heterotrophic bacteria that are removed from the outer layers of the biofilm during the washing process

In the future, it would have been interesting to perform similar long-term and short-term experiments in seawater and brackish reactors, and compare the results with those from the freshwater systems studied in this master thesis. In addition, it would have been interesting to perform similar short-term experiments in computer controlled reactors for better and more

precise metabolic activity measurements of carbon dioxide production and oxygen consumption under different C/N ratios. Long-term experiments with higher C/N ratios (3, 4 or 5) and regularly sampling of biofilm carriers would also be interesting for monitoring the change in microbial communities.

6. Conclusions

Conclusion from the MBBR experiments:

The following results were obtained:

- A C/N ratio of 1 did not affect the nitrification efficiency in the long-term stable continuous operations.
- The biofilm that had been exposed to a C/N ratio of 1 over a longer period of time had a considerably lower nitrification activity at acute high organic carbon concentrations compared to the biofilm with a long-term supply of a C/N ratio of 0.
- After the C/N ratio was increased to 3, the response time was under 24 hours before the reactor without previous exposure to organic substrate could consume organic carbon substrate equally fast as the reactor with previous exposure to organic substrate.
- After loading rate of carbon was increased, the nitrification efficiency was decreased in both the reactors.
- Denitrification was observed in both the reactors after loading rate of carbon was increased as loss of nitrogen (NH_4^+-N, NO_2^--N, NO_3^--N) was detected in the nitrogen budgets.

The conclusion based on these results is that the nitrification efficiency was not considerably reduced after long-term supply of a C/N ratio 1. In acute high organic carbon concentrations, the nitrification efficiency was reduced, which indicates reduced robustness of the biofilm that had been long-term exposed to organic carbon). However, higher loading rate of carbon gave reduction in the nitrification efficiency in both the systems (long-term continuous C/N ratio of 1 and long-term continuous C/N ratio of 0).

Conclusions from the nitrification filters in the BIOFOR system at VEAS:

The main results obtained from the nitrification filters at VEAS was:

- Compared to unwashed biofilter, the washed biofilter showed a 19 % increase in the ammonium consumption, and a 4 % reduction in the oxygen consumption.
- The differences in biofilm community structure between unwashed and washed filter were not statistical significant. However, the differences between the wash water and the biofilters communities were significant.

A 19 % difference in ammonium consumption is a strong indication that the washing process remove heterotrophic bacteria from the biofilm, however, the microbial community structure of the washed and unwashed did not indicate the same as the communities was similar. Therefore, it cannot be concluded that a high number of heterotrophic bacteria are removed from the nitrification filters after the washing process.

Conclusion for the two different nitrification systems:

The MBBR systems had higher nitrification efficiency and stability with lower C/N ratios. The washed biofilter had a higher ammonium consumption than the unwashed biofilter, which most likely consisted of a higher number of heterotrophic bacteria. The results from both the systems indicate that heterotrophic growth has negative effects on the nitrification process, and how important it is to avoid organic carbon for an optimal nitrification process and for avoiding high competition between heterotrophic and nitrifying bacteria.

References

ALMASI, A., MOUSAVI, S. A., BAHMAN, Z., ZOLFAGHARI, M. R. & ZINATIZADEH, A. A. 2016. Effect of hydraulic retention time and aeration time on the performance and microbial diversity in an upflow aerobic/anoxic sequential bioreactor. *Desalination and Water Treatment,* 57**,** 23589-23596.

ANDERSON, M. J. 2001. A new method for non-parametric multivariate analysis of variance. *Austral ecology,* 26**,** 32-46.

ANDERSON, M. J. 2005. Permutational multivariate analysis of variance. *Department of Statistics, University of Auckland, Auckland,* 26**,** 32-46.

AUSTIN SUTHANTHIRARAJ, P. P. & GRAVES, S. W. 2013. Fluidics. *Curr Protoc Cytom,* Chapter 1**,** Unit 1 2.

BLANCHETON, J. P. 2000. Developments in recirculation systems for Mediterranean fish species. *Aquacultural Engineering,* 22**,** 17-31.

BRAY, J. R. & CURTIS, J. T. 1957. An Ordination of the Upland Forest Communities of Southern Wisconsin. *Ecological Monographs,* 27**,** 325-349.

BRUCE, E. R. & PERRY, L. M. 2001. *Environmental biotechnology: principles and applications,* New York, McGrawHill 400.

CAMARGO, J. A. & ALONSO, A. 2006. Ecological and toxicological effects of inorganic nitrogen pollution in aquatic ecosystems: A global assessment. *Environment International,* 32**,** 831-849.

CAYLET, A., ESCUDIÉ, R., GÉVAUDAN, G., HAMELIN, J., BROCKMAN, D. & BERNET, N. 2011. Impact of Hydraulic Retention Time (HRT) on biofilm development: molecular analysis and modelling of microbial competition. https://www.researchgate.net/publication/256427135

CEUPPENS, S., DELBEKE, S., DE CONINCK, D., BOUSSEMAERE, J., BOON, N. & UYTTENDAELE, M. 2015. Characterization of the Bacterial Community Naturally Present on Commercially Grown Basil Leaves: Evaluation of Sample Preparation Prior to Culture-Independent Techniques. *Int J Environ Res Public Health,* 12**,** 10171-97.

CHENG, S.-S. & CHEN, W.-C. 1994. Organic carbon supplement influencing performance of biological nitritification in a fluidized bed reactor. *Water Science and Technology,* 30**,** 131-142.

COCOLIN, L., MANZANO, M., CANTONI, C. & COMI, G. 2001. Denaturing gradient gel electrophoresis analysis of the 16S rRNA gene V1 region to monitor dynamic changes in the bacterial population during fermentation of Italian sausages. *Appl Environ Microbiol,* 67**,** 5113-21.

COSTA, E., PÉREZ, J. & KREFT, J.-U. 2006. Why is metabolic labour divided in nitrification? *Trends in microbiology,* 14**,** 213-219.

CRAB, R., AVNIMELECH, Y., DEFOIRDT, T., BOSSIER, P. & VERSTRAETE, W. 2007. Nitrogen removal techniques in aquaculture for a sustainable production. *Aquaculture,* 270**,** 1-14.

CUA, L. S. & STEIN, L. Y. 2011. Effects of nitrite on ammonia-oxidizing activity and gene regulation in three ammonia-oxidizing bacteria. *FEMS microbiology letters,* 319**,** 169-175.

DARZYNKIEWICZ, Z., HALICKA, H. D. & ZHAO, H. 2010. Analysis of Cellular DNA Content by Flow and Laser Scanning Cytometry. *Polyploidization and Cancer,* 676**,** 137-147.

DAVIS, J. C. 1986. *Statistics and Data Analysis in Geology*, John Wiley & Son.

DONLAN, R. M. 2002. Biofilms: Microbial life on surfaces. *Emerging Infectious Diseases,* 8**,** 881-890.

DORAN, P. M. 2012. *Bioprocess Engineering Principles*, Elsevier Science.

EBELING, J. M., TIMMONS, M. B. & BISOGNI, J. 2006a. Engineering analysis of the stoichiometry of photoautotrophic, autotrophic, and heterotrophic removal of ammonia–nitrogen in aquaculture systems. *Aquaculture,* 257**,** 346-358.

EBELING, J. M., TIMMONS, M. B. & BISOGNI, J. J. 2006b. Engineering analysis of the stoichiometry of photoautotrophic, autotrophic, and heterotrophic removal of ammonia-nitrogen in aquaculture systems. *Aquaculture,* 257**,** 346-358.

EILER, A., LANGENHEDER, S., BERTILSSON, S. & TRANVIK, L. J. 2003. Heterotrophic bacterial growth efficiency and community structure at different natural organic carbon concentrations. *Applied and Environmental Microbiology,* 69**,** 3701-3709.

FIELDS, S. 2004. Global nitrogen - Cycling out of control. *Environmental Health Perspectives,* 112**,** A556-A563.

FIGUEROA, L. A. & SILVERSTEIN, J. 1992. The effect of particulate organic matter on biofilm nitrification. *Water environment research,* 64**,** 728-733.

FLEMMING, H. C., WINGENDER, J., SZEWZYK, U., STEINBERG, P., RICE, S. A. & KJELLEBERG, S. 2016. Biofilms: an emergent form of bacterial life. *Nat Rev Microbiol,* 14**,** 563-75.

GALLOWAY, J. N. & COWLING, E. B. 2002. Reactive nitrogen and the world: 200 years of change. *Ambio,* 31**,** 64-71.

GERARDI, M. H. 2016. Operator's Guide to Biological Nutrient Removal (BNR) in the Activated Sludge Process. *Operator's Guide to Biological Nutrient Removal.* Chemical Publishing Company Inc.

GINESTET, P., AUDIC, J. M., URBAIN, V. V. & BLOCK, J. C. 1998. Estimation of nitrifying bacterial activities by measuring oxygen uptake in the presence of the metabolic inhibitors allylthiourea and azide. *Appl Environ Microbiol,* 64**,** 2266-8.

GONZALEZ-SILVA, B. M., JONASSEN, K. R., BAKKE, I., ØSTGAARD, K. & VADSTEIN, O. 2016. Nitrification at different salinities: Biofilm community composition and physiological plasticity. *Water research,* 95**,** 48-58.

GOREAU, T. J., KAPLAN, W. A., WOFSY, S. C., MCELROY, M. B., VALOIS, F. W. & WATSON, S. W. 1980. Production of NO2-and N2O by nitrifying bacteria at reduced concentrations of oxygen. *Applied and environmental microbiology,* 40**,** 526-532.

GRADY, C. P. L. & LIM, H. C. 1980. *Biological Wastewater Treatment: Theory and Applications,* New York Marcel Dekker

GREEN, S. J., LEIGH, M. B. & NEUFELD, J. D. 2010. Denaturing Gradient Gel Electrophoresis (DGGE) for Microbial Community Analysis. *In:* TIMMIS, K. N. (ed.) *Handbook of Hydrocarbon and Lipid Microbiology.* Berlin, Heidelberg: Springer Berlin Heidelberg.

HAMMER, Ø., HARPER, D. & RYAN, P. 2001. PAST: Paleontological statistics software package for education and data analysis. Palaeontology Electronic 4: 9 pp.

HELBÆK, M. & KJELSTRUP, S. 2009. *Fysikalsk kjemi,* Bergen, Vigmostad & Bjørke AS.

HENRY, I. A., EINBU, A., SVENDSEN, H. F., BAKKE, I. & ØSTGAARD, K. 2016. Inhibition factors in biofilm N removal systems treating wastes generated by amine based CO 2 capture. *International Journal of Greenhouse Gas Control,* 45**,** 200-206.

HENZE, M., HARREMOES, P., JANSEN, J. L. C. & ARVIN, E. 2001. *Wastewater treatment : biological and chemical processes* Berlin, Springer.

HERRLING, M. P., GUTHAUSEN, G., WAGNER, M., LACKNER, S. & HORN, H. 2015. Determining the flow regime in a biofilm carrier by means of magnetic resonance imaging. *Biotechnology and bioengineering,* 112**,** 1023-1032.

HIBBING, M. E., FUQUA, C., PARSEK, M. R. & PETERSON, S. B. 2010. Bacterial competition: surviving and thriving in the microbial jungle. *Nature Reviews Microbiology,* 8**,** 15-25.

HU, J., LI, D., LIU, Q., TAO, Y., HE, X., WANG, X., LI, X. & GAO, P. 2009. Effect of organic carbon on nitrification efficiency and community composition of nitrifying biofilms. *J Environ Sci (China),* 21**,** 387-94.

ISAACS, S. H. & HENZE, M. 1995. Controlled carbon source addition to an alternating nitrification-denitrification wastewater treatment process including biological P removal. *Water Research,* 29**,** 77-89.

JACCARD, P. 1908. Nouvelles recherches sur la distribution florale. *Bulletin de la Société vaudoise des sciences naturelles,* 44**,** 223-270.

KACHEL, V., FELLNER-FELDEGG, H. & MENKE, E. 1990. *Hydrodynamic properties of flow cytometry instruments. Flow cytometry and sorting. ,* New York, John Wiley & Sons

KLAMMER, S., KNAPP, B., INSAM, H., DELL'ABATE, M. T. & ROS, M. 2008. Bacterial community patterns and thermal analyses of composts of various origins. *Waste Management & Research,* 26**,** 173-187.

KUENEN, J. G. 2008. Anammox bacteria: from discovery to application. *Nat Rev Microbiol,* 6**,** 320-6.

LEE, P. Y., COSTUMBRADO, J., HSU, C. Y. & KIM, Y. H. 2012. Agarose Gel Electrophoresis for the Separation of DNA Fragments. *Jove-Journal of Visualized Experiments*.

MADIGIAN, M., MARTINKO, J., STAHL, D. & CLARK, D. 2012. *Brock Biology of Microorganisms* Boston, Pearson.

MAO, Y., BAKKEN, L. R., ZHAO, L. & FROSTEGÅRD, Å. 2008. Functional robustness and gene pools of a wastewater nitrification reactor: comparison of dispersed and intact biofilms when stressed by low oxygen and low pH. *FEMS Microbiology Ecology,* 66**,** 167-180.

MICHAUD, L., BLANCHETON, J.-P., BRUNI, V. & PIEDRAHITA, R. 2006. Effect of particulate organic carbon on heterotrophic bacterial populations and nitrification efficiency in biological filters. *Aquacultural Engineering,* 34**,** 224-233.

NORLAND, S. 2004. Gel2K gel analysis software. University of Bergen, Norway.

ODEGAARD, H., GISVOLD, B. & STRICKLAND, J. 2000. The influence of carrier size and shape in the moving bed biofilm process. *Water Science and Technology,* 41**,** 383-391.

ODEGAARD, H., RUSTEN, B. & WESTRUM, T. 1994. A New Moving-Bed Biofilm Reactor - Applications and Results. *Water Science and Technology,* 29**,** 157-165.

OHASHI, A., DE SILVA, D. V., MOBARRY, B., MANEM, J. A., STAHL, D. A. & RITTMANN, B. E. 1995. Influence of substrate C/N ratio on the structure of multi-species biofilms consisting of nitrifiers and heterotrophs. *Water Science and Technology,* 32**,** 75-84.

PAINTER, H. 1986. *Nitrification in the treatment of sewage and waste-waters,* Washington, D.C : Society for General Microbiology, Oxford IRL Press 185–211.

PAWLOWSKI, L., DUDZINSKA, M. & PAWLOWSKI, A. 2007. *Environmental Engineering,* London, Taylor & Francis.

PEET, R. K. 1975. Relative diversity indexes. *Ecology,* 56**,** 496-498.

PEPPER, I. L., GERBA, C. P. & GENTRY, P. J. 2015. *Environmental microbiology,* San Diego, Calif, Academic Press.

PICOT, J., GUERIN, C. L., KIM, C. L. V. & BOULANGER, C. M. 2012. Flow cytometry: retrospective, fundamentals and recent instrumentation. *Cytotechnology,* 64**,** 109-130.

PICULELL, M., WELANDER, P., JÖNSSON, K. & WELANDER, T. 2016. Evaluating the effect of biofilm thickness on nitrification in moving bed biofilm reactors. *Environmental technology,* 37**,** 732-743.

PODANI, J. & MIKLOS, I. 2002. Resemblance coefficients and the horseshoe effect in principal coordinates analysis. *Ecology,* 83**,** 3331-3343.

POMMERVILLE, J. C. 2004. *Alcamo's fundamentals of microbiology, 7th ed,* Sudbury, Mass, Jones and Bartlett.

RASBAND, W. 1997-2012. ImageJ. Bethesda, MD: US National Institutes of Health. *imagej.nih.gov/ij/.*

ROSENZWEIG, M. L. 1995. *Species diversity in space and time,* Cambridge, Cambridge University Press.

RUSTEN, B., EIKEBROKK, B., ULGENES, Y. & LYGREN, E. 2006. Design and operations of the Kaldnes moving bed biofilm reactors. *Aquacultural Engineering,* 34**,** 322-331.

SANTORO, M. J. 2016. The do-it-all nitrifiers. *Science,* 351**,** 342-343.

SATOH, H., OKABE, S., NORIMATSU, N. & WATANABE, Y. 2000. Significance of substrate C/N ratio on structure and activity of nitrifying biofilms determined by in situ hybridization and the use of microelectrodes. *Water science and technology,* 41**,** 317-321.

SHANNON, C. E. & WEAVER, W. 1949. *The mathematical theory of communication,* Urbana, University of Illinois Press.

SHAPIRO, H. M. 2003. *Practical flow cytometry,* Hoboken, N.J, Wiley-Liss.

SHARMA, B. & AHLERT, R. 1977. Nitrification and nitrogen removal. *Water Research,* 11**,** 897-925.

SINGH, B., BAUDDH, K. & BUX, F. 2015. *Algae and Environmental Sustainability,* New Delhi, Springer India.

STOODLEY, P., DODDS, I., BOYLE, J. & LAPPIN-SCOTT, H. 1998. Influence of hydrodynamics and nutrients on biofilm structure. *Journal of applied microbiology,* 85.

STROUS, M., HEIJNEN, J., KUENEN, J. G. & JETTEN, M. 1998. The sequencing batch reactor as a powerful tool for the study of slowly growing anaerobic ammonium-oxidizing microorganisms. *Applied microbiology and biotechnology,* 50**,** 589-596.

SUN, G., XIAO, J., LU, M., WANG, H., CHEN, X., YU, Y., PAN, Y. & WANG, Y. 2015. Agarose gel purification of PCR products for denaturing gradient gel electrophoresis results in GC-clamp deletion. *Appl Biochem Biotechnol,* 175**,** 400-9.

THERMOFISHER. *SYBR® Green I Nucleic Acid Gel Stain* [Online]. Available: https://tools.thermofisher.com/content/sfs/manuals/mp07567.pdf [Accessed 14.04.2017 2017].

TIMMONS, M. B. & EBELING, J. M. 2013. *Recirculating Aquaculture* Ithaca, NY Ithaca Publishing Company.

VAN KESSEL, M. A. H. J., HARHANGI, H. R., VAN DE PAS-SCHOONEN, K., VAN DE VOSSENBERG, J., FLIK, G., JETTEN, M. S. M., KLAREN, P. H. M. & DEN CAMP, H. J. M. O. 2010. Biodiversity of N-cycle bacteria in nitrogen removing moving bed biofilters for freshwater recirculating aquaculture systems. *Aquaculture,* 306**,** 177-184.

VEAS. 2016. *Om VEAS* [Online]. Available: http://www.veas.nu/home/om-veas [Accessed 11 dec 2016].

VINDIMIAN, E. 2003. REGTOX: macro Excel™ for dose-response modelling.

WATSON, S. W., BOCK, E., HARMS, H., KOOPS, H.-P. & HOOPER, A. B. 1989. *Bergey's manual of systematic bacteriology: Nitrifying bacteria,* Baltimore, Williams & Wilkins.

WHITTAKER, R. H. 1960. Vegetation of the Siskiyou Mountains, Oregon and California. *Ecological Monographs,* 30**,** 279-338.

WIEN, A. 1995. 25% reduksjon i utbyggingen av nitrogenrensetrinnet på VEAS etter utvikling av et optimalt filtermedium i nitrifikasjonstrinnet. *VANN,* 30**,** 44-50.

WIEN, A., BERG, K. G., KRISTIN GREIFF JOHNSEN, K. G., SAGEBERG, P. & RYRFORS, P. 1995. Erfaringer med oppstrøms biofilter prosess for nitrogenfjerning ved VEAS – status for utviklingen av VEAS konseptet. *VANN,* 30**,** 33-43.

YOU, J., DAS, A., DOLAN, E. M. & HU, Z. Q. 2009. Ammonia-oxidizing archaea involved in nitrogen removal. *Water Research,* 43**,** 1801-1809.

ZHU, S. M. & CHEN, S. L. 2001. Effects of organic carbon on nitrification rate in fixed film biofilters. *Aquacultural Engineering,* 25**,** 1-11.

ZIEMBINSKA-BUCZYNSKA, A., CEMA, G., KALBARCZYK, M. & ZABCZYNSKI, S. 2014. Application of PCR-DGGE to Study Genotypic Variability of Bacteria Inhabiting Rotating Biological Contactors Treating Synthetic Coke Wastewater. *Ochrona Srodowiska,* 36**,** 3-8.

Appendix A: Experimental details MBBR

Deviation values caused by the various problems in the long-term continuous experiments were removed from the average calculations. Days and explanation for the different incidences are shown in Table A.1-A.2.

Table A.1 Deviation values from 1. Period for reactor 1 (R1) and reactor 2 (R2).

1. period		
day	**Explanation**	**Reactor**
3	Unstable flow	R2
19	Unstable flow	R2
33	Unstable flow	R1 & R2
36	Unstable flow	R1

Table A.2 Deviation values from 2. Period for reactor 1 (R1) and reactor 2 (R2).

2. period		
day	**Explanation**	**Reactor**
3	Not in balance & low flow	R1& R2
17	Unstable flow (U F)	R1
24	Unstable flow	R1 & R2
27	Unstable flow	R2
30	Unstable flow	R2
43	Oxygen problem and U F	R1 & R2
45	Continuing oxygen problems	R2
48	Continuing oxygen problems	R2
63	Curl on the pump tubing	R1
118	Low flow	R1 & R2
138	Low flow	R1 & R2

Appendix B: Protocol for DNA Isolation

Experienced User Protocol

Please wear gloves at all times

1. To the **PowerBead Tubes** provided, add 0.25 grams of soil sample.
2. Gently vortex to mix.
3. **Check Solution C1.** If **Solution C1** is precipitated, heat solution to 60ºC until dissolved before use.
4. Add 60 µl of **Solution C1** and invert several times or vortex briefly.
5. Secure **PowerBead Tubes** horizontally using the MO BIO Vortex Adapter tube holder for the vortex (MO BIO Catalog# 13000-V1-24) or secure tubes horizontally on a flat-bed vortex pad with tape. Vortex at maximum speed for 10 minutes. **Note:** If you are using the 24 place Vortex Adapter for more than 12 preps, increase the vortex time by 5-10 minutes.
6. Make sure the PowerBead Tubes rotate freely in your centrifuge without rubbing. Centrifuge tubes at 10,000 x *g* for 30 seconds at room temperature. **CAUTION:** Be sure not to exceed 10,000 x *g* or tubes may break.
7. Transfer the supernatant to a clean **2 mL Collection Tube** (provided). **Note**: Expect between 400 to 500 µl of supernatant. Supernatant may still contain some soil particles.
8. Add 250 µl of **Solution C2** and vortex for 5 seconds. Incubate at 4ºC for 5 minutes.
9. Centrifuge the tubes at room temperature for 1 minute at 10,000 x *g*.
10. Avoiding the pellet, transfer up to, but no more than, 600 µl of supernatant to a clean **2 mL Collection Tube** (provided).
11. Add 200 µl of **Solution C3** and vortex briefly. Incubate at 4□C for 5 minutes.
12. Centrifuge the tubes at room temperature for 1 minute at 10,000 x *g*.
13. Avoiding the pellet, transfer up to, but no more than, 750 µl of supernatant into a clean **2 mL Collection Tube** (provided).
14. Shake to mix Solution C4 before use. Add 1200 µl of **Solution C4** to the supernatant and vortex for 5 seconds.
15. Load approximately 675 µl onto a **Spin Filter** and centrifuge at 10,000 x *g* for 1 minute at room temperature. Discard the flow through and add an additional 675 µl of supernatant to the **Spin Filter** and centrifuge at 10,000 x *g* for 1 minute at room temperature. Load the remaining supernatant onto the **Spin Filter** and centrifuge at 10,000 x *g* for 1 minute at room temperature. **Note**: A total of three loads for each sample processed are required.
16. Add 500 µl of **Solution C5** and centrifuge at room temperature for 30 seconds at 10,000 x *g*.
17. Discard the flow through.
18. Centrifuge again at room temperature for 1 minute at 10,000 x *g*.
19. Carefully place spin filter in a clean **2 mL Collection Tube** (provided). Avoid splashing any **Solution C5** onto the **Spin Filter**.
20. Add 100 µl of **Solution C6** to the center of the white filter membrane. Alternatively, sterile DNA-Free PCR Grade Water may be used for elution from the silica Spin Filter membrane at this step (MO BIO Catalog# 17000-10).
21. Centrifuge at room temperature for 30 seconds at 10,000 x *g*.
22. Discard the **Spin Filter**. The DNA in the tube is now ready for any downstream application. No further steps are required.

    We recommend storing DNA frozen (-20ºC to -80 ºC). **Solution C6** contains no EDTA. To concentrate the DNA see the Hints & Troubleshooting Guide.

Thank you for choosing the PowerSoil® DNA Isolation Kit.

Technical information: Toll free 1-800-606-6246, or 1-760-929-9911 Email: technical@mobio.com
Website: www.mobio.com

Appendix C: DGGE

Solutions used in PCR and DGGE are described in Table C1-C7.

Table C.1 1 L 50x TAE-buffer

Chemical	Amount	pH	Start concentration
Tris base	242 g	-	
Glacial acetic acid	57.1 mL	-	0.5 M
EDTA	100 mL	8	
MQ-water	Added to final volume: 1 L	-	

Table C.2 100 mL 10 % APS**.**

Chemical	Amount
Ammonium persulfate	10 g
MQ-water	100 mL

Table C.3 200 mL deionized formamide.

Chemical	Amount
Formamide	200 mL
DOWEX RESINAG 501X8	7.5 g
MQ-water	Added to final volume: 200 mL

Table C.4 250 mL 0 % Denaturing acrylamide solution.

Chemical	Amount
50x TAE-buffer	2.5 mL
40 % acrylamide solution	50 mL
MQ-water	Added to final volume: 250 mL

Table C.5 250 mL 80 % Denaturing acrylamide solution.

Chemical	Amount

50x TAE-buffer	2.5 mL
40 % acrylamide solution	50 mL
Deionizied formamide	80 mL
Urea	84 g
MQ-water	Added to final volume: 250mL

Appendix D: VEAS

Complete picture of the DGGE gel 3 analysed in Figure 4.26 is shown in Figure D.1.

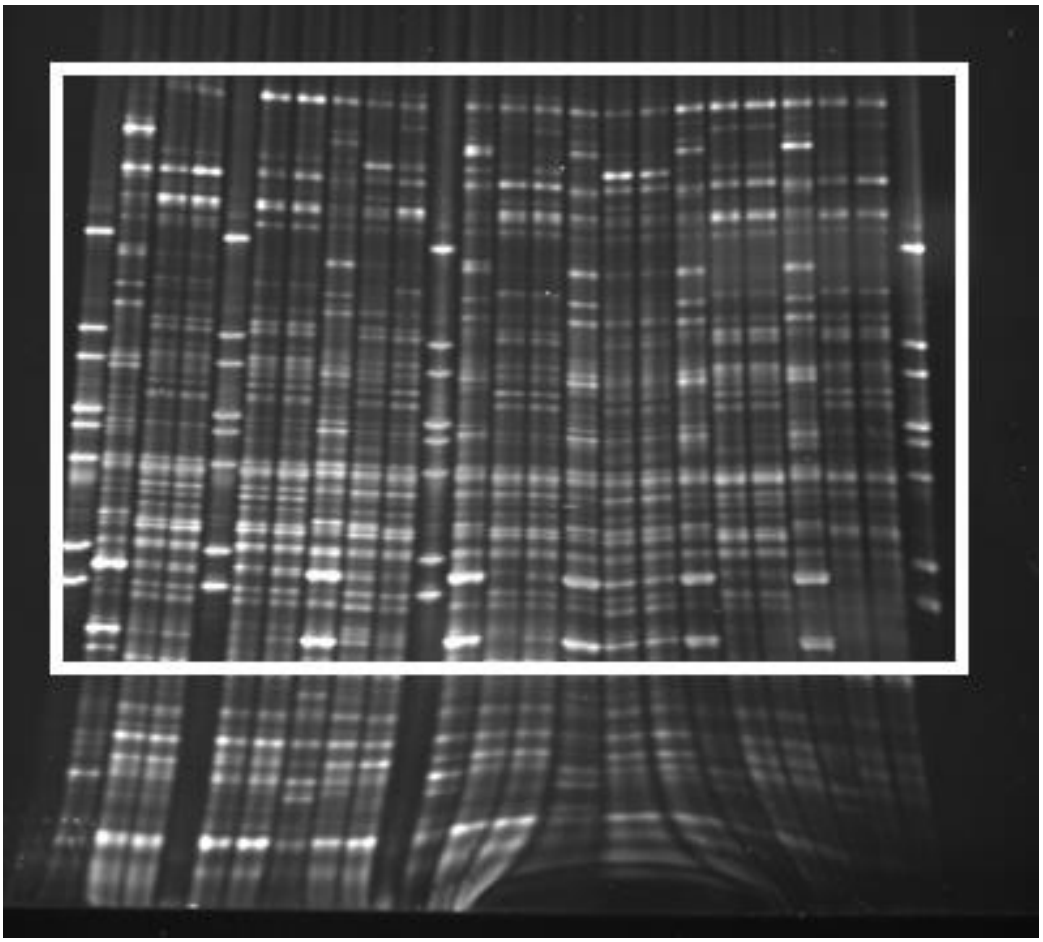

Figure D.1 Complete picture of gel 3 (Figure 4.26). White frame indicates the analysed area.

Appendix E: Flow cytometer

For freshwater is 1x Tris-EDTA (TE)-buffer used as working solution (Table E.1)

Table E.1 Working solution (1x TE-buffer) used in analysis with flow cytometer.

Chemical	Amount (mL)
H_2O	495.5
0.5 EDTA (pH 8.0)	1.0
Tris-HCl (pH 7.5)	2.5

1x TE-buffer and MQ-water were filtrated with syringe filter with 0.2 μm acetate membrane (VWR International, USA) for avoiding contamination in the working solution.